Summer 8-14-2015

Role of Hippo-YAP signaling in Mitosis and Prostate Cancer

Lin Zhang
University of Nebraska Medical Center

ROLE OF HIPPO-YAP SIGNALING IN MITOSIS AND PROSTATE CANCER

BY

LIN ZHANG

A DISSERTATION

Presented to the Faculty of

The University of Nebraska Graduate College

In Partial Fulfillment of the Requirements
for the Degree of Doctor of Philosophy

Pathology and Microbiology graduate Program

Under the Supervision of Professor Jixin Dong

University of Nebraska Medical Center

Omaha, Nebraska

May, 2015

Supervisor Committee

Kaustubh Datta, Ph.D. **Kai Fu, M.D., Ph.D.**

Keith Johnson, Ph.D. **Robert Lewis, Ph.D.**

Acknowledgements

My PhD training in UNMC marks a great milestone in my life. I want to thank all these people who helped and supported me a lot in different ways during my doctoral study in the past four years.

First and foremost, I would like to express my sincerest gratitude to my mentor, Dr. Jixin Dong, for taking me as his student. His suggestions, patience, guidance, and encouragement support me throughout my 4-year Ph.D. training. It is because of him I have this precious opportunity to study here. He respects me a lot and never yells at me even when I made stupid mistakes. His door was always open and he was more than happy to keep up with my projects and help me to figure out the problem I met in my projects. His enthusiasm in scientific research always encourages me, and he exhibited what an excellent scientist should be. Additionally, he led our group towards a happy family, in which we treat everyone in the lab friendly, honestly and gratefully. I want to express my full respect and gratitude to Dr. Dong. My thesis projects would never have been possible without his tremendous help and support. I will keep working hard to live up to his expectations to become a very good doctor, scientist and a good mentor in the future.

I am honored to have a graduate committee composed of excellent scientists, Dr. Kaustubh Datta, Dr. Kai Fu, Dr. Keith Johnson, and Dr. Robert Lewis. Thanks for

everything they have done throughout my PhD training. I felt so blessed that they accepted my invitations to be on my committee. I deeply appreciate their insightful suggestion and critical comments which greatly improved my scientific knowledge.

Many thanks to current and former lab members in the Dong laboratory, Dr. Ming Ji, Dr. Ling Xiao, Dr. Shuping Yang, Xingcheng Chen and Seth Stauffer. We always freely offered scientific suggestions to help each other, making the lab an enjoyable place to work. Especially, I would like to say special thanks to our lab manager, Yuanhong Chen. She helps us to prepare solutions, order supplies, organize reagents and maintain security standards. Her hard work ensures that our lab operate smoothly, safely and efficiently. It is really a wonderful experience to work with these great people in such a friendly laboratory.

I wish to thank Ming-Fong Lin (University of Nebraska Medical Center) for providing us the LNCaP-C33 (equivalent to LNCaP) and LNCaP-C81 cell lines. I am grateful to the Prostate Cancer Biorepository Network (PCBN, New York University site) for providing hormonal resistant tissue array. I would also like to thank the Department of Pathology and Microbiology, the Chinese Scholarship Council, and the funding sources, without their support I would not be able to study at UNMC. I also want to thank Tuire Cechin, who helped me a lot arranging

the seminars and exams. In addition, I thank Dr. Joyce Solheim for critical reading and comments on my manuscripts before publication.

I am really grateful to all my friends who have helped me along the way and helped me a lot through the difficult moments in my life. No words can express my gratitude towards my beloved mother Aiyun Wang, my father Chuanfu Zhang, my mother in-law Zaihong Wu and my father in-law Xuegang Li, for their endless love and cares, especially in days when I was facing challenges and frustrations. I owe more than I could ever repay to them. I also want to thank my husband Song Li, who always stand by my side whenever I need him. Lastly, I thank my little baby Anderson Sihan Li, who made me realize the truth of life.

ROLE OF HIPPO-YAP SIGNALING IN MITOSIS AND PROSTATE CANCER

Lin Zhang, Ph.D.

University of Nebraska, 2015

Advisor: **Jixin Dong, Ph.D.**

Abstract:

The Hippo pathway controls organ size and tumorigenesis by inhibiting cell proliferation and promoting apoptosis. KIBRA [kidney and brain expressed protein] is an upstream regulator of the Hippo-YAP signaling. The role KIBRA plays in mitosis has not been established. We show that KIBRA activates the Aurora kinases during mitosis and KIBRA promotes the phosphorylation of large tumor suppressor 2 by activating Aurora-A. We further show that knockdown of KIBRA causes mitotic abnormalities, including defects of spindle and centrosome formation and chromosome misalignment. The transcriptional co-activator with PDZ-binding motif is a downstream effector of the Hippo tumor suppressor pathway. In the current study, we define a new layer of regulation of TAZ activity that is critical for its oncogenic function. We found that TAZ is phosphorylated *in vitro* and *in vivo* by the mitotic kinase CDK1 at S90, S105, T326, and T346 during the G2/M phase of the cell cycle. Interestingly, the non-phosphorylatable mutant

possesses higher activity in epithelial-mesenchymal transition, anchorage-independent growth, cell migration and invasion. Functional studies show that the non-phosphorylatable mutant of TAZ was sufficient to induce spindle and centrosome defects in immortalized epithelial cells. Together, our results reveal a previously unrecognized connection between TAZ oncogenicity and mitotic phospho-regulation.

Recent studies have demonstrated that the Hippo signaling pathway plays a critical role in tumorigenesis. The functional significance of the main effector of the Hippo tumor suppressor pathway, YAP, in prostate cancer has remained elusive. We show that enhanced expression of YAP transformed immortalized prostate epithelial cells and promoted migration and invasion in both immortalized and cancerous prostate cells. YAP knockdown largely blocked cell division in LNCaP-C4-2 cells under androgen-deprivation conditions. In addition, ectopic expression of YAP was sufficient to promote LNCaP cells from androgen-sensitive to androgen-insensitive *in vitro* and YAP conferred castration resistance *in vivo*. Our results identify YAP as a novel regulator in prostate cancer and as a potential therapeutic target for castration-resistant prostate cancer.

TABLE OF CONTENTS

List of Figures

List of Abbreviations

ANKRD1: Ankyrin repeat domain-containing protein 1

AR: androgen receptor

CAMTA1: calmodulin-binding transcription activator 1

CDK1: cyclin dependent kinase 1

CRPC: castration-resistant prostate cancer

CSS: charcoal-stripped serum

CTGF: connective tissue growth factor

Cyr61: Cysteine-rich angiogenic inducer 61

DHT: dihydrotestosterone

EMT: epithelial-to-mesenchymal transition

ERK: extracellular signal-regulated kinases

FBS: fetal bovine serum

GAPDH: glyceraldehyde-3-phosphate dehydrogenase

GSK3: Glycogen synthase kinase 3

GST: glutathione S-transferase

HCC: hepatocellular carcinoma

ITGB2: Integrin beta-2

KIBRA: kidney and brain expressed protein

KLK2: kallikrein-2

Lats1/2: large tumor suppressor kinase 1/2

MAPK: mitogen-activated protein kinases

MEK: mitogen-activated protein kinase

MOB1: Mps one binder 1

Mst1/2: mammalian sterile-20 like 1/2

NF2: neurofibromatosis type 2

NKX3.1: NK3 homeobox 1

NRK cells: normal rat kidney epithelial cells

PB: probasin

PGC-1: Peroxisome proliferator-activated receptor gamma coactivator 1

PIN: prostatic intraepithelial neoplasia

PLK1: polo-like kinase 1

PP1: protein phosphatase 1

PSA: prostate-specific antigen

PTEN: phosphatase and tensin homolog

RSK1/2: p90 ribosomal S6 kinase 1/2

rtTA: reverse tetracycline-controlled transactivator

TAZ: transcriptional coactivator with PDZ-binding motif

TEAD1-4: TEA domain family member 1-4

TGF: transforming growth factor

TRAMP: transgenic adenocarcinoma of the prostate

TRE: tetracycline response element

WW45: protein salvador homolog 1, 45 kD WW domain protein

YAP: yes-associated protein

Chapter 1

Regulation and Functional Dissection of KIBRA and TAZ in Mitosis

Part of the contents is from the original publication:

J Biol. Chem. 2012 Oct 5; 287(41):34069-77.

1.1 Introduction

Mitosis is tightly controlled in order to achieve proper separation of chromosomes during cell division. Aberration in mitosis often causes genome instability or aneuploidy, a phenotype that many human malignant tumors exhibit. Various cellular surveillance mechanisms ensure the fidelity of cell cycle progression (1). The spindle assembly checkpoint ensures that mitosis proceeds accurately by arresting the cells in mitosis until all chromosomes are properly aligned at the metaphase plate (2). Defects in mitosis, such as chromosome misalignment or abnormal spindle formation, will therefore result in activation of the spindle assembly checkpoint and subsequent cell cycle arrest in metaphase. Thus, several antimitotic drugs have been developed, and they induce abnormal or prolonged cell cycle arrest in mitosis by perturbing microtubule dynamics, leading to mitotic catastrophe or cell death (3-5).

The Hippo signaling pathway was originally discovered in *Drosophila* and plays an important role in tumorigenesis by regulating cell proliferation and apoptosis (6-8). In mammals, the core components of Hippo pathway form a kinase cascade comprising the tumor suppressors Mst1/2, WW45, Lats1/2 and Mob1. Protein kinases Mst1/2 form a complex with WW45 that phosphorylate and activate Lats1/2 as well as the adaptor protein Mob1. In turn, activated Lats1/2 phosphorylates and inactivates the downstream effector YAP and its paralog TAZ. The phosphorylation of YAP at Serine 127 and TAZ at Serine 89 from the upstream Hippo pathway serve as 14-3-3-binding sites and sequesters YAP/TAZ

in the cytoplasm and further leads to protein degradation. Without the inhibition from the Hippo pathway, YAP and TAZ translocate into the nucleus, where they bind to transcription factors and induce transcription of genes that promote cell proliferation and inhibit apoptosis.

Although many studies have demonstrated the important roles of the Hippo pathway in tumorigenesis, the underlying mechanisms remain unclear. Recent studies have shown that several key members of the Hippo pathway, such as Mst1/2, Lats1/2, WW45, and Mob1, are involved in regulating mitosis (9). Aberration of mitosis often causes genome instability/aneuploidy and subsequent oncogenesis. Thus, the Hippo pathway may contribute to tumorigenesis by regulating mitosis-related events.

The WW domain-containing protein KIBRA (enriched in kidney and brain (10)) was recently identified as a novel regulator of the Hippo pathway in both *Drosophila* and mammalian cells (11-14). In *Drosophila*, *kibra* was shown to function as a tumor suppressor that regulates the Hippo signaling pathway, which controls tissue growth and organ size (11-13). *Kibra* associates with Mer and Ex and directly binds to the Hippo–Sav complex to regulate the Hippo signaling pathway. Loss of *kibra* results in imaginal disc overgrowth, oogenesis defects and increased target gene expression of Hippo signaling (13). Human KIBRA was originally identified as a memory performance-associated protein in humans (15-19), and this function was recently confirmed in mice (20). The physiological function of KIBRA in non-neuronal cells is much less defined, although KIBRA

has been shown to be involved in cell migration in podocytes (21) and NRK cells (22) and in epithelial cell polarity (23). KIBRA also interacts with the motor protein dynein light chain 1 to positively regulate cell growth in breast cancer cells (24). Interestingly, KIBRA expression is frequently down-regulated by promoter methylation in B-cell acute lymphocytic leukemia (25) and chronic lymphocytic leukemia (26) but not in epithelial cancers, including breast, colorectal, kidney, lung, and prostate, suggesting a potential cell type-specific tumor suppressive function of KIBRA. Recent studies demonstrated that KIBRA functions together with NF2 to stimulate phosphorylation of Lats1/2, thus inducing activation of the Hippo pathway to suppress the transcriptional activity of YAP, indicating that the tumor suppressive function of KIBRA may be conserved in the mammalian system. However, a role of KIBRA in development of cancer has not been established.

Our group previously reported that KIBRA associates with Aurora-A (27) and Lats2 (14). Furthermore, we showed that KIBRA is phosphorylated by Aurora-A and -B kinases during mitosis (27). The functions of Aurora kinases and Lats2 in mitosis are well defined, but whether KIBRA has a mitotic role is currently unknown. It is largely unclear how KIBRA, Aurora, and Lats2 regulate each other within the KIBRA-Aurora-Lats2 axis. In this study, we show that KIBRA activates the Aurora kinases and stimulates the phosphorylation of Lats2 on Ser83 through activating Aurora-A. Lats2, in turn, inhibits Aurora-mediated phosphorylation of KIBRA. Importantly, knockdown of KIBRA causes mitotic defects. We propose

that KIBRA, in conjunction with Aurora-A and Lats2, is a novel mitotic component that regulates proper mitosis.

TAZ (also called WWTR1-WW domain-containing transcription regulator protein 1) is a transcriptional co-activator (28). TAZ is involved in human cancer and stem cell function (29-31). TAZ promotes tumor growth and metastasis in several types of cancers, including breast cancer (32-34), colon cancer (35-37), non-small cell lung cancer (38-40) and glioblastoma (41). Correspondingly, TAZ expression/activity is upregulated in several human malignancies (29, 34, 42, 43) and the TAZ locus is amplified in some triple-negative breast cancers (33) and non-small cell lung cancer tumors (39). Recent studies showed that the TAZ gene is frequently fused with calmodulin-binding transcription activator 1 (CAMTA1) in epithelioid hemangioendothelioma although the underlying mechanism of this fusion protein in cancer is still unclear (44, 45). TAZ also plays an important role in embryonic stem-cell self-renewal (46) and confers cancer stem cell-like properties in breast (33) and oral cancer cells (47).

TAZ activity/function is regulated largely through the Hippo tumor suppressor pathway, which was originally discovered in *Drosophila* (48) and is highly conserved in mammals (7, 49, 50). The Hippo core kinases large tumor suppressor 1/2 (Lats1/2) phosphorylate and inactivate TAZ by sequestering it in the cytoplasm and promoting ubiquitination-dependent protein degradation (51, 52). Many cues (e.g. the G-protein coupled receptor-Rho GTPase axis,

mechanical force and actin cytoskeleton etc.) regulate TAZ activity in a Hippo-dependent manner (29, 31). Recent work has shown that other signals (e.g. GSK3 or Rho GTPase) can regulate TAZ in a Hippo-independent manner (53, 54). TAZ also crosstalks with and is regulated by Wnt/β-catenin signaling. For example, TAZ, along with β-catenin, is degraded in the absence of Wnt signaling (8) and TAZ (and its paralog YAP) orchestrates the Wnt response by forming a complex with the β-catenin destruction complex (55). Furthermore, cytoplasmic TAZ (phosphorylated by Hippo) restricts β-catenin nuclear localization/activation directly (56) or through inhibiting Dishevelled phosphorylation (57). Besides the above regulation, however, it is not known whether and how TAZ is regulated during cell cycle progression/mitosis.

We recently showed that some members of the Hippo pathway are phosphorylated by mitotic kinases Aurora and CDK1 during mitosis (27, 58). We and others found that TAZ was up shifted on a SDS-polyacrylamide gel (due to phosphorylation) during anti-microtubule drug-induced G2/M arrest (59, 60); however, the phosphorylation sites and the biological significance of this phosphorylation have remained elusive. In this study, we show that mitotic phosphorylation of TAZ on a number of sites occurs dynamically in cells in a CDK1-dependent manner. Interestingly, mitotic phosphorylation inactivates TAZ's oncogenic activity. Therefore our data reveal a new layer of regulation for TAZ activity, implicating a link between mitosis and TAZ oncogenicity.

1.2 Materials and Methods

Expression constructs

We used the human full-length KIBRA cDNA (isoform 1) as a PCR template to clone KIBRA into the pcDNA3.1/FLAG (Invitrogen) vector or pcDNA3.1 (Invitrogen) to generate N-terminal FLAG-tagged KIBRA. A human full-length Aurora-A cDNA clone (identification number 3051177, OpenBiosystems) was subcloned in-frame into the pEGFP-C1 vector (Clontech) to make the GFP-Aurora-A construct. A human PP1c clone (identification number 3956353) was purchased from OpenBiosystems and subcloned into the pcDNA-HA vector. HA-TAZ was a gift from Kun-Liang Guan (Addgene plasmid #32839) (47). To make the retroviral-mediated and GFP tagged TAZ expression constructs, the above cDNA was cloned into MaRX^{TM}IV vector (14) and pEGFP-C1 vector (Clontech), respectively. Deletion constructs were made by PCR and verified by sequencing and restriction enzyme digestion. Point mutations were generated by the Quik Change Site-Directed PCR mutagenesis kit (Stratagene) and verified by sequencing.

Cell culture and transfection

HEK293T, HeLa, and MCF-7 cell lines (purchased from American Type Culture Collection (ATCC), Manassas, VA) were maintained in Dulbecco's modified Eagle's medium containing 10% fetal bovine serum and antibiotics (Clontech Laboratories, Mountain View, CA). MCF-10A cells were cultured as described (34). The immortalized human pancreatic epithelial (HPNE) cells were cultured

as we previously described (34). Attractene (Qiagen) were used for transient overexpression transfections following the manufacturer's instructions. Aurora-A siRNA (27) (SMART pool) and siRNA against Lats2 (SMART pool) were purchased from Dharmacon, Inc. (Lafayette, CO). PP1c siRNA (27) was purchased from Santa Cruz Biotechnology (Santa Cruz, CA). SiRNA-1 and -2 against KIBRA have been described previously (14). Nocodazole (100 ng/ml for 16-20 h) and Taxol (0.1 μM for 16 h) were used to arrest cells in G2/M phase unless otherwise indicated. RO-3306 (CDK1 inhibitor) and roscovitine (CDKs inhibitor) were from ENZO Life Sciences. Purvalanol A (CDKs inhibitor) was purchased from Selleck. All other chemicals were either from Sigma or Thermo Fisher.

Establishment of Tet-On-inducible Cell Lines

The parental HeLa-rtTA cell line was purchased from Clontech Laboratories. We utilized the pRetroX-Tet-On advanced/pRetroX-Tight-Pur system (Clontech) to establish the cell lines expressing wild-type (WT) KIBRA or KIBRA S539A mutant (both are siRNA-resistant constructs). Cells were maintained in medium containing Tet system-approved fetal bovine serum (Clontech Laboratories).

Cell Cycle Synchronization

A double thymidine block was used as described previously with slight modification (61). Briefly, thymidine was added to subconfluent HeLa cells (2.5 mm final), and the culture was incubated for 17 h. Cells were washed three times with PBS and allowed to recover with fresh medium for 10 h. The cells were then

incubated with 2.5 mm thymidine for another 18 h. The culture medium was replaced with fresh medium without the drug to release the cells from the block.

Luciferase reporter assay

Luciferase reporter assays were performed in 24-well platesin HEK293T cells. 8XGTIIC-Luciferase (Addgene #34615, (62)), SV40-Renilla (Addgene #27163,(63)) and various TAZ mutants were co-transfected in triplicate as we have described previously (34). Luciferase activity was assayed at 48 hours post-transfection by the Dual-luciferase reporter assay system (Promega) following the manufacturer's instructions.

Recombinant protein purification

To make His-tagged human TAZ, full-length TAZ cDNA was subcloned into the pET-21c vector (Novagen/EMD Chemicals). The His-tagged proteins were bacterially expressed and purified on HisPur^{TM} Cobalt spin columns (Pierce) following the manufacturer's instructions.

In vitro kinase assay

About 1µg of His-TAZ was incubated with 100 ng recombinant CDK1/cyclin B complex (Signal Chem) or HeLa cell total lysates (treated with DMSO or Taxol) in kinase buffer (27) in the presence of 10 µCi γ-^{32}P-ATP (3000 Ci/mmol, PerkinElmer). The samples were resolved by SDS-PAGE, transferred onto PVDF (Millipore) and visualized by autoradiography followed by Western blotting or detected by phospho-specific antibodies.

Antibodies

Rabbit polyclonal and mouse monoclonal antibodies against human KIBRA have been described (27). The rabbit polyclonal phospho-specific antibody against KIBRA Ser539 has been described (27). Anti-FLAG, anti-HA, and anti-Myc antibodies were from Sigma. Anti-HA and anti-Myc antibodies from Santa Cruz Biotechnology were also used. Anti-β-actin, anti-cyclin B, anti-PP1c (pan), and anti-GFP antibodies were also from Santa Cruz Biotechnology. Mouse monoclonal anti-Aurora-A antibody was from Sigma. Anti-Lats2 was purchased from Bethyl Laboratories (Montgomery, TX). Rabbit polyclonal anti-α-tubulin and mouse monoclonal anti-γ-tubulin were from Abcam (Cambridge, MA). Anti-phospho-Thr288 Aurora-A/Thr232 Aurora-B was from Cell Signaling Technology (Danvers, MA). Mouse monoclonal anti-phospho-Ser83 Lats2 (64) was obtained from Abnova (Taipei, Taiwan). The TAZ (V386) antibody from Cell Signaling Technology was used for Western blotting throughout the study. Rabbit polyclonal phospho-specific antibodies against TAZS90, S105, T326, and T346 were generated and purified by AbMart. Anti-β-actin, anti-GFP, and anti-cyclin B antibodies were from Santa Cruz Biotechnology. Anti-glutathione S-transferase (GST) and anti-His antibodies were from Bethyl Laboratories. Anti-phospho-S10 H3and anti-vimentin antibodies were from Cell Signaling Technology. Anti-E-cadherin antibody was from BD Biosciences. Anti-β-tubulin (Sigma), anti-α-tubulin (Abcam), and anti-γ-tubulin (Biolegend) antibodies were used for immunofluorescence staining.

Immunoprecipitation, Western blot analysis and lambda phosphatase treatment

For Immunoprecipitation, at 48 h after transfection, cells were lysed in radioimmune precipitation assay buffer (150 mM NaCl, 50 mM Tris-HCl, pH 7.4, 1% Nonidet P-40, 0.5% sodium deoxycholate, 0.1% SDS, 1 mM PMSF with protease inhibitor mixture (Roche Applied Science), and phosphatase inhibitors (10 mM pyrophosphate, 10 mM-glycerophosphate, 1.5 mM sodium orthovanadate, and 25 mM sodium fluoride). Proteins were immunoprecipitated with appropriate antibodies and Sepharose 4 Fast Flow Protein G beads (GE Healthcare). The proteins were separated on SDS polyacrylamide gels and transferred onto PVDF membranes (Millipore). HRP-conjugated anti-mouse or anti-rabbit IgG were from Pierce. ECL and SuperSignal West Pico Chemiluminescent substrate kits (Pierce) were used as HRP substrates. For lambda phosphatase treatment, Cells were lysed in Nonidet P-40 buffer (50 mM Tris-HCl, pH 8.0, 150 mM NaCl, and 1% Nonidet P-40). The lysates were treated or not with 400 units (1 ul) lamda phosphatase (P0753, NewEngland Biolabs) in the presence of 1 mM MnCl2 at 30°C for 30 min. A mixed solution of 10 mM sodium orthovanadate and 50 mM sodium fluoride was used as lamda phosphatase inhibitor. The reaction was stopped by the addition of SDS sample buffer followed by 5 min of heating at 95°C.

Immunofluorescence staining

Cells were fixed for 10 min with 100% methanol at −20°C, and then permeabilized with 1% Triton X-100 in PBS for 15 min at room temperature.

Nonspecific epitopes were blocked with 4% BSA in PBS for 1 h. After three washes with PBS (each for 10 min), cells were incubated with the primary antibodies diluted in 4% BSA in PBS for 2 h at room temperature or overnight at 4 °C. Texas Red (GE Healthcare) and/or Alexa Fluor 594-conjugated (Molecular Probes, Eugene, OR) anti-rabbit/mouse IgG were incubated with the cells for 40 min with 4% BSA in PBS at room temperature. After washing the cells three times (each wash for 10 min, with DAPI added in the final wash) with PBS, the stained cells were mounted with Fluoromount (Vector Laboratories, Burlingame, CA) and visualized with an upright, inverted, Axiovert 200 m Zeiss fluorescence microscope (Carl Zeiss, New York, NY). The Slidebook software (version 4.2, Intelligent Imaging Innovations, Denver, CO) was used for analyzing and processing all immunofluorescence images. For phenotypic analysis, we independently analyzed and scored the mitotic defects in each experiment. For peptide blocking, a protocol from Abcam website was used and as we previously described (59).

Soft agar assay, cell migration, and invasion assays

Soft agar assays were conducted in 6-well plates. The base layer of each well consisted of 1.5ml with final concentrations of 1 x media and 1% agarose. Plates were chilled at room temperature until solid, at which point a 2 ml growth medium with 0.5% agarose layer was poured, consisting of cells suspended (MCF10A cells: 5000 cells per well, HPNE cells: $1X10^4$ cells per well). Plates were again chilled at room temperature until the growth layer congealed. A further 1 ml of 1x

culture media without agarose was added on top of the growth layer. The growth medium was changed every week for 3-4 weeks, after which colonies were fixed with 3.7% PFA and stained with 0.005% crystal violet for 1 minute followed by PBS wash for 3 times of 5 minutes each. Data were obtained from three independent experiments.

In vitro analysis of invasion and migration was assessed using the BioCoat invasion system (BD Biosciences) and Transwell system (Corning), respectively, according to the manufacturer's instructions. The cells were trypsinized and resuspended in the medium without serum and/or growth factor at the indicated concentration (MCF10A: $1.0X10^5$/well, HPNE $1.0X10^5$/well for migration assay; MCF10A: $5.0X10^4$/well, HPNE: $5.0X10^4$/well for invasion assay). 600 µl of basal medium with 10%FBS was added to the bottom of the migration assay chamber, and 750 µl for BioCoat invasion chamber. The insert was carefully placed into each well to avoid leaving a bubble between insert and the medium in the bottom chamber. 100 µl or 500 µl of the above mentioned cell suspension was added to the insert for migration and invasion assay, respectively. After the incubation at 37°C for 18 to 24 hours, the plate was removed from the incubator. The cells were fixed with 3.7% PFA and the cells inside the inserts were removed with cotton swabs. Then, the invasive and migratory cells were stained with ProLong® Gold Antifade Reagent with DAPI. The relative invading and migrating rate were calculated by the number of cells invading and migrating through the membrane, divided by the number of cells that invaded and migrated in the control group.

Statistical analysis

Statistical significance was performed using a two-tailed, unpaired Student's t-test. A P value of <0.05 was considered as indicating statistical significance.

1.3 Results

1.3.1 KIBRA Regulates Aurora Kinase Activity and Is Required for Precise Chromosome Alignment During Mitosis.

1.3.1.1 KIBRA activates Aurora kinases and is required for Aurora activation during mitosis

We previously identified Ser539 of KIBRA as a major phosphorylation site for Aurora kinases in mitosis (27). As many Aurora substrates also function as activators of the kinase, we tested whether this is also the case for KIBRA. To this end, we examined Aurora kinase activity by using the phospho-specific antibody against the autophosphorylation sites (Thr288 for Aurora-A, Thr232 for Aurora-B, and Thr198 for Aurora-C). As shown in Fig. 1.1A, overexpression of KIBRA strongly stimulated Aurora-A kinase activation, as indicated by an increase of phosphorylation of Aurora-A on Thr288. As expected, the phosphorylation of Thr288 of Aurora-A-KD (kinase dead/inactive) form was not increased by KIBRA. Interestingly, KIBRA S539A, a mutant that is not phosphorylated by Aurora-A, also promoted the phosphorylation of Aurora-A on Thr288 and did so as well as wild-type KIBRA, suggesting that Aurora-mediated phosphorylation is not required for KIBRA to activate Aurora-A. Similarly, overexpression of KIBRA enhanced the phosphorylation of Aurora-B on Thr232 (Fig. 1.1B). We noticed that there was still some phosphorylation of Thr232 when Aurora-B KD was used (Fig. 1.1B, lanes 4–6), suggesting the existence of another kinase that phosphorylated Aurora-B on Thr232.

The expression of Aurora-A is diminished in interphase cells, whereas Aurora-A is stabilized and activated by phosphorylation during mitosis (61). To further explore the involvement of KIBRA in the activation of Aurora kinase, we established doxycycline-inducible HeLa cells expressing siRNA-resistant KIBRA or KIBRA S539A and employed a double thymidine block to synchronize these cells in mitosis (Fig. 1.1C). As shown in Fig. 1.1D, Aurora kinases were clearly activated in control cells (revealed by an increase of phosphorylation of Aurora-A Thr288 and Aurora-B Thr232) 14 h after being released from the double thymidine block (compare lane 3 with lane 1). However, activation of Aurora kinases is largely diminished in KIBRA knockdown cells at the same time point, indicating that KIBRA is required for full activation of Aurora kinases when cells enter mitosis (Fig. 1.1D, compare lane 6 with lane 3). Aurora-A and cyclin B levels are increased similarly in both control and KIBRA knockdown cells when the cells are released into mitosis, suggesting that KIBRA knockdown did not affect the overall entry into mitosis at the time points examined. Importantly, the defect caused by KIBRA knockdown was completely rescued by re-expression of either siRNA-resistant wild-type KIBRA or KIBRA S539A, further confirming that Aurora-mediated phosphorylation is not required for KIBRA to promote activation of Aurora (Fig. 1.1D, compare lanes 9 and 12 with lane 6). Taken together, the data show KIBRA activates Aurora-A and -B kinases by stimulating their autophosphorylation.

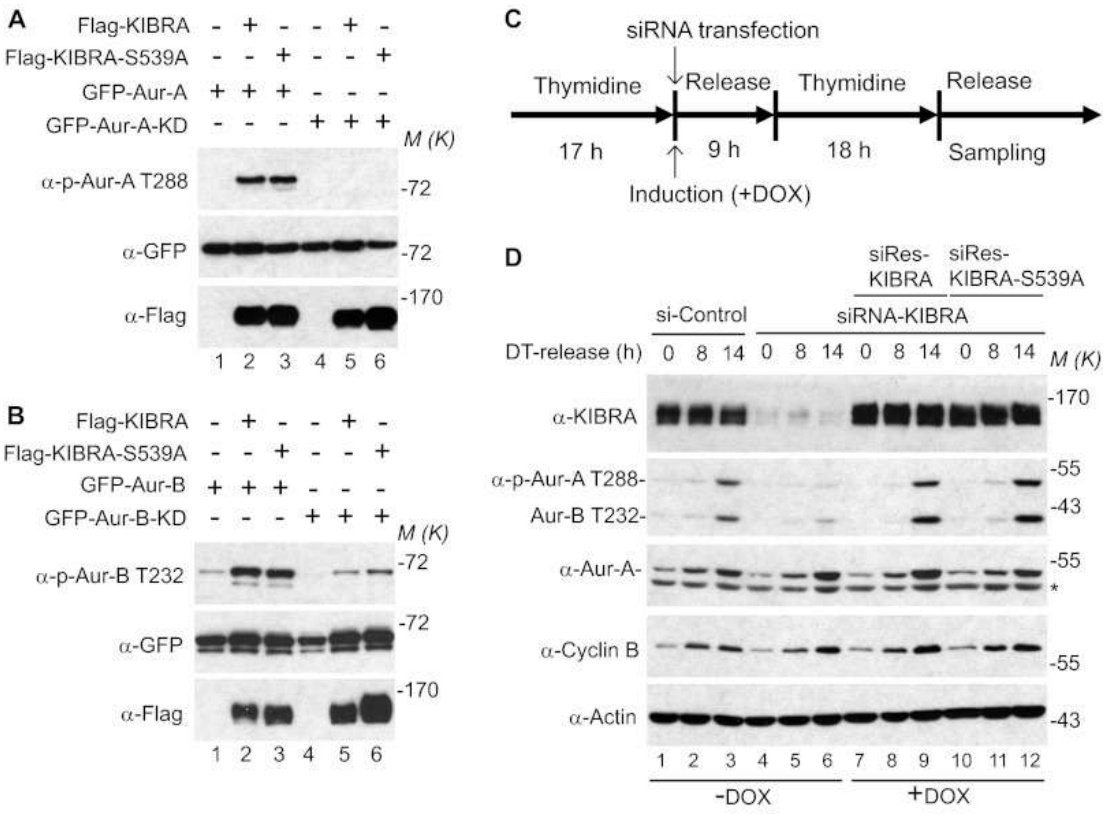

Figure 1.1 KIBRA activates Aurora kinases.

A, various plasmids were transfected into HEK293T cells as indicated. At 48 h after transfection, cells were lysed, and proteins were separated by SDS-PAGE and transferred onto PVDF membranes, followed by Western blot analysis with the indicated antibodies. In all of the figures, M(K) indicates positions where the relevant molecular markers migrated.

B, transfection and Western blotting were done as described in A.

C, schematic diagram for D. Double thymidine block was employed as described under “Materials and Methods.” siRNA transfection and doxycycline (DOX) addition were done after the first thymidine block.

D, the doxycycline-inducible HeLa cell lines expressing siRNA-resistant (siRes) wild-type KIBRA or KIBRA S539A were established, and the cells were treated as described in C. The samples were probed with the indicated antibodies. DT, double thymidine block. The asterisk marks the incompletely stripped actin. Doxycycline (Sigma) was used at 50–100 ng/ml to induce exogenous siRNA-resistant KIBRA. Aur-B, Aurora-B.

1.3.1.2 KIBRA promotes phosphorylation of Lats2 on Ser83 through Aurora-A

Ser83 of Lats2 was shown to be phosphorylated during mitosis by Aurora-A (64). We recently reported that KIBRA associates with both Lats2 (14) and Aurora-A (27). These findings, along with the data from Fig. 1.1, led us to determine whether KIBRA is involved in controlling phosphorylation of Ser83 on Lats2. Figure 1.2A shows that enhanced expression of either KIBRA or KIBRA S539A similarly promoted the phosphorylation of Lats2 on Ser83. However, deletion of the WW domains (which abolishes the interaction between KIBRA and Lats2(14)) did not affect the ability of KIBRA to stimulate the phosphorylation on Ser83 of Lats2. At this point, we reasoned that KIBRA promotes the phosphorylation of Lats2 on Ser83 by activating Aurora-A kinase. To test this hypothesis, we introduced Aurora-A-KD (kinase dead/inactive) or Aurora-A siRNA to determine the role of Aurora-A in mediating the KIBRA-dependent phosphorylation of Lats2 on Ser83. As shown in Fig. 1.2, B and C, overexpression of Aurora-A-KD or knocking down Aurora-A greatly impaired the phosphorylation of Ser83 on Lats2 induced by KIBRA, suggesting that KIBRA promotes Ser83 phosphorylation of Lats2 by activating Aurora-A kinase and that the Aurora-A-KD form has a dominant-negative function. Interestingly, although Aurora-A robustly phosphorylated Lats2 on Ser83 (Fig. 1.2B, lane 3), overexpression of Aurora-B did not increase the phosphorylation of Lats2 on Ser83 and expression of Aurora-B-KD had no effect on the ability of KIBRA to promote Ser83 phosphorylation of Lats2 (Fig. 1.2D).

Because KIBRA, Aurora-A, and Lats2 associate with each other and Aurora-A is required for KIBRA to promote Lats2 phosphorylation, we further explored whether the interaction between KIBRA and Lats2 is Aurora-A-dependent. Surprisingly, neither overexpression of Aurora-A nor Aurora-A knockdown affected the association between KIBRA and Lats2 (Fig. 1.2E). In addition, neither knockdown nor enhanced expression of KIBRA affected the interaction between Lats2 and Aurora-A (Fig. 1.2F). These data suggest that KIBRA, Aurora-A, and Lats2 interact with each other in an independent or mutually exclusive manner.

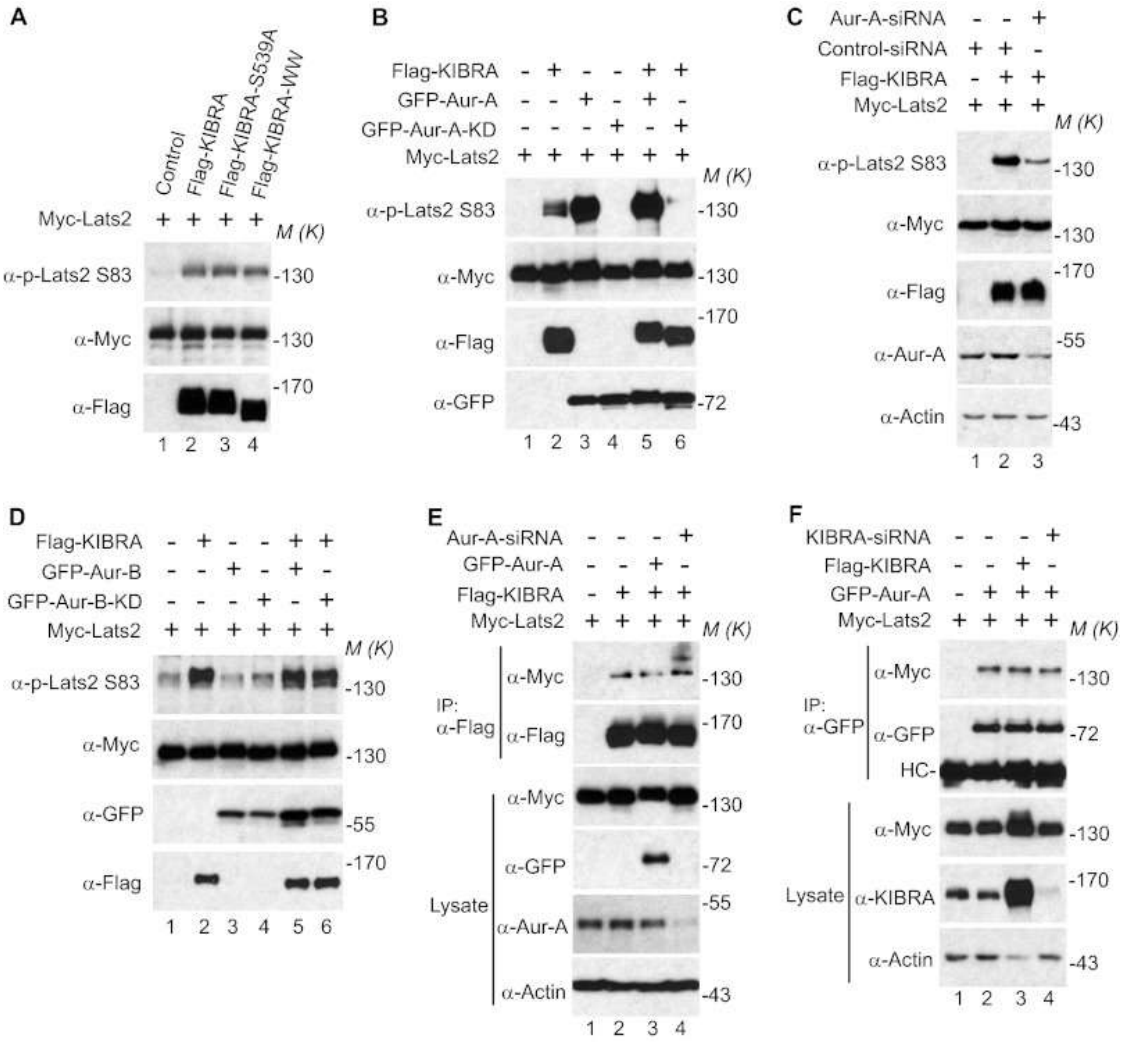

Figure 1.2 KIBRA promotes phosphorylation of Lats2 on Ser83 through Aurora-A.

A, Myc-tagged Lats2 was transfected into HEK293T cells with FLAG-tagged KIBRA or KIBRA mutants as indicated. At 48 h after transfection, cells were lysed, and proteins were immunoprecipitated with Myc antibody followed by Western blot analysis with the indicated antibodies. Lysates were also probed with FLAG antibody to check the expression of transfected KIBRA.

B, HEK293T cells were transiently transfected with plasmids as indicated. At 48 h after transfection, Myc-Lats2 was immunoprecipitated and probed with p-Lats2 Ser83 and Myc antibodies. Lysates without immunoprecipitation were also probed with FLAG and GFP antibodies to check the expression of KIBRA and Aurora-A (Aur-A).

C, HEK293T cells were transiently transfected with control siRNA (lanes 1 and 2) or siRNA against Aurora-A (lane 3) and plasmids as indicated. Immunoprecipitation and Western blotting were done as described in B.

D, transfection, immunoprecipitation, and Western blot analysis were performed as described in B except GFP-Aurora-B and GFP-Aurora-B-KD were used.

E, HEK293T cells were transiently transfected with control siRNA (lanes 1–3) or siRNA against Aurora-A (lane 4) and plasmids as indicated. At 48 h post-transfection, cells were lysed and immunoprecipitated with FLAG antibody. The immunoprecipitates were probed with the indicated antibodies. Total cell lysates were used to check the expression of Aurora-A and Myc-Lats2.

F, HEK293T cells were transiently transfected with control siRNA (lanes 1–3) or siRNA targeting KIBRA and various plasmids as indicated. Cells were harvested at 48 h post-transfection. The immunoprecipitates and total cell lysates without immunoprecipitation were probed with the indicated antibodies. HC, IgG heavy chain. M(K) indicates positions where the relevant molecular markers migrated.

1.3.1.3 Lats2 overexpression enhances KIBRA mobility

During our experiments, we noticed the migration of KIBRA increased on SDS gels when Lats2 was overexpressed ((14); Fig. 1.3A, compare lane 2 with lane 1). The kinase activity and Aurora-A-mediated phosphorylation on Ser83 were not required for this function of Lats2 (Fig. 1.3A, compare lanes 2–4 with lane 1). Interestingly, Lats2, but not Mst1 or its close homolog Lats1, possessed this function (Fig. 1.3A, compare lanes 5 and 6 with lanes 2–4), confirming the specificity. To further explore which domain/region is required for Lats2 to enhance the mobility of KIBRA, we generated a series of truncated Lats2 constructs (Fig. 1.3B). Deletion of the C-terminal 400 amino acids did not significantly alter the ability of Lats2 to enhance the mobility of KIBRA (Fig. 1.3C). However, deletion of an additional 100 amino acids abolished the ability of Lats2 to increase the mobility of KIBRA, suggesting that the region encompassing amino acids 588–689 is required for Lats2 to perform this function. Additional truncated constructs were made with deletions within this region, and our data suggest that the highly conserved region (amino acids 598–619 of human Lats2, Fig. 1.3B) is required for Lats2 to enhance the mobility of KIBRA (Fig. 1.3D). Internal deletion of these 22 amino acids in Lats2 (Lats2Δ22) largely abolished its function to increase KIBRA mobility (Fig. 1.3E).

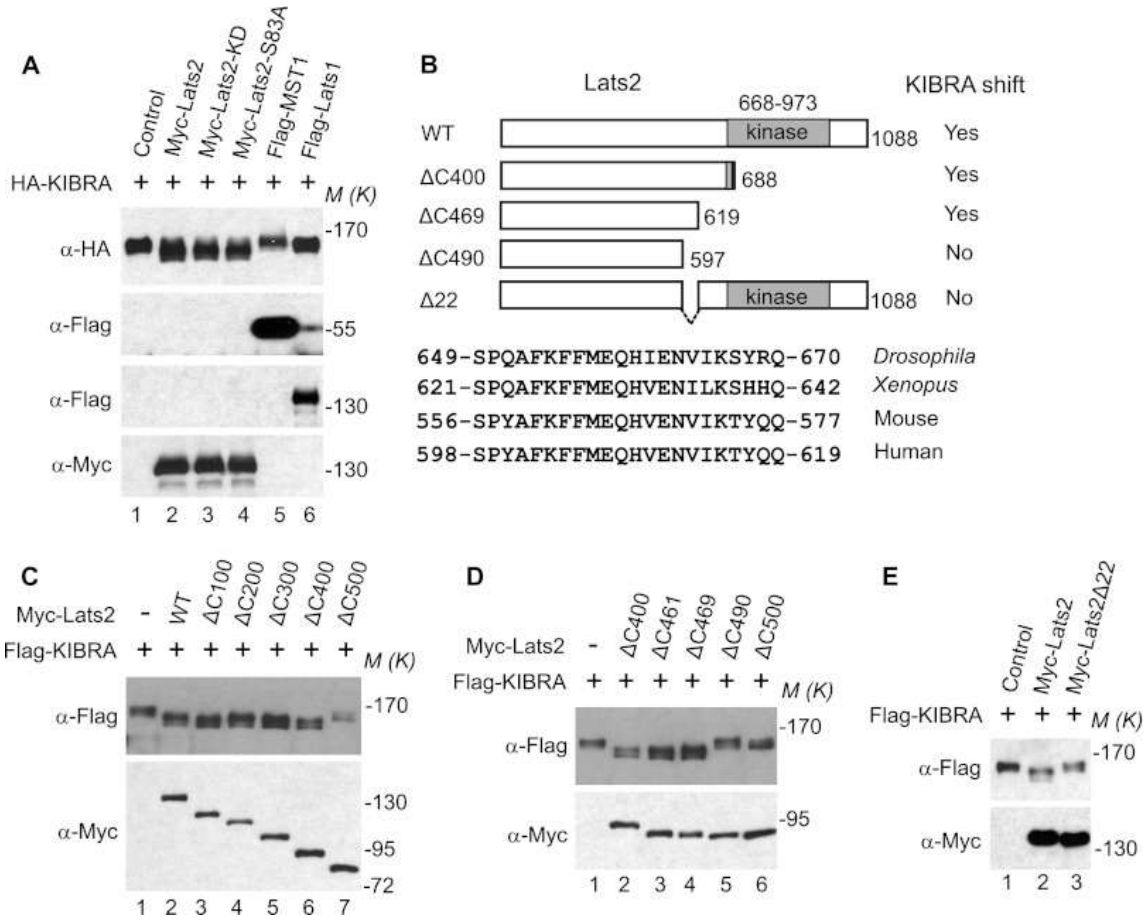

Figure 1.3 Overexpression of Lats2 enhances mobility shift of KIBRA.

A, HA-tagged KIBRA was transfected into HEK293T cells with empty vector or various DNAs as indicated. At 48 h post-transfection, total cell lysates were probed with the indicated antibodies.

B, schematic diagram of various Lats2 constructs used for C--E.

C–E, FLAG-tagged KIBRA was transfected into HEK293T cells with empty vector or plasmids as indicated. At 48 h post-transfection, total cell lysates were probed with the indicated antibodies. M(K) indicates positions where the relevant molecular markers migrated.

1.3.1.4 Lats2 inhibits phosphorylation of KIBRA on Ser539

We previously reported that during mitosis Ser539 of KIBRA is phosphorylated by Aurora kinases and that KIBRA migrates differently on SDS-polyacrylamide gels depending on its phosphorylation status (27). Thus, we tested whether expression of Lats2 might inhibit the phosphorylation of KIBRA using phospho-specific antibodies. Overexpression of Lats2, but not Lats2Δ22, strongly decreased the phosphorylation of KIBRA on Ser539 (Fig. 1.4A). In addition, knockdown of Lats2 increased the phosphorylation of transfected KIBRA on Ser539 (Fig. 1.4B). Taken together, these data suggest that during mitosis Lats2 antagonizes Aurora-mediated phosphorylation of KIBRA on Ser539.

We recently reported that PP1 can dephosphorylate Ser539 of KIBRA (27). Thus, we explored whether PP1 is required for the Lats2-dependent reduction of phosphorylation of KIBRA Ser539. As shown in Fig. 1.4C, in the presence of siRNA against PP1c (catalytic subunit), Lats2 inhibited the phosphorylation of KIBRA on Ser539 less efficiently (compare lane 3 with lane 2), indicating that Lats2 may inhibit KIBRA phosphorylation on Ser539, at least partially through regulating PP1c.

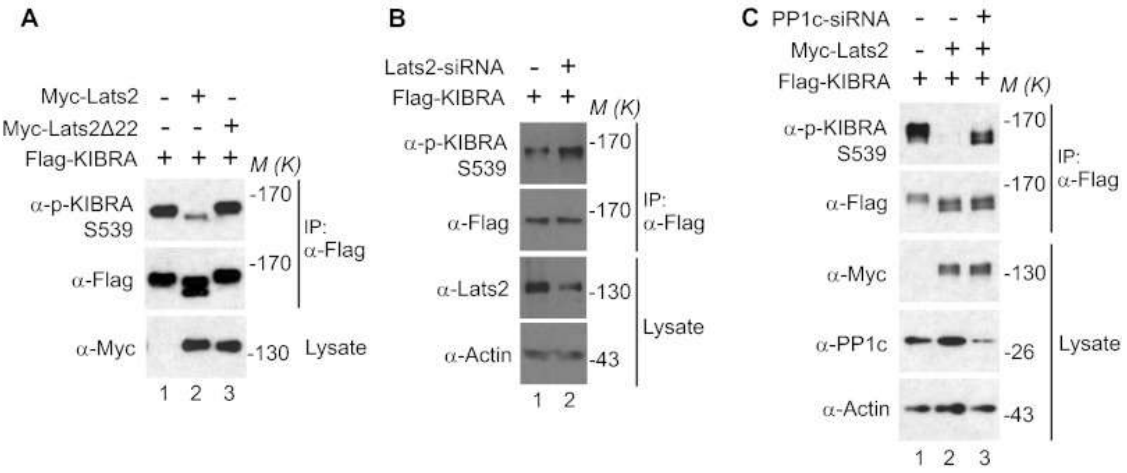

Figure 1.4 Lats2 inhibits the phosphorylation of KIBRA on Ser539 via PP1.

A, HEK293T cells were transfected with FLAG-KIBRA and plasmids as indicated. At 48 h post-transfection, the cells were lysed and immunoprecipitated with FLAG antibody. The immunoprecipitates were probed with anti-phospho-Ser539 KIBRA and subsequent anti-FLAG antibodies.

B, HeLa cells were transfected with FLAG-KIBRA and control siRNA (lane 1) or siRNA against Lats2 (lane 2) for 48 h. FLAG-KIBRA was immunoprecipitated and probed with the indicated antibodies. Total cell lysates without immunoprecipitation were also analyzed.

C, HeLa cells were transfected with control siRNA (lanes 1 and 2) or siRNA targeting PP1 (lane 3) and plasmids as indicated. FLAG-KIBRA was immunoprecipitated and probed with phospho-KIBRA Ser539 and subsequent anti-FLAG antibodies. Total cell lysates without immunoprecipitation were also analyzed. M(K) indicates positions where the relevant molecular markers migrated.

1.3.1.5 KIBRA knockdown causes mitotic defects

We found that KIBRA activates the important mitotic kinase, Aurora-A (Fig. 1.1). Moreover, KIBRA is a verified substrate of both Aurora- A and -B. Therefore, we expected KIBRA to play an important role in the process of mitosis. To test the function of KIBRA in mitosis, we knocked down KIBRA in both MCF-7 and HeLa cells using two different siRNA oligonucleotides. As seen in Fig. 1.5A, 48 h after transfection, both oligonucleotides efficiently depleted KIBRA in HeLa as well as MCF-7 cells. We first depleted KIBRA in MCF-7 cells and used immunofluorescence to identify any mitotic defects. The depletion of KIBRA in MCF-7 cells caused striking defects in spindle assembly (Fig. 1.5B and C) as well as the centrosome number (Fig. 1.5B and D). KIBRA activates Aurora-A and Aurora-A activity is known to be required for proper spindle assembly and centrosome function. Hence, it is likely for these reasons that depleting KIBRA caused defects in spindle assembly and centrosome number. We observed that the knockdown of KIBRA strongly affected the spindle structure (Fig. 1.5B). The spindle microtubules were abnormally organized in KIBRA siRNA cells (Fig. 1.5B, middle panels). Furthermore, the centrosomes appeared fragmented (Fig. 1.5B, lowest panels). About 48% of the cells that were transfected with KIBRA siRNA-1 and 35% of the cells that were transfected with KIBRA siRNA-2 displayed abnormally assembled metaphase spindles (Fig. 1.5C). Furthermore, 38% of the cells that were transfected with KIBRA siRNA-1 and >33% of the cells that were transfected with KIBRA siRNA-2 exhibited defects in centrosome numbers (Fig. 1.5D). These data show that KIBRA plays a crucial role in mitosis by regulating

centrosome function and spindle assembly, possibly via regulating Aurora-A activity.

Because we detected abnormal spindles in KIBRA siRNA MCF-7 cells, we expected that the knockdown of KIBRA would also impair chromosome alignment during mitosis. To test this hypothesis, HeLa cells were transfected with either a scrambled, non-targeting siRNA or with siRNA against KIBRA. Furthermore, these cells were either treated with dimethyl sulfoxide (control) or with monastrol (an Eg5 inhibitor that arrests cells in mitosis). The monastrol was then washed out, and the cells were allowed to proceed normally through mitosis (65, 66). All cells were then subjected to immunofluorescence analysis to visualize abnormalities in chromosome alignment. Remarkably, the depletion of KIBRA from HeLa cells caused the appearance of lagging chromosomes (Fig. 1.6A, panel iv), chromosome bridges (Fig. 1.6A, panel v), and micronuclei (Fig. 1.6A, panel vi) during different stages of mitosis. Additionally, we observed that the knockdown of KIBRA by another siRNA in HeLa cells also yielded abnormal metaphase chromosome alignment (Fig. 1.6B). In addition, we observed that the enrichment of mitotic cells by monastrol treatment further increased the percentage of cells with lagging chromosomes that were obtained upon knockdown of KIBRA (Fig. 1.6C). All these data establish a very important role for KIBRA for the proper progression of mitosis.

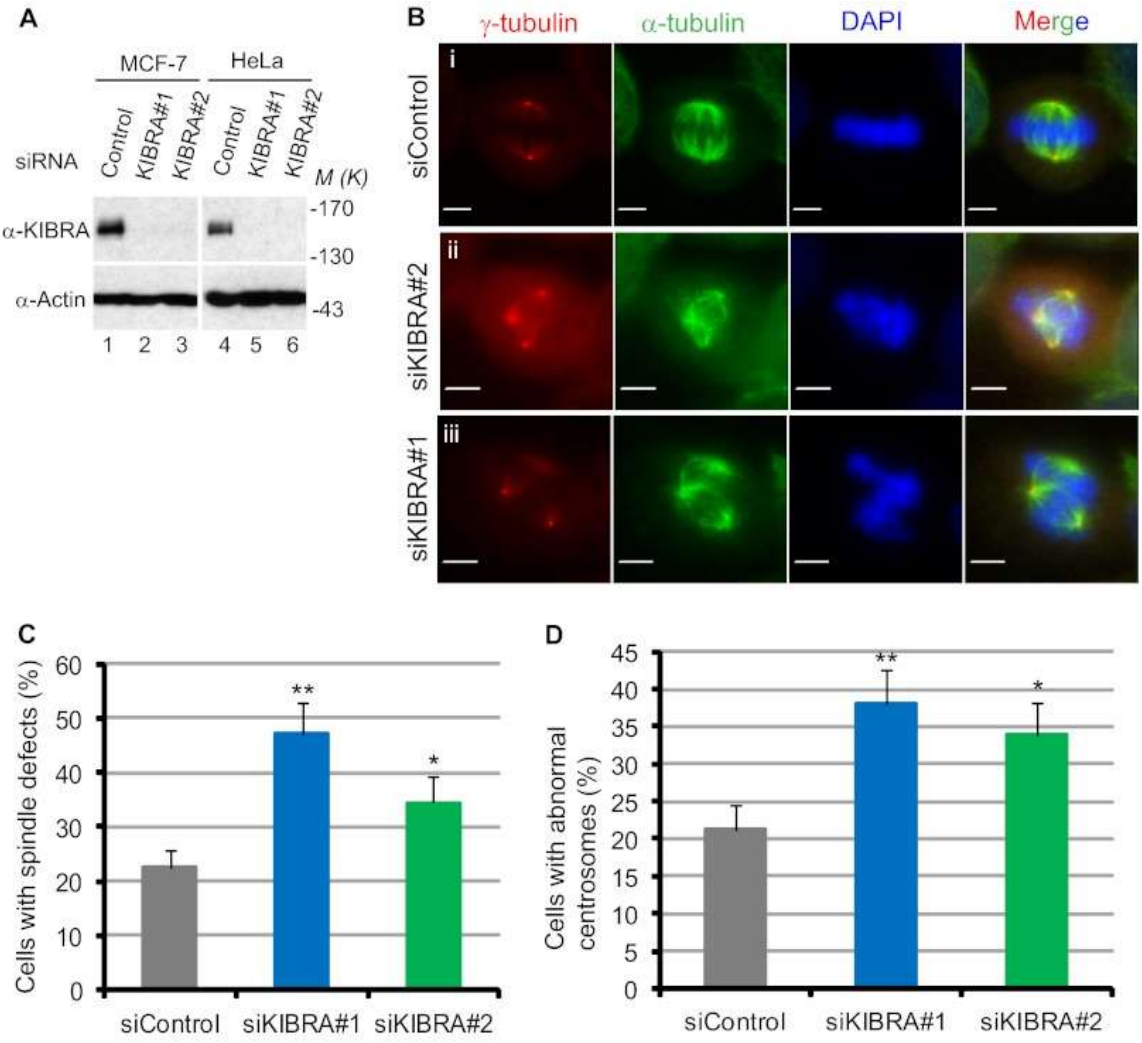

Figure 1.5 KIBRA knockdown causes mitotic defects in MCF-7 cells.

A, MCF-7 and HeLa cells were treated with control siRNA (20 nm, lanes 1 and 4) and siRNA targeting KIBRA (20 nm, lanes 2, 3, 5, and 6) for 48 h, and knockdown efficiency was analyzed by Western blotting.

B, MCF-7 cells were transfected with KIBRA siRNA. At 24–48 h post-transfection, cells were fixed, permeabilized, and stained (see “Experimental Procedures”) with antibodies as indicated. Representative confocal images are shown. Scale bar, 10 μm.

C, quantification of spindle defects in KIBRA knockdown cells. The graph represents the percentage of cells from three independent experiments, and at least 150 mitotic cells were counted in each group. Error bars represent S.E. **, $p < 0.01$; *, $p < 0.05$(t test).

D, quantification of centrosome defects in KIBRA knockdown cells. The graph represents the percentage of cells from three independent experiments, and at least 150 mitotic cells were counted in each group. Error bars represent S.E. **, $p < 0.01$; *, $p < 0.05$(t test). M(K) indicates positions where the relevant molecular markers migrated.

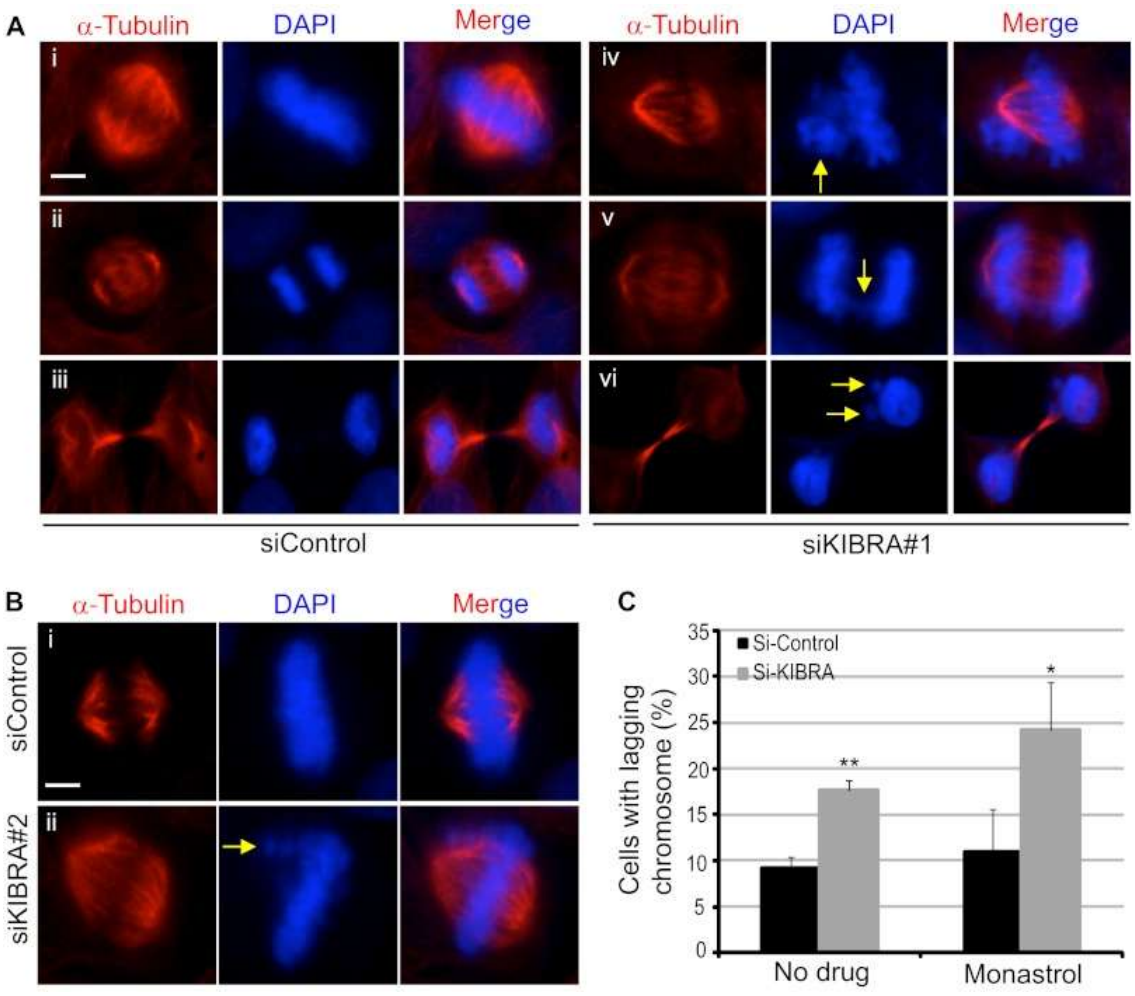

Figure 1.6 KIBRA knockdown causes chromosome misalignment in HeLa cells.

A and B, HeLa cells were transfected with the siRNA oligonucleotides as indicated (20 nm). At 48 h post-transfection, cells were treated with monastrol (an Eg5 inhibitor that arrests cells in mitosis) for 2 h. The monastrol was then washed out, and the cells were allowed to proceed normally through mitosis (65, 66). These cells were then fixed and stained with α-tubulin antibody. DAPI was used to visualize the DNA. Cells at various mitotic phases are shown. Yellow arrows mark the abnormalities in KIBRA knockdown cells. Scale bar, 10 μm.

C, Quantification of chromosome misalignment (lagging chromosome) in KIBRA knockdown cells. The graph represents the percentage of cells from three independent experiments, and at least 150 mitotic cells were counted in each group. Error bars represent S.E. **, $p < 0.01$; *, $p < 0.05$(t test).

1.3.2 CDK1 Phosphorylation of TAZ in Mitosis Inhibits its Oncogenic Activity.

1.3.2.1 TAZ is phosphorylated during anti-mitotic drug-inducedG2/M arrest

We and others showed that TAZ protein is upshifted on SDS-polyacrylamide gels during Taxol or nocodazole (both agents arrest cells in G2/M) -induced mitotic arrest (59, 60). As shown in Figure 7A, the dramatic mobility up-shift of TAZ was readily detected by a phos-tag gel (Fig. 1.7A).Lambda phosphatase treatment converted all slow-migrating bands to fast-migrating bands, confirming that the mobility shift of TAZ during G2/M is caused by phosphorylation (Fig. 1.7B). Since TAZ is a paralog of YAP and mitotic phosphorylation of YAP is mediated by the mitotic kinase CDK1, we tested whether CDK1 is also responsible for TAZ phosphorylation. As shown in Figure 7C, both RO3306 (a CDK1 inhibitor) and Purvalanol A (an inhibitor for CDK1 and other CDKs) completely reverted the mobility shift of TAZ, suggesting that CDK1 is likely to be responsible for TAZ phosphorylation. Inhibition of other mitotic kinases Aurora-A, B, C (with VX-680) and PLK1 (with BI2536) did not alter the TAZ phosphorylation (data not shown).

1.3.2.2 CDK1 phosphorylates TAZ *in vitro*

Next, we determined whether CDK1 kinase can directly phosphorylate TAZ *in vitro* with His-tagged TAZ as substrates. Figure 1.7D shows that Taxol-treated mitotic lysates robustly phosphorylated TAZ and that CDK1 inhibitors greatly reduced phosphorylation of His-TAZ (Fig. 1.7D). Furthermore, purified

CDK1/cyclin B complex phosphorylated His-TAZ *in vitro* (Fig. 1.7E). These results indicate that CDK1 phosphorylated TAZ *in vitro*.

There are a total of six sites that fit the proline-directed consensus sequence of CDK1-phosphorylation sites(67). Two of them (threonine 175 and threonine 285) do not exist in mouse and rat and are excluded for further study. Interestingly, the remaining four sites (serine 90, serine 105, threonine 326, and threonine 346) have been identified as mitotic phosphorylation sites from large scale proteomic studies(68). Mutating these four sites to non-phosphorylatable alanines (TAZ-4A) almost completely abolished the ^{32}P incorporation into TAZ, suggesting that S90, S105, T326 and T346 are the main CDK1 phosphorylation sites (Fig. 1.7F). Metabolic labeling confirmed that wild type TAZ was phosphorylated during Taxol-treatment and TAZ-4A was not able to be further phosphorylated during Taxol-induced G2/M arrest (Fig. 1.7G), indicating that these four sites are the main phosphorylation sites during G2/M in cells.

1.3.2.3 CDK1/cyclin B complex phosphorylates TAZ at S90 and S105 *in vitro*

We have generated phospho-specific antibodies against S90, S105, T326, and T346. Using these antibodies we demonstrated that CDK1 phosphorylated TAZ atS90 and S105 *in vitro* (Fig. 1.7H,I). Addition of RO3306 abolished the phosphorylation (Fig. 1.7H,I). We could not detect a signal when anti-p-TAZ T326 and T346 antibodies were used with these conditions (data not shown).

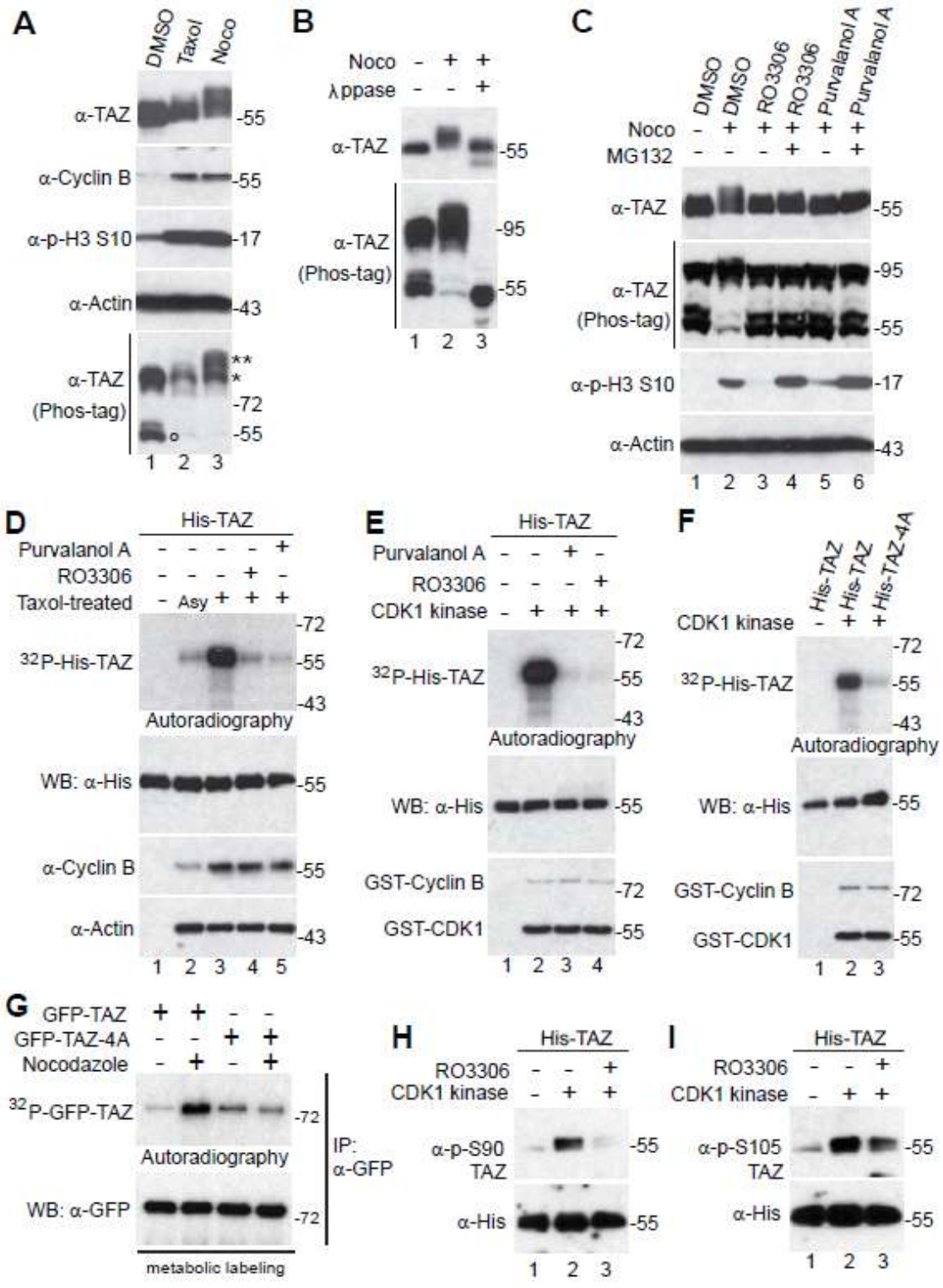
A
DMSO
Taxol
Noco
α-TAZ
-55
α-Cyclin B
-55
α-p-H3 S10
-17
α-Actin
-43
α-TAZ
(Phos-tag)
**
*
o
-72
-55
1 2 3
B
Noco - + +
λppase - - +
α-TAZ
-55
α-TAZ
(Phos-tag)
-95
-55
1 2 3
C
DMSO
DMSO
RO3306
RO3306
Purvalanol A
Purvalanol A
Noco - + + + + +
MG132 - - - + - +
α-TAZ
-55
α-TAZ
(Phos-tag)
-95
-55
α-p-H3 S10
-17
α-Actin
-43
1 2 3 4 5 6
D
His-TAZ
Purvalanol A - - - - +
RO3306 - - - + -
Taxol-treated - Asy + + +
32P-His-TAZ
-72
-55
-43
Autoradiography
WB: α-His
-55
α-Cyclin B
-55
α-Actin
-43
1 2 3 4 5
E
His-TAZ
Purvalanol A - - + -
RO3306 - - - +
CDK1 kinase - + + +
32P-His-TAZ
-72
-55
-43
Autoradiography
WB: α-His
-55
GST-Cyclin B
-72
GST-CDK1
-55
1 2 3 4
F
His-TAZ
His-TAZ
His-TAZ-4A
CDK1 kinase - + +
32P-His-TAZ
-72
-55
-43
Autoradiography
WB: α-His
-55
GST-Cyclin B
-72
GST-CDK1
-55
1 2 3
G
GFP-TAZ + + - -
GFP-TAZ-4A - - + +
Nocodazole - + - +
32P-GFP-TAZ
-72
Autoradiography
WB: α-GFP
-72
IP:
α-GFP
metabolic labeling
H
His-TAZ
RO3306 - - +
CDK1 kinase - + +
α-p-S90
TAZ
-55
α-His
-55
1 2 3
I
His-TAZ
RO3306 - - +
CDK1 kinase - + +
α-p-S105
TAZ
-55
α-His
-55
1 2 3

Figure 1.7 TAZ is phosphorylated by CDK1 during G2/M arrest.

A, HeLa cells were treated with DMSO (control), Taxol (0.1 μM for 16 h) or Nocodazole (Noco, 100 ng/ml for 16 h). Total cell lysates were probed with the indicated antibodies. o marks the non-phosphorylated TAZ; * and ** mark the phosphorylated TAZ.

B, HeLa cells were treated with Nocodazole (Noco) as indicated and cell lysates were further treated with (+) or without (-) λ phosphatase (ppase). Total cell lysates were probed with anti-TAZ antibody.

C, HeLa cells were treated with Nocodazole (Noco). RO3306 (CDK1 inhibitor) or Purvalanol A (CDKs inhibitor) were added (with or without MG132) into the cells 2 h before harvesting the cells. Proteasome inhibitor MG132 was also added (together with inhibitors) to prevent cyclin B from degradation and cells from exiting from mitosis.Total cell lysates were subjected to Western blotting with the indicated antibodies.

D, *In vitro* kinase assays using HeLa cell lysates to phosphorylate recombinant His-TAZ in the presence of ^{32}P. Asy: asynchronized; Tax: Taxol-treated.The samples were also probed with cyclin B and β-actin antibodies.

E, *In vitro* kinase assays with purified CDK1/cyclin B complex. RO3306 (5 μM) or Purvalanol (10 μM) was used to inhibit CDK1 kinase activity.

F, *In vitro* kinase assays with purified CDK1/cyclin B complexto phosphorylate recombinant His-TAZ or His-TAZ-4A.

G, GFP-tagged TAZ or –TAZ-4A were transfected into HeLa cells. At 24 h post-transfection, cells were treated with nocodazole (Noco) for 16 h and metabolically

labeled in the presence of ^{32}P for an additional 2 h as we previously described(58).

H,I, *In vitro* kinase assays were done as in E except anti-phospho-TAZS90 and S105 antibodies were used.

1.3.2.4 Phosphorylation of TAZ occurs in cells during normal mitosis

Next, we performed immunofluorescence microscopy with these phospho-specific antibodies. Strong and specific signals were detected in nocodazole-arrested prometaphase cells for all antibodies against S90, S105, T326, and T346 (Fig. 1.8A-D, top panels, red arrows). Very weak or no signal was detected in interphase cells (Fig. 1.8A-D, yellow arrows). Importantly, phosphopeptide-, but not non-phosphopeptide- (control peptide), incubation largely blocked the signal, suggesting that these antibodies specifically recognize phosphorylated TAZ (Fig. 1.8A-D, middle panels). Addition of RO3306 largely abolished the signals detected by p-TAZS90, S105, T326, and T346 antibodies in prometaphase cells, further indicating that the phosphorylation is CDK1 dependent (Fig. 1.8A-D, low panels).

To further investigate the dynamics of TAZ phosphorylation in cells during unperturbed/normal mitosis, we utilized double thymidine block and release and determined the phospho-status of TAZ during different cell-cycle phases. We found that the p-TAZS90 signal was readily detectable in prophase and peaked in prometaphase/metaphase. The signal was then weakened in anaphase and further diminished in telophase and cytokinesis (Fig. 1.9A). We observed similar staining patterns when the p-TAZ S105, T326, and T346 antibodies were used for staining (Fig. 1.9B,C and data not shown). These data strongly indicate that mitotic phosphorylation of TAZ occurs dynamically in cells.

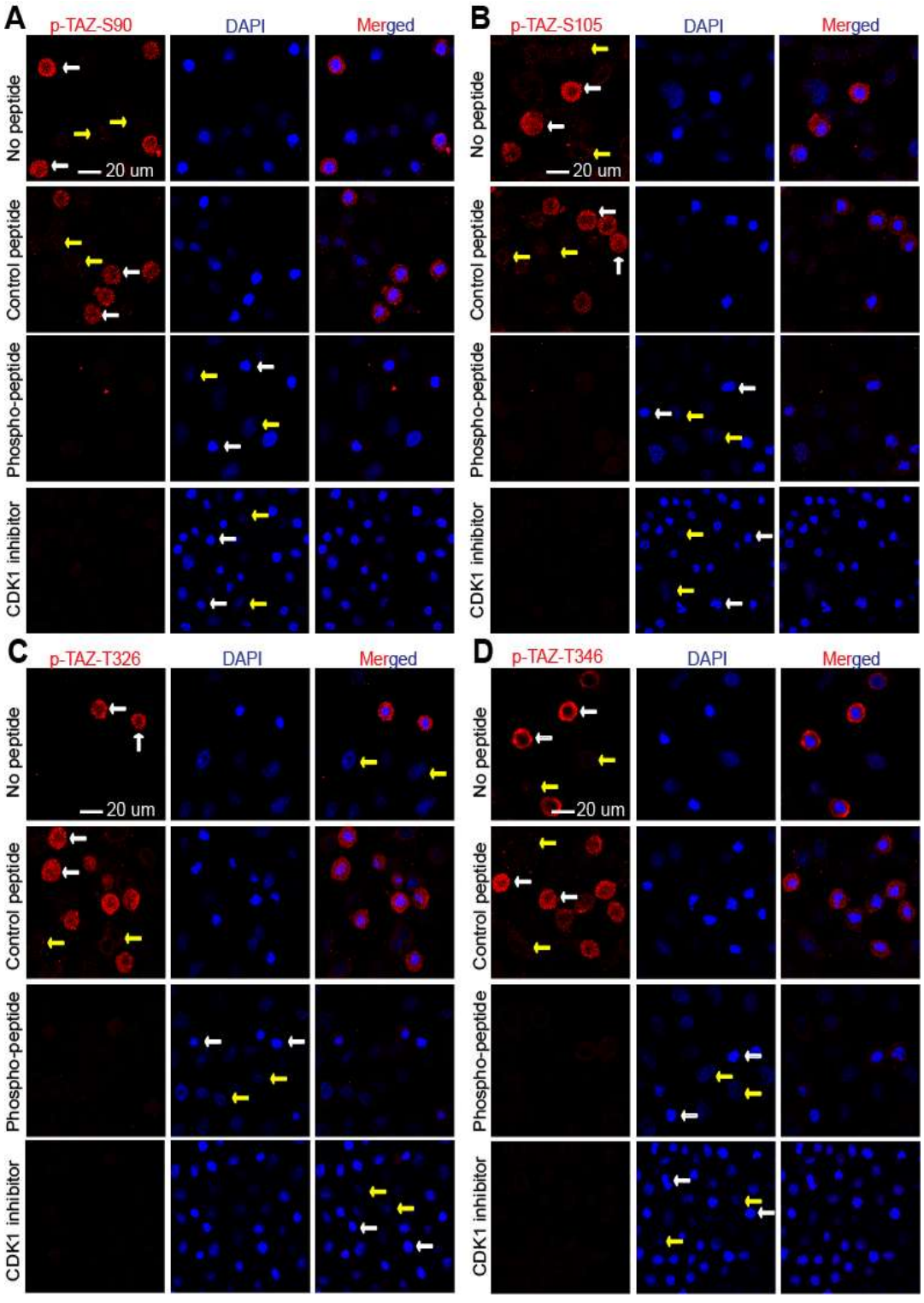
A
p-TAZ-S90
DAPI
Merged
No peptide
20 um
Control peptide
Phospho-peptide
CDK1 inhibitor
B
p-TAZ-S105
DAPI
Merged
No peptide
20 um
Control peptide
Phospho-peptide
CDK1 inhibitor
C
p-TAZ-T326
DAPI
Merged
No peptide
20 um
Control peptide
Phospho-peptide
CDK1 inhibitor
D
p-TAZ-T346
DAPI
Merged
No peptide
20 um
Control peptide
Phospho-peptide
CDK1 inhibitor

Figure 1.8 TAZ is phosphorylated at multiple sites by CDK1 during nocodazole-arrested G2/M phase.

A, HeLa cells were treated with nocodazole for overnight and fixed. The cells were then incubated with or without peptides used for immunonizing rabbits prior to phospho-TAZ S90 staining. CDK1 inhibitor (RO3306) was added 2 h before the cells were fixed (bottom low).

B-D, Similar experiments were done as in A with different phospho-specific antibodies. Red and yellow arrows mark some of the prometaphase cells and the interphase cells, respectively.

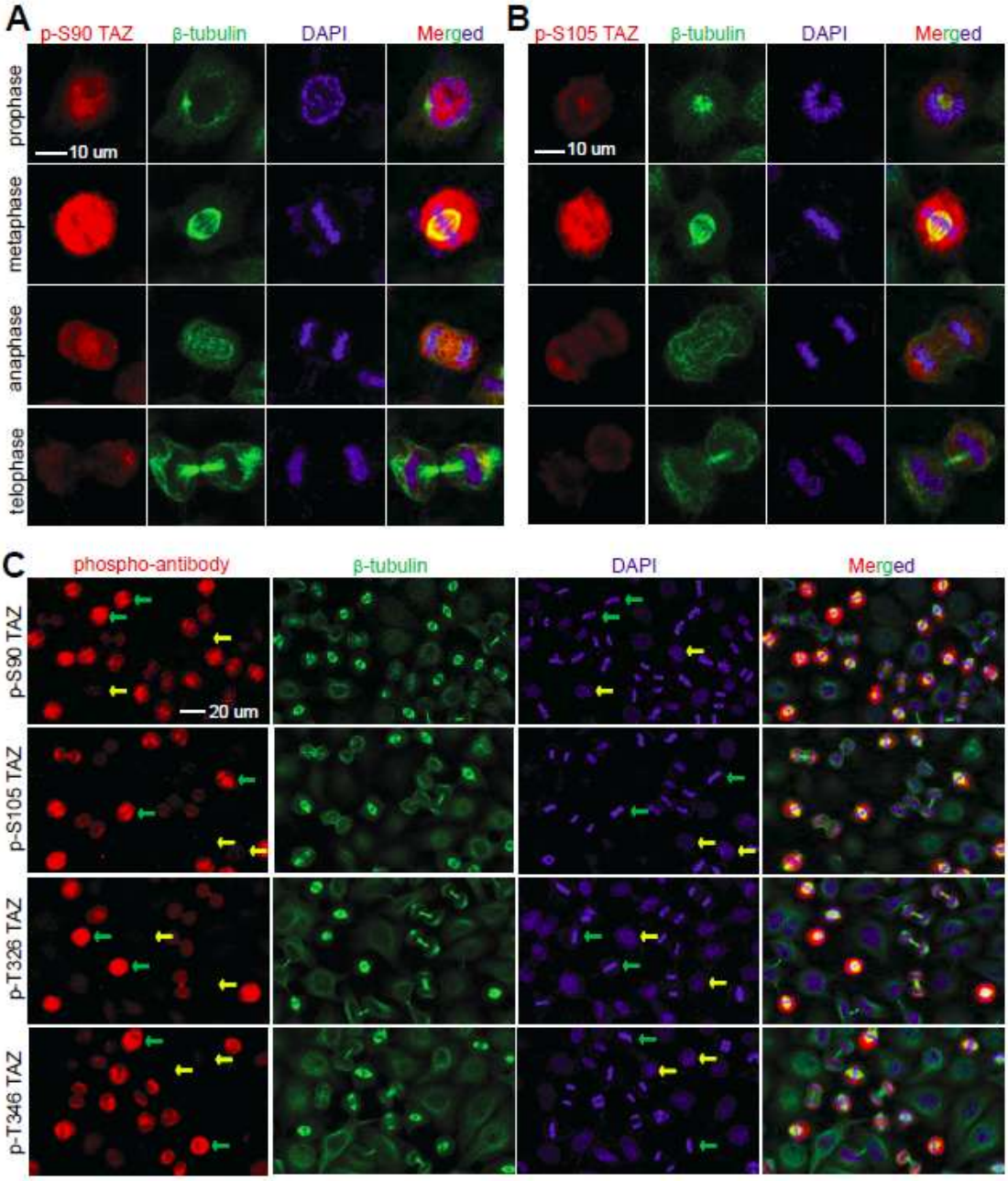

Figure 1.9 TAZ is phosphorylated at S90, S109, T326 and T346 during normal mitosis.

A,B, HeLa cells were synchronized by a double thymidine (DT) block and release method. Cells were stained with p-TAZ S90 (A) and p-TAZS105 (B).Cells were co-stained with DAPI and β-tubulin to indicate the various phases.

C, HeLa cells were synchronized as in (A) and stained with DAPI, phospho-specific antibodies against TAZ, and β-tubulin. A lower power (40X) objective lens was used for photography to view various phases of the cells in a field. Red and yellow arrows in (C) mark the mitotic and interphase cells, respectively.

1.3.2.5 Mitotic phosphorylation inhibits TAZ in EMT and cellular transformation

We next examined the biological significance of mitotic phosphorylation of TAZ. Overexpression of TAZ promotes epithelial-mesenchymal transition (EMT) and transforms MCF10A cells (51, 69). We first established pooled cell lines stably expressing TAZ or TAZ mutants (Fig. 1.10A). We confirmed that the epithelial marker E-cadherin was downregulated and vimentin (a mesenchymal marker) was greatly upregulated in cells expressing active TAZ (TAZ-S89A) (Fig. 1.10A). Interestingly, TAZ-4A (non-mitotic phosphorylatable mutant) possesses higheractivity in regulating EMT in MCF10A cells when compared to wild type TAZ (Fig. 1.10A,B). In contrast, ectopic expression of TAZ-4D (a mitotic phosphomimetic mutant) failed to alter EMT in MCF10A cells (Fig. 1.10A,B). Mutating phosphorylation sites to alanines (TAZ-S89A/4A) further increased TAZ-S89A activity in promoting EMT (Fig. 1.10A,B), suggesting that mitotic phosphorylation inhibits TAZ in EMT. Consistent with the EMT results, we observed significant morphology change of MCF10A cells expressing TAZ-4A, but not vector, wild type TAZ or TAZ-4D (Fig. 1.10C). Again, the most significant change was observed in TAZ-S89A/4A-expressing cells (Fig. 1.10A-C).

MCF10A cells expressing TAZ-S89A/4A formed colonies in soft agar, however, all other cells failed to produce any obvious colonies when fewer cells were seeded (Fig. 1.10D). Again, TAZ-S89A/4Apossesses higher activity compared to TAZ-S89A in stimulating anchorage-independent growth in soft agar (Fig.

1.10E,F). TAZ, TAZ-4A or TAZ-4D overexpression failed to produce colonies in soft agar even when 10,000 cells were seeded (data not shown). Similarly, only TAZ-S89A/4A-expressing HPNE (an immortalized pancreatic epithelial cell line) cells were able to produce colonies in soft agar (Fig. 1.10G-I). Together, these data strongly suggest that mitotic phosphorylation inhibits TAZ-mediated cellular transformation in immortalized epithelial cells.

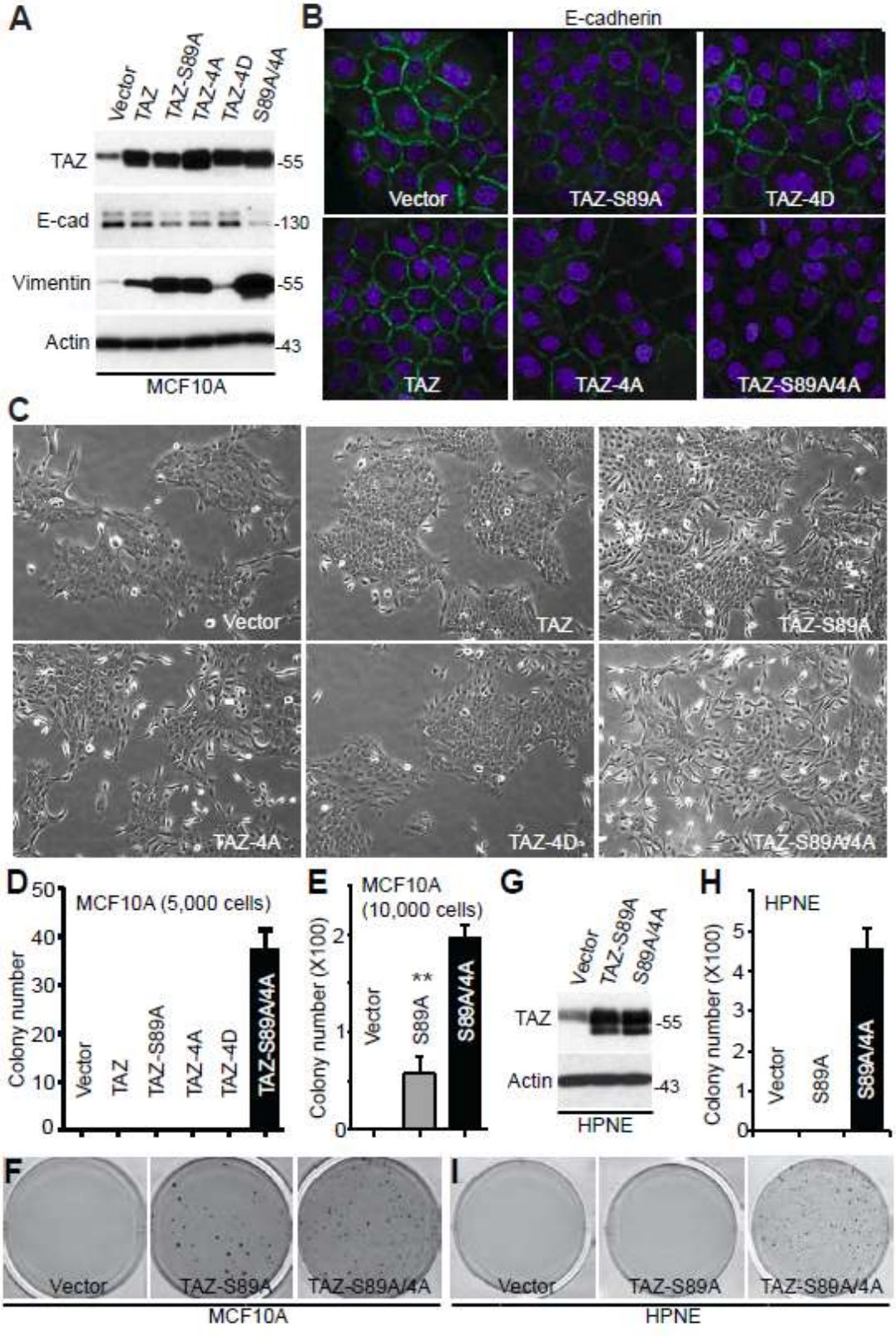
A
Vector
TAZ
TAZ-S89A
TAZ-4A
TAZ-4D
S89A/4A
TAZ
-55
E-cad
-130
Vimentin
-55
Actin
-43
MCF10A
B
E-cadherin
Vector
TAZ-S89A
TAZ-4D
TAZ
TAZ-4A
TAZ-S89A/4A
C
Vector
TAZ
TAZ-S89A
TAZ-4A
TAZ-4D
TAZ-S89A/4A
D
MCF10A (5,000 cells)
Colony number
Vector
TAZ
TAZ-S89A
TAZ-4A
TAZ-4D
TAZ-S89A/4A
E
MCF10A
(10,000 cells)
Colony number (X100)
Vector
**
S89A
S89A/4A
G
Vector
TAZ-S89A
S89A/4A
TAZ
-55
Actin
-43
HPNE
H
HPNE
Colony number (X100)
Vector
S89A
S89A/4A
F
Vector
TAZ-S89A
TAZ-S89A/4A
MCF10A
I
Vector
TAZ-S89A
TAZ-S89A/4A
HPNE

Figure 1.10 Mitotic phosphorylation of TAZ inhibits EMT and anchorage-independent growth.

A, Establishment of MCF10A cells stably express vector, TAZ, TAZ-S89A, TAZ-4A, TAZ-4D, and TAZ-S89A/4A (TAZ-5A).4A: S90A/S105A/T326A/T346A; 5A: S89A/4A; 4D: S90D/S105D/T326D/T346D. The total cell lysates were probed with the indicated antibodies.

B, Immunofluorescence staining with E-cadherin inMCF10A cells established in A.

C, Morphology change of MCF10A cells expressing vector or various TAZ mutants.

D-F, Colony assays in soft agar (anchorage-independent growth) in MCF10A cells established in A.

G, Establishment of HPNE cells stably express vector, TAZ-S89A, TAZ-5A (S89A/4A).

H,I, Colony assays in HPNE cells established in G.

1.3.2.6 Mitotic phosphorylation of TAZ impairs cell motility and transcriptional activity

Several studies showed that TAZ/TAZ-S89A also promotes cell migration, invasion and metastasis in animal (70, 71). We therefore tested whether mitotic phosphorylation affects TAZ's activity in cell motility. As expected, ectopic expression of TAZ or TAZ-S89A increased migration of MCF10A cells assayed by wound healing (Fig. 1.11A). Mutating CDK1-mediated phosphorylation sites to alanines (TAZ-4A) increased migration to a greater extent when compared to wildtype TAZ (Fig. 1.11A). In contrast, cells expressingTAZ-4D possess much lower migratory activity than cells expressing wild type TAZ (Fig. 1.11A). Cells expressing TAZ-S89A/4A migrate the fastest (Fig. 1.11A). We further examined the TAZ activity in invasion using Matrigel. Expression of TAZ-S89A greatly enhanced invasion of both MCF10A (Fig. 1.11B,C) and HPNE (Fig. 1.11D,E) cells. In line with the observations from Fig. 1.10 and Figure 10A, non-mitotic phosphorylatable mutant (TAZ-S89A/4A) further increased the invading activity when compared to TAZ-S89A (Fig. 1.11B-E). Again, TAZ-4D-expressing cells (similar to control cells) possess the lowest activity in invasion (data not shown). Together, these data suggest that mitotic phosphorylation of TAZ inhibits cell motility in immortalized epithelial cells.

TAZ is a transcriptional co-activator, and functions mainly through the TEAD1-4 transcription factors in the Hippo pathway (69, 72, 73). We determined whether mitotic phosphorylation affects TAZ's transcriptional activity using luciferase

reporter assays. As shown in Figure 5F, expression of TAZ-5A (TAZ-S89A/4A) significantly increased the luciferase activity compared with TAZ-S89A (Fig. 1.11F). Expression of TAZ-4D failed to significantly induce TEAD-luciferase activity (data not shown). These results suggest that mitotic phosphorylation impairs TAZ's transcriptional activity. Consistent with these observations, the target genes expression was further induced by overexpression of TAZ-5A when compared with TAZ-S89A (Fig. 1.11G).Collectively, these data strongly indicate that mitotic phosphorylation inhibits TAZ's oncogenic activity.

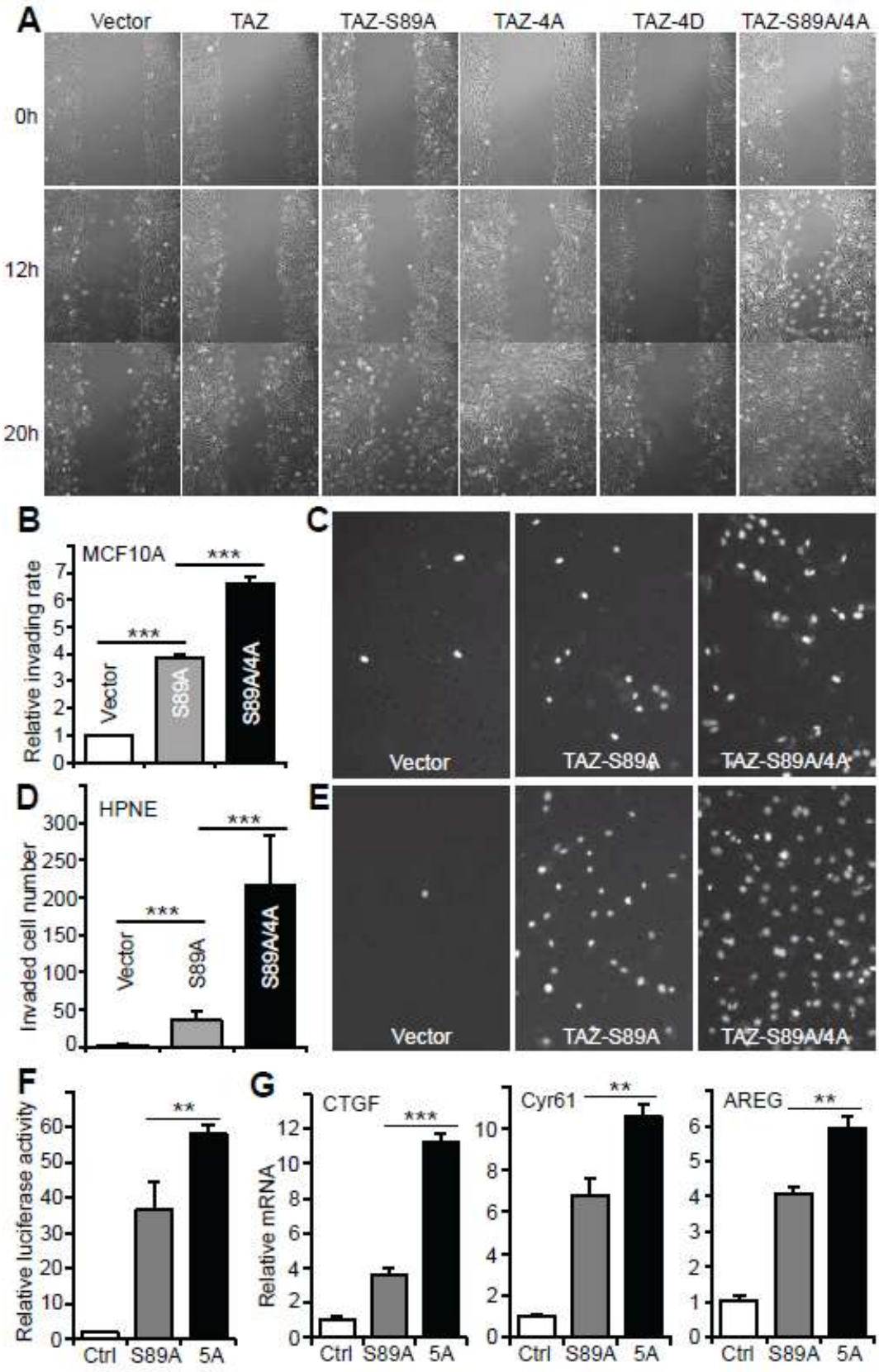
A
Vector
TAZ
TAZ-S89A
TAZ-4A
TAZ-4D
TAZ-S89A/4A
0h
12h
20h
B
MCF10A
Relative invading rate
Vector
S89A
S89A/4A
***
C
Vector
TAZ-S89A
TAZ-S89A/4A
D
HPNE
Invaded cell number
E
F
Relative luciferase activity
**
Ctrl
S89A
5A
G
CTGF
Cyr61
AREG
Relative mRNA

Figure 1.11 Mitotic phosphorylation of TAZ inhibits its oncogenic and transcriptional activity.

A, Wound healing assays in MCF10A cells expressing various TAZ constructs.

B,C, Cell invasion assays with MCF10A cells expressing vector, TAZ-S89A or TAZ-S89A/4A. Invaded cells were stained with DAPI and representative fields were shown (C).

D,E, Cell invasion assays with HPNE cells expressing vector, TAZ-S89A or TAZ-S89A/4A. Invaded cells were stained with DAPI and representative fields were shown (E).

F, Luciferase reporter assays in HEK293T cells. Expression levels of TAZ-S89A and TAZ-S89A/4A are similar in all transfections (data not shown). Ctrl: control (empty vector); 5A: S89A/4A. Data are expressed as the mean ± s.e.m. of three independent experiments (each in triplicate). **: $p<0.01$ (TAZ5A vs TAZ-S89A)(t-test).

G, Quantitative RT-PCR of YAP targets in MCF10A cells expressing vector, TAZ-S89A or TAZ-S89A/4A. Data are expressed as the mean ± s.e.m. of three independent experiments (in duplicate). ***: $p< 0.001$; **: $p< 0.01$ (TAZ5A vs TAZ-S89A) (t-test).

1.3.2.7 Non-phosphorylatable (active) TAZ induces mitotic abnormalities

We next examined whether TAZ or its phosphorylation mutants are able to trigger mitotic defects. MCF10A cells stably expressing vector, TAZ-S89A, and TAZ-5A (TAZ-S89A/4A) were used for this purpose. Consistent with our recent studies, immunofluoresence staining with α-tubulin and γ-tubulin showed normal microtubule/spindle formation and centrosome number during mitosis in most control cells (Fig. 1.12A). In contrast, mitotic abnormalities (disorganization of microtubules and formation of multipolar spindles) were detected in a significantly higher percentage of cells expressing TAZ-S89A, and to a greater extent in TAZ-S89A/4A-expressing cells (Fig. 1.12A,B). Overexpression of TAZ-S89A or TAZ-S89A/4A also induced abnormal centrosome (γ-tubulin staining) number (Fig. 1.12A,C). Not surprisingly, massive chromosome misalignment and chromosome missegregation were observed in a higher percentage of TAZ-S89A- or TAZ-S89A/4A-expressing cells when compared with vector-expressing cells (Fig. 1.12A,D). These data suggest that ectopic expression of non-phosphorylatable (active) TAZ is sufficient to trigger mitotic abnormalities in immortalized epithelial cells.

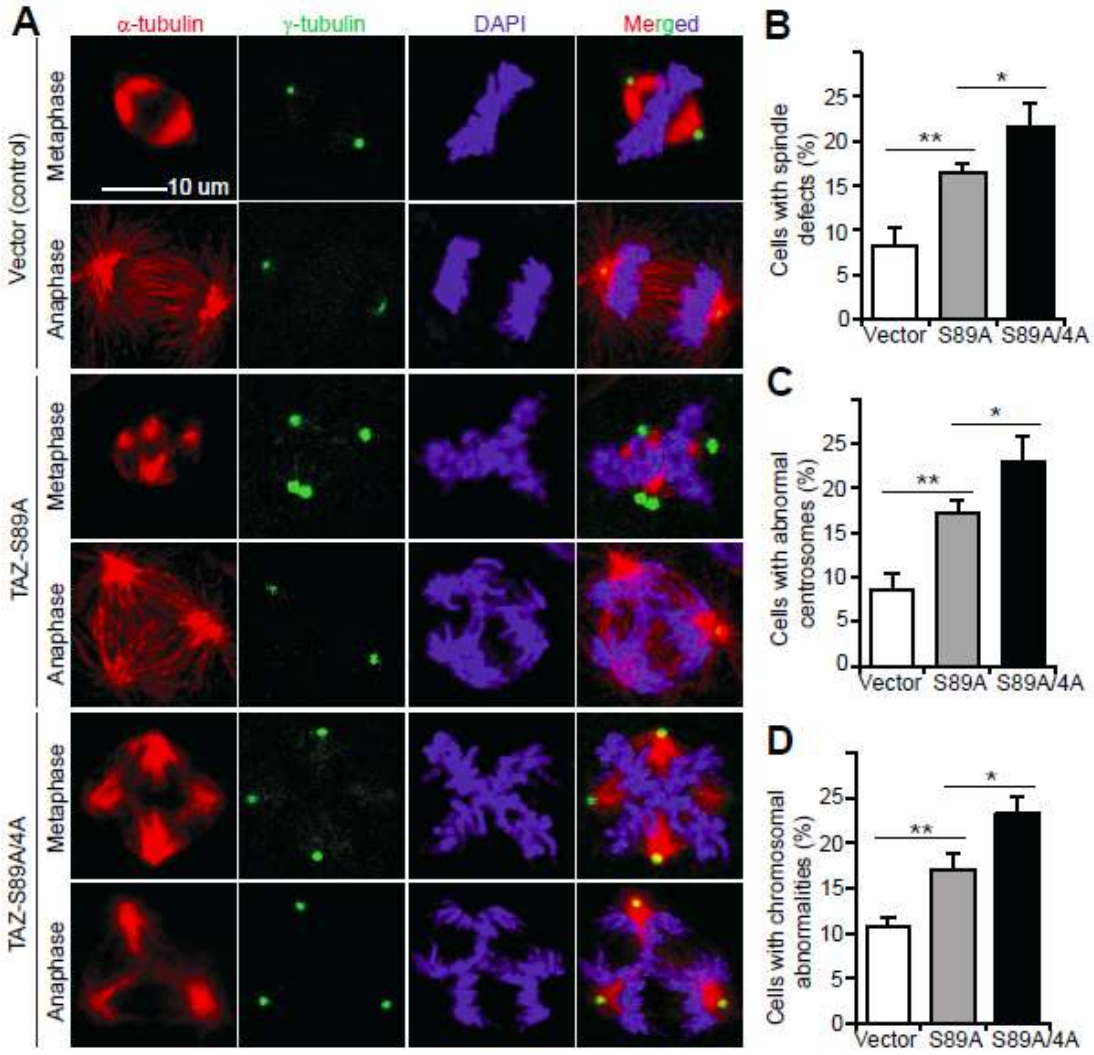

Figure 1.12 Non-phosphorylatable TAZ induces mitotic defects in MCF10A cells.

A, Representative photos of normal mitosis (vector control) and mitotic abnormalities (TAZ-S89A or TAZ-S89A/4A) in MCF10A cells. MCF10A cells stably expressing vector, TAZ-S89A, and TAZ-S89A/4A (TAZ5A) were established at the same time and maintained at similar passage (around 22-24 at the time of experiments conducted).Cells were stained with α-tubulin, γ-tubulin

antibodies and DAPI to visualize microtubules (red), centrosomes (green), and chromosomes (blue), respectively.

B-D, Quantification of mitotic characteristics including microtubule organization/multipolar spindles. (B), centrosome number (C), and chromosome alignment. (D). Data were collected from n=106,185, and 243 mitotic cells for vector control, TAZ-S89A, and TAZ-S89A/4A-expressing cells, respectively. Data were expressed as the mean ± s.e.m. of four independent experiments. **: $p< 0.01$; *: $p<0.05$ (t-test).

Discussion

Aurora kinases are important regulators of cell cycle progression and are potential oncogenes (74, 75). Thus, identification of modulators and/or substrates of Aurora kinases is important for understanding the function and mechanisms of action of Aurora kinase family proteins and the basic principles of cell cycle regulation. In fact, many regulators or substrates of Aurora kinase have been implicated in controlling mitotic entry, chromosome alignment/segregation, and cytokinesis (76). We previously showed that KIBRA is phosphorylated by Aurora kinases in mitosis (27). In the present study, we have further demonstrated that KIBRA is required for full activation of Aurora kinases during mitosis (Fig. 1.1). Future studies are needed to examine whether Aurora-mediated phosphorylation of KIBRA is involved in the mitotic defects induced by knocking down KIBRA.

Both Aurora-A and Lats2 are localized to the centrosome during mitosis, raising the possibility that KIBRA or phosphorylated KIBRA is also localized to this mitotic structure, but this has not been investigated and demonstrated. Interestingly, a previous report showed that KIBRA associates with the microtubule motor protein dynein light chain 1 (24). These findings, along with the demonstration of mitotic defects induced by KIBRA knockdown, strongly suggest that KIBRA may also be required for proper construction of the mitotic apparatus. We are currently investigating the spatial and temporal localization of KIBRA and phosphorylated KIBRA, and such studies are anticipated to further

strengthen the importance of KIBRA in cell cycle progression, especially in mitosis.

The mechanism through which Lats2 regulates KIBRA phosphorylation is currently unknown. Phosphorylation of KIBRA on Ser539 is regulated by Aurora kinase and PP1. Thus, it is possible that overexpression of Lats2 stimulates dephosphorylation of KIBRA by inhibiting Aurora kinase activity and/or activating PP1. However, although we showed that PP1 is required for Lats2 to inhibit phosphorylation of KIBRA on Ser539 (Fig. 1.4), a solid connection between Lats2 and PP1 has not been established. We previously demonstrated that KIBRA also associates with PP1 (27). Therefore, it will be interesting to explore whether Lats2 or Lats2Δ22 affects PP1 activity or the interaction between KIBRA and PP1. Moreover, it is of particular interest to determine the difference between Lats2 and Lats1 with regards to their activity toward inhibiting the phosphorylation of KIBRA.

We noticed that cells with Lats2 knockdown or knock-out also exhibit defects similar to those caused by knocking down KIBRA, including failure of centrosome maturation, spindle disorganization, and chromosome misalignment, which further supports the notion that KIBRA-Aurora-Lats2 may form a novel signaling axis that regulates mitosis. It will be interesting to explore to what extent these

proteins regulate mitosis in a mutually dependent way. Interestingly, recent reports have also connected other members of the Hippo pathway with mitosis. For example, the tumor suppressors Mst1 and Mob1 are involved in centrosome duplication, and Mob1 also localizes to the centrosome during mitosis (77). WW45 and Mst2 control centrosome disjunction and the localization of Nek2 to centrosomes (78). In addition, Mats (*Drosophila* ortholog of Mob1) is required for proper chromosomal segregation in developing embryos (79). Thus, it may be a common feature that Hippo pathway components control mitotic-related events and that deregulation of their function may result in mitotic defects, contributing to genome instability/aneuploidy and subsequent tumorigenesis. One would expect that YAP and TAZ, downstream effectors in the Hippo pathway, may also have a mitotic role. Therefore, it is worth investigating whether Hippo pathway activity is cell cycle-regulated.

Intriguingly, recent studies have shown that most of the Hippo core tumor suppressor proteins, such as Mst1/2, Lats1/2, WW45, Mob1 are involved in regulating mitosis (9, 78, 80, 81). Furthermore, several other regulators of the Hippo pathway, such as Ajuba, Zyxin, as well as the effector YAP are known to be regulated (phosphorylated) during mitosis and they all play a role in mitotic progression (27, 58, 59, 61, 82-86). Therefore, these studies suggest that the Hippo-YAP/TAZ pathway ensures normal mitosis and deregulation of the pathway causes mitotic aberrations and tumorigenesis.

Upon treatment with anti-microtubule agents including Taxol, YAP (59, 60) and KIBRA (27, 58) are phosphorylated by mitotic kinases independently of the Hippo pathway. Another prominent change is the marked increase of Lats2 proteins in response to Taxol treatment (59, 87). Interestingly, induction of Lats2 and phosphorylation of YAP regulate Taxol-sensitivity in cancer cells (60, 87). Furthermore, TAZ and its downstream targets Cyr61 and CTGF have been shown to be important regulators for Taxol-resistance in breast cancer cells (60). Our current studies showed that TAZ is phosphorylated during Taxol treatment and this phosphorylation inhibits its transcriptional activity (Figs. 1.7,11). Taxol (trademark: Paclitaxel) is widely used for treating breast and ovarian cancer patients and drug-resistance is one of the major clinical challenges. Therefore, it will be interesting to determine the role of mitotic phosphorylation of TAZ in mediating anti-Taxol drug resistance.

Although recent studies have demonstrated the important roles for TAZ in promoting tumorigenesis, the underlying mechanisms are largely unclear. The current study identified novel phosphorylation of TAZ during mitosis and importantly, the mitotic phosphorylation regulates TAZ's oncogenic activity (Figs. 1.10,11). Interestingly, TAZ-5A (a non-phosphorylatable mutant), but not TAZ-4D (L.Z. and J.D., unpublished observations), drives massive mitotic defects (Fig. 1.12). Thus, TAZ may contribute to cancer development by regulating mitosis-related events, since aberration of mitosis often causes genome instability/aneuploidy and subsequent tumor formation (88).

Our data not only reveal a new layer of regulation for TAZ's oncogenic activity, but also highlight a previously unrecognized mechanism through which TAZ exerts its oncogenic function. We found that mitotic phosphorylation did not affect TAZ's binding with the major transcription factor TEAD1 and Lats2 kinase (L.Z. and J.D., unpublished observations). Thus, it is not clear how CDK1 phosphorylation of TAZ increases its transcriptional activity. Does this phosphorylation regulate TAZ's transcriptional activity with other transcription factors? We recently found that YAP (a paralog of TAZ) is required for the spindle checkpoint activation induced by Taxol (82). YAP regulates the spindle checkpoint through upregulating the spindle checkpoint protein BubR1 in a mitotic phosphorylation-dependent manner (82). Since the spindle checkpoint is a surveillance mechanism in mitosis (89), these studies suggest that YAP and its mitotic phosphorylation trigger mitotic defects through the dysregulation of the spindle checkpoint machinery. Surprisingly, knockdown of TAZ had no effects on the spindle checkpoint activation and mitotic arrest in the presence of anti-mitotic agents (L.Z. and J.D., unpublished observations), suggesting a distinct function of TAZ and YAP in mitosis. Future studies are needed to address how TAZ and its mitotic phosphorylation are involved in mitosis and how they promote the mitotic defects. Furthermore, mitotic phosphorylation activates YAP (59) and in contrast, TAZ is inhibited by mitotic phosphorylation regarding their oncogenic activity (Figs. 1.10,11). It is currently not known how TAZ and YAP achieved opposite regulation (negatively and positively, respectively) during mitosis by the same kinase.

References

1. Storchova Z, and Pellman D. From polyploidy to aneuploidy, genome instability and cancer. *Nature reviews Molecular cell biology.* 2004;5(1):45-54.
2. Musacchio A, and Salmon ED. The spindle-assembly checkpoint in space and time. *Nature reviews Molecular cell biology.* 2007;8(5):379-93.
3. Jackson JR, Patrick DR, Dar MM, and Huang PS. Targeted anti-mitotic therapies: can we improve on tubulin agents? *Nature reviews Cancer.* 2007;7(2):107-17.
4. Janssen A, and Medema RH. Mitosis as an anti-cancer target. *Oncogene.* 2011;30(25):2799-809.
5. Jordan MA, and Wilson L. Microtubules as a target for anticancer drugs. *Nature reviews Cancer.* 2004;4(4):253-65.
6. Zhao B, Li L, Lei Q, and Guan KL. The Hippo-YAP pathway in organ size control and tumorigenesis: an updated version. *Genes & development.* 2010;24(9):862-74.
7. Pan D. The hippo signaling pathway in development and cancer. *Developmental cell.* 2010;19(4):491-505.
8. Halder G, and Johnson RL. Hippo signaling: growth control and beyond. *Development.* 2011;138(1):9-22.
9. Hergovich A, and Hemmings BA. Hippo signalling in the G2/M cell cycle phase: lessons learned from the yeast MEN and SIN pathways. *Seminars in cell & developmental biology.* 2012;23(7):794-802.

10. Kremerskothen J, Plaas C, Buther K, Finger I, Veltel S, Matanis T, Liedtke T, and Barnekow A. Characterization of KIBRA, a novel WW domain-containing protein. *Biochemical and biophysical research communications.* 2003;300(4):862-7.

11. Genevet A, Wehr MC, Brain R, Thompson BJ, and Tapon N. Kibra is a regulator of the Salvador/Warts/Hippo signaling network. *Developmental cell.* 2010;18(2):300-8.

12. Baumgartner R, Poernbacher I, Buser N, Hafen E, and Stocker H. The WW domain protein Kibra acts upstream of Hippo in Drosophila. *Developmental cell.* 2010;18(2):309-16.

13. Yu J, Zheng Y, Dong J, Klusza S, Deng WM, and Pan D. Kibra functions as a tumor suppressor protein that regulates Hippo signaling in conjunction with Merlin and Expanded. *Developmental cell.* 2010;18(2):288-99.

14. Xiao L, Chen Y, Ji M, and Dong J. KIBRA regulates Hippo signaling activity via interactions with large tumor suppressor kinases. *The Journal of biological chemistry.* 2011;286(10):7788-96.

15. Schneider A, Huentelman MJ, Kremerskothen J, Duning K, Spoelgen R, and Nikolich K. KIBRA: A New Gateway to Learning and Memory? *Frontiers in aging neuroscience.* 2010;2(4.

16. Schaper K, Kolsch H, Popp J, Wagner M, and Jessen F. KIBRA gene variants are associated with episodic memory in healthy elderly. *Neurobiology of aging.* 2008;29(7):1123-5.

17. Bates TC, Price JF, Harris SE, Marioni RE, Fowkes FG, Stewart MC, Murray GD, Whalley LJ, Starr JM, and Deary IJ. Association of KIBRA and memory. *Neuroscience letters.* 2009;458(3):140-3.

18. Almeida OP, Schwab SG, Lautenschlager NT, Morar B, Greenop KR, Flicker L, and Wildenauer D. KIBRA genetic polymorphism influences episodic memory in later life, but does not increase the risk of mild cognitive impairment. *Journal of cellular and molecular medicine.* 2008;12(5A):1672-6.

19. Papassotiropoulos A, Stephan DA, Huentelman MJ, Hoerndli FJ, Craig DW, Pearson JV, Huynh KD, Brunner F, Corneveaux J, Osborne D, et al. Common Kibra alleles are associated with human memory performance. *Science.* 2006;314(5798):475-8.

20. Makuch L, Volk L, Anggono V, Johnson RC, Yu Y, Duning K, Kremerskothen J, Xia J, Takamiya K, and Huganir RL. Regulation of AMPA receptor function by the human memory-associated gene KIBRA. *Neuron.* 2011;71(6):1022-9.

21. Duning K, Schurek EM, Schluter M, Bayer M, Reinhardt HC, Schwab A, Schaefer L, Benzing T, Schermer B, Saleem MA, et al. KIBRA modulates directional migration of podocytes. *Journal of the American Society of Nephrology : JASN.* 2008;19(10):1891-903.

22. Rosse C, Formstecher E, Boeckeler K, Zhao Y, Kremerskothen J, White MD, Camonis JH, and Parker PJ. An aPKC-exocyst complex controls

paxillin phosphorylation and migration through localised JNK1 activation. *PLoS biology.* 2009;7(11):e1000235.

23. Yoshihama Y, Sasaki K, Horikoshi Y, Suzuki A, Ohtsuka T, Hakuno F, Takahashi S, Ohno S, and Chida K. KIBRA suppresses apical exocytosis through inhibition of aPKC kinase activity in epithelial cells. *Current biology : CB.* 2011;21(8):705-11.

24. Rayala SK, den Hollander P, Manavathi B, Talukder AH, Song C, Peng S, Barnekow A, Kremerskothen J, and Kumar R. Essential role of KIBRA in co-activator function of dynein light chain 1 in mammalian cells. *The Journal of biological chemistry.* 2006;281(28):19092-9.

25. Hill VK, Dunwell TL, Catchpoole D, Krex D, Brini AT, Griffiths M, Craddock C, Maher ER, and Latif F. Frequent epigenetic inactivation of KIBRA, an upstream member of the Salvador/Warts/Hippo (SWH) tumor suppressor network, is associated with specific genetic event in B-cell acute lymphocytic leukemia. *Epigenetics : official journal of the DNA Methylation Society.* 2011;6(3):326-32.

26. Shinawi T, Hill V, Dagklis A, Baliakas P, Stamatopoulos K, Agathanggelou A, Stankovic T, Maher ER, Ghia P, and Latif F. KIBRA gene methylation is associated with unfavorable biological prognostic parameters in chronic lymphocytic leukemia. *Epigenetics : official journal of the DNA Methylation Society.* 2012;7(3):211-5.

27. Xiao L, Chen Y, Ji M, Volle DJ, Lewis RE, Tsai MY, and Dong J. KIBRA protein phosphorylation is regulated by mitotic kinase aurora and protein

phosphatase 1. *The Journal of biological chemistry.* 2011;286(42):36304-15.

28. Kanai F, Marignani PA, Sarbassova D, Yagi R, Hall RA, Donowitz M, Hisaminato A, Fujiwara T, Ito Y, Cantley LC, et al. TAZ: a novel transcriptional co-activator regulated by interactions with 14-3-3 and PDZ domain proteins. *The EMBO journal.* 2000;19(24):6778-91.
29. Piccolo S, Dupont S, and Cordenonsi M. The biology of YAP/TAZ: hippo signaling and beyond. *Physiological reviews.* 2014;94(4):1287-312.
30. Mo JS, Park HW, and Guan KL. The Hippo signaling pathway in stem cell biology and cancer. *EMBO reports.* 2014;15(6):642-56.
31. Moroishi T, Hansen CG, and Guan KL. The emerging roles of YAP and TAZ in cancer. *Nature reviews Cancer.* 2015;15(2):73-9.
32. Chan SW, Lim CJ, Guo K, Ng CP, Lee I, Hunziker W, Zeng Q, and Hong W. A role for TAZ in migration, invasion, and tumorigenesis of breast cancer cells. *Cancer research.* 2008;68(8):2592-8.
33. Cordenonsi M, Zanconato F, Azzolin L, Forcato M, Rosato A, Frasson C, Inui M, Montagner M, Parenti AR, Poletti A, et al. The Hippo transducer TAZ confers cancer stem cell-related traits on breast cancer cells. *Cell.* 2011;147(4):759-72.
34. Dong J, Feldmann G, Huang J, Wu S, Zhang N, Comerford SA, Gayyed MF, Anders RA, Maitra A, and Pan D. Elucidation of a universal size-control mechanism in Drosophila and mammals. *Cell.* 2007;130(6):1120-33.

35. Azzolin L, Zanconato F, Bresolin S, Forcato M, Basso G, Bicciato S, Cordenonsi M, and Piccolo S. Role of TAZ as mediator of Wnt signaling. *Cell.* 2012;151(7):1443-56.

36. Wang L, Shi S, Guo Z, Zhang X, Han S, Yang A, Wen W, and Zhu Q. Overexpression of YAP and TAZ is an independent predictor of prognosis in colorectal cancer and related to the proliferation and metastasis of colon cancer cells. *PloS one.* 2013;8(6):e65539.

37. Yuen HF, McCrudden CM, Huang YH, Tham JM, Zhang X, Zeng Q, Zhang SD, and Hong W. TAZ expression as a prognostic indicator in colorectal cancer. *PloS one.* 2013;8(1):e54211.

38. Noguchi S, Saito A, Horie M, Mikami Y, Suzuki HI, Morishita Y, Ohshima M, Abiko Y, Mattsson JS, Konig H, et al. An integrative analysis of the tumorigenic role of TAZ in human non-small cell lung cancer. *Clinical cancer research : an official journal of the American Association for Cancer Research.* 2014;20(17):4660-72.

39. Lau AN, Curtis SJ, Fillmore CM, Rowbotham SP, Mohseni M, Wagner DE, Beede AM, Montoro DT, Sinkevicius KW, Walton ZE, et al. Tumor-propagating cells and Yap/Taz activity contribute to lung tumor progression and metastasis. *The EMBO journal.* 2014;33(5):468-81.

40. Xie M, Zhang L, He CS, Hou JH, Lin SX, Hu ZH, Xu F, and Zhao HY. Prognostic significance of TAZ expression in resected non-small cell lung cancer. *Journal of thoracic oncology : official publication of the International Association for the Study of Lung Cancer.* 2012;7(5):799-807.

41. Bhat KP, Salazar KL, Balasubramaniyan V, Wani K, Heathcock L, Hollingsworth F, James JD, Gumin J, Diefes KL, Kim SH, et al. The transcriptional coactivator TAZ regulates mesenchymal differentiation in malignant glioma. *Genes & development.* 2011;25(24):2594-609.

42. Johnson R, and Halder G. The two faces of Hippo: targeting the Hippo pathway for regenerative medicine and cancer treatment. *Nature reviews Drug discovery.* 2014;13(1):63-79.

43. Overholtzer M, Zhang J, Smolen GA, Muir B, Li W, Sgroi DC, Deng CX, Brugge JS, and Haber DA. Transforming properties of YAP, a candidate oncogene on the chromosome 11q22 amplicon. *Proceedings of the National Academy of Sciences of the United States of America.* 2006;103(33):12405-10.

44. Tanas MR, Sboner A, Oliveira AM, Erickson-Johnson MR, Hespelt J, Hanwright PJ, Flanagan J, Luo Y, Fenwick K, Natrajan R, et al. Identification of a disease-defining gene fusion in epithelioid hemangioendothelioma. *Science translational medicine.* 2011;3(98):98ra82.

45. Errani C, Zhang L, Sung YS, Hajdu M, Singer S, Maki RG, Healey JH, and Antonescu CR. A novel WWTR1-CAMTA1 gene fusion is a consistent abnormality in epithelioid hemangioendothelioma of different anatomic sites. *Genes, chromosomes & cancer.* 2011;50(8):644-53.

46. Varelas X, Sakuma R, Samavarchi-Tehrani P, Peerani R, Rao BM, Dembowy J, Yaffe MB, Zandstra PW, and Wrana JL. TAZ controls Smad

nucleocytoplasmic shuttling and regulates human embryonic stem-cell self-renewal. *Nature cell biology.* 2008;10(7):837-48.

47. Wang Q, Xu Z, An Q, Jiang D, Wang L, Liang B, and Li Z. TAZ promotes epithelial to mesenchymal transition via the upregulation of connective tissue growth factor expression in neuroblastoma cells. *Molecular medicine reports.* 2015;11(2):982-8.

48. Pan D. Hippo signaling in organ size control. *Genes & development.* 2007;21(8):886-97.

49. Harvey KF, Zhang X, and Thomas DM. The Hippo pathway and human cancer. *Nature reviews Cancer.* 2013;13(4):246-57.

50. Zhao B, Tumaneng K, and Guan KL. The Hippo pathway in organ size control, tissue regeneration and stem cell self-renewal. *Nature cell biology.* 2011;13(8):877-83.

51. Lei QY, Zhang H, Zhao B, Zha ZY, Bai F, Pei XH, Zhao S, Xiong Y, and Guan KL. TAZ promotes cell proliferation and epithelial-mesenchymal transition and is inhibited by the hippo pathway. *Molecular and cellular biology.* 2008;28(7):2426-36.

52. Liu CY, Zha ZY, Zhou X, Zhang H, Huang W, Zhao D, Li T, Chan SW, Lim CJ, Hong W, et al. The hippo tumor pathway promotes TAZ degradation by phosphorylating a phosphodegron and recruiting the SCF{beta}-TrCP E3 ligase. *The Journal of biological chemistry.* 2010;285(48):37159-69.

53. Huang W, Lv X, Liu C, Zha Z, Zhang H, Jiang Y, Xiong Y, Lei QY, and Guan KL. The N-terminal phosphodegron targets TAZ/WWTR1 protein for

SCFbeta-TrCP-dependent degradation in response to phosphatidylinositol 3-kinase inhibition. *The Journal of biological chemistry.* 2012;287(31):26245-53.

54. Sorrentino G, Ruggeri N, Specchia V, Cordenonsi M, Mano M, Dupont S, Manfrin A, Ingallina E, Sommaggio R, Piazza S, et al. Metabolic control of YAP and TAZ by the mevalonate pathway. *Nature cell biology.* 2014;16(4):357-66.

55. Azzolin L, Panciera T, Soligo S, Enzo E, Bicciato S, Dupont S, Bresolin S, Frasson C, Basso G, Guzzardo V, et al. YAP/TAZ incorporation in the beta-catenin destruction complex orchestrates the Wnt response. *Cell.* 2014;158(1):157-70.

56. Imajo M, Miyatake K, Iimura A, Miyamoto A, and Nishida E. A molecular mechanism that links Hippo signalling to the inhibition of Wnt/beta-catenin signalling. *The EMBO journal.* 2012;31(5):1109-22.

57. Varelas X, Miller BW, Sopko R, Song S, Gregorieff A, Fellouse FA, Sakuma R, Pawson T, Hunziker W, McNeill H, et al. The Hippo pathway regulates Wnt/beta-catenin signaling. *Developmental cell.* 2010;18(4):579-91.

58. Ji M, Yang S, Chen Y, Xiao L, Zhang L, and Dong J. Phospho-regulation of KIBRA by CDK1 and CDC14 phosphatase controls cell-cycle progression. *The Biochemical journal.* 2012;447(1):93-102.

59. Yang S, Zhang L, Liu M, Chong R, Ding SJ, Chen Y, and Dong J. CDK1 phosphorylation of YAP promotes mitotic defects and cell motility and is

essential for neoplastic transformation. *Cancer research.* 2013;73(22):6722-33.

60. Zhao Y, Khanal P, Savage P, She YM, Cyr TD, and Yang X. YAP-induced resistance of cancer cells to antitubulin drugs is modulated by a Hippo-independent pathway. *Cancer research.* 2014;74(16):4493-503.

61. Hirota T, Kunitoku N, Sasayama T, Marumoto T, Zhang D, Nitta M, Hatakeyama K, and Saya H. Aurora-A and an interacting activator, the LIM protein Ajuba, are required for mitotic commitment in human cells. *Cell.* 2003;114(5):585-98.

62. Dupont S, Morsut L, Aragona M, Enzo E, Giulitti S, Cordenonsi M, Zanconato F, Le Digabel J, Forcato M, Bicciato S, et al. Role of YAP/TAZ in mechanotransduction. *Nature.* 2011;474(7350):179-83.

63. Chen X, and Prywes R. Serum-induced expression of the cdc25A gene by relief of E2F-mediated repression. *Molecular and cellular biology.* 1999;19(7):4695-702.

64. Toji S, Yabuta N, Hosomi T, Nishihara S, Kobayashi T, Suzuki S, Tamai K, and Nojima H. The centrosomal protein Lats2 is a phosphorylation target of Aurora-A kinase. *Genes to cells : devoted to molecular & cellular mechanisms.* 2004;9(5):383-97.

65. Kim Y, Holland AJ, Lan W, and Cleveland DW. Aurora kinases and protein phosphatase 1 mediate chromosome congression through regulation of CENP-E. *Cell.* 2010;142(3):444-55.

66. Kapoor TM, Lampson MA, Hergert P, Cameron L, Cimini D, Salmon ED, McEwen BF, and Khodjakov A. Chromosomes can congress to the metaphase plate before biorientation. *Science.* 2006;311(5759):388-91.

67. Nigg EA. Cellular substrates of p34(cdc2) and its companion cyclin-dependent kinases. *Trends in cell biology.* 1993;3(9):296-301.

68. Hornbeck PV, Kornhauser JM, Tkachev S, Zhang B, Skrzypek E, Murray B, Latham V, and Sullivan M. PhosphoSitePlus: a comprehensive resource for investigating the structure and function of experimentally determined post-translational modifications in man and mouse. *Nucleic acids research.* 2012;40(Database issue):D261-70.

69. Chan SW, Lim CJ, Loo LS, Chong YF, Huang C, and Hong W. TEADs mediate nuclear retention of TAZ to promote oncogenic transformation. *The Journal of biological chemistry.* 2009;284(21):14347-58.

70. Li Z, Wang Y, Zhu Y, Yuan C, Wang D, Zhang W, Qi B, Qiu J, Song X, Ye J, et al. The Hippo transducer TAZ promotes epithelial to mesenchymal transition and cancer stem cell maintenance in oral cancer. *Molecular oncology.* 2015.

71. Bartucci M, Dattilo R, Moriconi C, Pagliuca A, Mottolese M, Federici G, Benedetto AD, Todaro M, Stassi G, Sperati F, et al. TAZ is required for metastatic activity and chemoresistance of breast cancer stem cells. *Oncogene.* 2015;34(6):681-90.

72. Zhang H, Liu CY, Zha ZY, Zhao B, Yao J, Zhao S, Xiong Y, Lei QY, and Guan KL. TEAD transcription factors mediate the function of TAZ in cell

growth and epithelial-mesenchymal transition. *The Journal of biological chemistry.* 2009;284(20):13355-62.

73. Zhao B, Ye X, Yu J, Li L, Li W, Li S, Yu J, Lin JD, Wang CY, Chinnaiyan AM, et al. TEAD mediates YAP-dependent gene induction and growth control. *Genes & development.* 2008;22(14):1962-71.

74. Bischoff JR, Anderson L, Zhu Y, Mossie K, Ng L, Souza B, Schryver B, Flanagan P, Clairvoyant F, Ginther C, et al. A homologue of Drosophila aurora kinase is oncogenic and amplified in human colorectal cancers. *The EMBO journal.* 1998;17(11):3052-65.

75. Zhou H, Kuang J, Zhong L, Kuo WL, Gray JW, Sahin A, Brinkley BR, and Sen S. Tumour amplified kinase STK15/BTAK induces centrosome amplification, aneuploidy and transformation. *Nature genetics.* 1998;20(2):189-93.

76. Marumoto T, Zhang D, and Saya H. Aurora-A - a guardian of poles. *Nature reviews Cancer.* 2005;5(1):42-50.

77. Florindo C, Perdigao J, Fesquet D, Schiebel E, Pines J, and Tavares AA. Human Mob1 proteins are required for cytokinesis by controlling microtubule stability. *Journal of cell science.* 2012;125(Pt 13):3085-90.

78. Mardin BR, Lange C, Baxter JE, Hardy T, Scholz SR, Fry AM, and Schiebel E. Components of the Hippo pathway cooperate with Nek2 kinase to regulate centrosome disjunction. *Nature cell biology.* 2010;12(12):1166-76.

79. Shimizu T, Ho LL, and Lai ZC. The mob as tumor suppressor gene is essential for early development and regulates tissue growth in Drosophila. *Genetics.* 2008;178(2):957-65.

80. Nishio M, Hamada K, Kawahara K, Sasaki M, Noguchi F, Chiba S, Mizuno K, Suzuki SO, Dong Y, Tokuda M, et al. Cancer susceptibility and embryonic lethality in Mob1a/1b double-mutant mice. *The Journal of clinical investigation.* 2012;122(12):4505-18.

81. Yabuta N, Okada N, Ito A, Hosomi T, Nishihara S, Sasayama Y, Fujimori A, Okuzaki D, Zhao H, Ikawa M, et al. Lats2 is an essential mitotic regulator required for the coordination of cell division. *The Journal of biological chemistry.* 2007;282(26):19259-71.

82. Yang S, Zhang L, Chen X, Chen Y, and Dong J. Oncoprotein YAP Regulates the Spindle Checkpoint Activation in a Mitotic Phosphorylation-dependent Manner through Up-regulation of BubR1. *The Journal of biological chemistry.* 2015;290(10):6191-202.

83. Abe Y, Ohsugi M, Haraguchi K, Fujimoto J, and Yamamoto T. LATS2-Ajuba complex regulates gamma-tubulin recruitment to centrosomes and spindle organization during mitosis. *FEBS letters.* 2006;580(3):782-8.

84. Hirota T, Morisaki T, Nishiyama Y, Marumoto T, Tada K, Hara T, Masuko N, Inagaki M, Hatakeyama K, and Saya H. Zyxin, a regulator of actin filament assembly, targets the mitotic apparatus by interacting with h-warts/LATS1 tumor suppressor. *The Journal of cell biology.* 2000;149(5):1073-86.

85. Iida S, Hirota T, Morisaki T, Marumoto T, Hara T, Kuninaka S, Honda S, Kosai K, Kawasuji M, Pallas DC, et al. Tumor suppressor WARTS ensures genomic integrity by regulating both mitotic progression and G1 tetraploidy checkpoint function. *Oncogene.* 2004;23(31):5266-74.

86. Zhang L, Iyer J, Chowdhury A, Ji M, Xiao L, Yang S, Chen Y, Tsai MY, and Dong J. KIBRA regulates aurora kinase activity and is required for precise chromosome alignment during mitosis. *The Journal of biological chemistry.* 2012;287(41):34069-77.

87. Aylon Y, Michael D, Shmueli A, Yabuta N, Nojima H, and Oren M. A positive feedback loop between the p53 and Lats2 tumor suppressors prevents tetraploidization. *Genes & development.* 2006;20(19):2687-700.

88. Kops GJ, Weaver BA, and Cleveland DW. On the road to cancer: aneuploidy and the mitotic checkpoint. *Nature reviews Cancer.* 2005;5(10):773-85.

89. Lara-Gonzalez P, Westhorpe FG, and Taylor SS. The spindle assembly checkpoint. *Current biology : CB.* 2012;22(22):R966-80.

Chapter 2

Functional Study of Hippo-YAP Signaling in Prostate Cancer

This part is a modified version of the original publication:

Mol Cell Biol. 2015 Apr 15;35(8):1350-62.

2.1 Introduction

In 2014, there were 233,000 estimated new cases of prostate cancer and 29，480 estimated deaths caused by prostate cancer in the United States. In the past 10 years, prostate cancer remains the most common malignancy and the second leading cause of cancer deaths among men in the United States. The treatment regimens of prostate cancer are based on the stage of the disease. For localized cancer, the conventional treatments are surgical excision (radical prostatectomy) and radiotherapy. In cases of advanced or invasive cancer, including those have metastatic lesions, androgen deprivation therapy is the major strategy (1). Androgen ablation initially decreases the volume of both primary and metastatic lesions and reduces PSA to low or undetectable level, however, in most cases the tumors will recur and become chemotherapy-resistant and androgen-independent (2, 3). This recurrence of prostate cancer is termed “castration resistant prostate cancer (CRPC)”, since the removal of testicular androgen by chemical or surgical castration does not effect as in the initial response, ultimately the disease will be lethal (4, 5).

Circulating androgens are essential for both normal prostate development and the onset of prostate cancer through interactions with the androgen receptor (AR). Testosterone is the major androgen produced by testis and adrenal gland. When testosterone enters prostate cells, it is converted to dihydrotestosterone (DHT) by the enzyme 5-reductase. This more potent form of androgen binds to the AR and induces its dimerization and phosphorylation. Then the androgen

receptor complex translocates into nucleus, where it binds to androgen-response elements in the promoter regions of target genes, and leads to biological responses including growth, survival and the produce of prostate-specific antigen (PSA).

During castration-resistant progression, prostate cancer relies on various cellular pathways, some involving the androgen receptor and others bypassing it. In the former type of pathway, amplification of AR gene copy number happens in about one-third of CRPC patients (6-8). Another 10%–30% of tumors have mutations of AR that may confer increased protein stability, greater sensitivity to androgens, novel responses to other steroid hormones, ligand-independent activity, or increased recruitment of AR coactivator proteins (9-11). In the pathways that bypass the androgen receptor, the loss of PTEN (phosphatase and tensin homolog) results in up-regulation of the Akt/mTOR signaling pathway in prostate cancer, primarily through activation of Akt1 (12, 13). In addition, Erk-MAPK signaling is also frequently activated in prostate cancer, particularly in advanced disease, and is often coordinately deregulated together with Akt signaling (14, 15).

In the past two decades, the use of genetically engineered transgenic and knockout mice has represented a major progress of prostate cancer investigations. A well-studied model is the TRAMP (transgenic adenocarcinoma of the prostate) mouse model, which carries a probasin promoter driving both

SV40 large T and small t antigen and results in adenocarcinoma and CRPC (16). Loss of Nkx3.1 and Pten showed accelerated formation of high-grade PIN (prostate intraepithelial neoplasia) and invasive cancer (17). Conditional deletion of PTEN and p53 in the prostate driven by a minimal probasin promoter driving Cre recombinase developed PIN and adenocarcinoma. However, none of these models closely mimics the human prostate cancer progression.

Recent genetic mouse models and studies with cancer patients have firmly demonstrated the critical roles of Hippo pathway in cancer development and progression. For example, Mst1 and Mst2 suppress development of hepatocellular carcinoma (HCC) in mice (18-20). WW45 heterozygous mice and mice with a conditional deletion of WW45 in the liver develop osteosarcoma and hepatoma (21). Although mutations are rare in Hippo pathway, mutation or deletion of Lats2 is significant in malignant mesothelioma (22).

As the main downstream effectors of the Hippo pathway, YAP and TAZ do not have any DNA binding domain thus they function as the transcriptional co-activators, promoting the downstream gene expression through binding with multiple transcription factors. Among these transcription factors, the TEAD/TEF family, which represent homologs of the *Drosophila* Sd protein, are the prime mediators of YAP/TAZ function in Hippo Signaling. The YAP/TAZ-TEAD transcription factor complex represents a common target of oncogenic transformation. The oncoprotein YAP has been implicated in promoting several

types of tumor formation, such as liver and skin tumorigensis and rhabdomyosarcoma (23-27). Specifically, the Tet-on inducible YAP transgenic mice developed numerous discrete nodules in the liver after 8 weeks feeding with water containing doxycycline, and further developed to widespread HCC after 3 months (24). As expected, overexpression or hyperactivation (nuclear localization) of YAP is frequently detected in several human malignancies including liver, ovarian, breast, lung and pancreatic cancer (24-26, 28-34). In addition to the role of Hippo-YAP signaling in cancer development, recent studies also implicate YAP involved in the metastatic progression of breast cancer and melanoma (35). Although one study have shown that TAZ overexpression was detected in 21% of primary breast cancers (36), a comprehensive study of TAZ protein expression across multiple tumor types is unavailable at present.

Accumulated evidence has shown that the Hippo-YAP pathway activity is regulated by many cues and factors, including cell adhesion, cell polarity, contact inhibition/cell density, and cytoskeleton dynamics/mechanical forces (37, 38). Recent studies have also demonstrated that YAP/TAZ activity can be regulated independently of Hippo signaling and YAP/TAZ crosstalks with many other canonical signaling pathways including Wnt/β-catenin (39-45), TGF-β/Smad (46-48) and Ras-ERK (34, 49, 50) in the regulation of cancer cell proliferation, survival and tumorigenesis. Although YAP signaling is largely involved in mediating these physiological processes, the biological significance of YAP in prostate cancer has not been previously defined.

Our study is the first study that explored the functional role of YAP in prostate cancer cell motility, invasion and castration-resistant growth and determined the clinical relevance of YAP in CRPC. Our data identify YAP as a critical regulator in prostate cancer, especially for CRPC, providing an alternative mechanism underlying the development of castration-resistance of prostate tumor cells.

2.2 Materials and Methods

Expression constructs

The pcDNA-YAP expression construct has been described (24). Point mutations were generated by the QuikChange Site-Directed PCR mutagenesis kit (Stratagene, La Jolla, CA, USA) and verified by sequencing. To make the retroviral-mediated YAP expression construct, the above cDNA was cloned into MaRXTMIV vector. The lentiviral YAP shRNA constructs and packaging vectors (psPAX2 and pMD2.G) were from Addgene (Cambridge, MA, USA).

Cell culture and transfection

HEK293T, HEK293GP, RWPE-1, LNCaP cell lines were purchased from American Type Culture Collection (ATCC, Manassas, VA, USA). HEK293T and HEK293GP cell lines were maintained in DMEM containing 10% FBS and L-glutamine plus 100 units/ml penicillin and 100 µg/ml streptomycin (Invitrogen) at 37 °C in a humidified atmosphere containing 5% CO2. The LNCap cell lines were maintained in ATCC-formulated RPMI-1640 Medium containing 10% FBS at 37 °C in a humidified atmosphere containing 5% CO2. The cell lines were

authenticated at ATCC and were used at low (<25) passages. The LNCaP-C4-2 and LNCaP-C81 sublines have been described (51-53). All the transient overexpression transfections were performed using Attractene (Qiagen) following the manufacturer's instructions. Cells were harvested at 2 days post-transfection. RNA interference was performed using HiPerFect (Qiagen). For DNA and siRNA co-transfection, Attractene reagents were used. siRNA oligonucleotides were purchased from Dharmacom and GenePharma. YAP siRNA was synthesized by GenePharma based on the following target sequence (YAP-1: 5'-CAGGTGATACTATCAACCAAA-3'; YAP-2: 5'-GACCAATAGCTCAGATCCTTT (selected by Invitrogen online software). R1881 was purchased from PerkinElmer (Waltham, MA, USA) All other chemicals were either from Sigma or Thermo Fisher.

Retrovirus packaging and infection

To generate wild type YAP and YAP mutant overexpression stable cell lines, retrovirus infection was performed by transfecting HEK293GP cells with empty MXIV-neo vector or MXIV-neo wild type YAP or YAP mutant constructs, following the company's instructions (Oligoengine). Each plasmid was co-transfected with a construct expressing the VSV-G gene into the virus packaging cell line HEK293GP to produce retrovirus expressing wild type YAP or YAP mutant. The obtained retroviral supernatant was further filtered with 0.45μM filter and used to infect the RWPE-1 and LNCaP cells with polybrene (Millipore) with the final concentration of 10 μg/ml. At 24hours after infection, virus supernatant was

replaced with fresh growth medium. The transduced cells were then selected at 800 µg/ml of neomycin (at 48hours post-infection) to establish stably expressing YAP or YAP mutant cell lines. Western blot was used to test the expression level of YAP.

Lentivirus packaging and infection

The LNCap-C4-2 cells were stably transfected with YAP shRNAs (purchased from Addgene). Briefly, lentivirus infection was performed by transfecting HEK293T cells with pLKO1-shYAP1 and pLKO1-shYAP2, following the company's instructions (Oligoengine). The plasmid (2.5 µg) was co-transfected with the construct expressing psPAX2 (2.0µg) and pMD2.G (1.0µg) gene into the virus packaging cell line HEK293T to produce lentivirus expressing YAP shRNA with puromycin as the selectable marker, when HEK293T cells reached 50% confluence. At 16hours after transfection, the medium was replaced and HEPES (10 mM) and Sodium Butyrate (10 mM) were added to increase the half-life and production of the virus. At 48 hours after transfection, the obtained lentiviral supernatant was collected and further filtered with a 0.45 µM filter and used to infect the LNCaP-C4-2 cells with polybrene (Millipore, Billerica, MA, USA) in the presence of 10 µg/ml of polybrene. At 24hours after infection, the virus supernatant was replaced with fresh growth medium. The transduced cells were then selected with puromycin (2µg/ml) to establish cell lines in which YAP expression was stably knocked down. Western blot was used to test the expression level of YAP.

Quantitative real time-PCR

Total RNA isolation, RNA reverse transcription and quantitative real time-PCR were done as described previously (54). Other primer sequences are as follows: TEAD1: cttgaatgtgcaatgaagcg (forward, F), cgaagtttgcctcggactc (reverse, R); TEAD2: ctcactccgtagaagccacc (F), tgccttcttcctggtcaagt (R); TEAD3: gcaccttcttccgagctaga (F), tacggccgaaatgagttgat (R); TEAD4: gctccactcgttggaggtaa (F), cttagcgcacccatccc (R); YAP: acgttcatctgggacagcat (F), gttgggagatggcaaagaca (R); TAZ: attcatcgccttcctagggt (F), ggctgggagatgaccttcac (R); CTGF: ttggcaggctgatttctagg (F), ggtgcaaacatgtaacttttgg (R); ITGB2: actcctgagagaggacgcac (F), cagggcagactggtagcaa (R); ANKRD1: gtgtagcaccagatccatcg (F), cggtgagactgaaccgctat (R); Cyr61: cccgttttggtagattctgg (F), gctggaatgcaacttcgg (R); SOX4: aatgtatgtttccccctccc (F), tcgctgtcgggtctctagtt (R); Survivin: cgaggctggcttcatccact (F), acggcgcactttcttcgca (R); PSA: atatcgtagagcgggtgtgg (F), tcctcacagctgcccact (R); NKX3.1: cagataagaccccaagtgcc (F), cagagccagagccagagg (R); KLK2: tgtcttcaggctcaaacagg (F), gtacagtcatggatgggcac (R); PGC-1: ctgctagcaagtttgcctca (F), agtggtgcagtgaccaatca (R).

Cell fractionation assay

Cell fractionation assays were done by NE-PER Nuclear and Cytoplasmic Extraction Reagents following the manufacturer's instructions (Thermo Scientific/Pierce, Rockford, IL, USA).

Antibodies and Western blot analysis

The YAP antibodies from Cell Signaling Technology (#4912, Danvers, MA, USA) and Abcam (52771, Cambridge, MA, USA) were used for Western blotting throughout the study. Anti-β-actin, anti-androgen receptor, anti-ERK1/2, anti-Akt, anti-GSK3β, anti-β-catenin, anti-RSK1 and anti-RSK2 antibodies were from Santa Cruz Biotechnology (Santa Cruz, CA, USA). Anti-Mst1, anti-Mst2, anti-Lats1 and anti-Lats2 antibodies were from Bethyl Laboratory (Montgomery, TX, USA). Anti-phospho-YAP S127, anti-phospho-Akt T308, anti-phospho-Akt S473, anti-phospho-GSK3β S9, anti-phospho-ERK1/2, anti-phospho-Mst2 T180, anti-E-cadherin, anti-vimentin and anti-PARP antibodies were from Cell Signaling Technology. Mouse monoclonal antibody against N-cadherin was provided by Dr. Keith Johnson (University of Nebraska Medical Center) (55). Anti-phospho-RSK S380 antibody was from Biolegend (San Diego, CA, USA). Anti-NF2 and anti-β-tubulin antibodies were from Sigma (St. Louis, MO, USA). The cells were harvested and cell lysate were prepared by 2XSDS lysis buffer. The proteins were separated on SDS polyacrylamide gels and transferred onto PVDF membranes (Millipore). HRP-conjugated anti-mouse or anti-rabbit IgG were from Pierce. ECL and SuperSignal West Pico Chemiluminescent substrate kits (Pierce) were used as HRP substrates.

Cell proliferation and anchorage-independent growth assays

For cell proliferation assays, 5,000 (LNCaP-C4-2) or 10,000 (LNCaP) cells were seeded in wells of a 24-well plate in triplicate. Cells were counted by a hemocytometer (Thermo, Waltham, MA, USA) and proliferation curves were

made based on cell numbers of each well from three independent experiments. Soft agar assays were conducted in 6-well plates. The base layer of each well consisted of 1.5ml with final concentrations of 1 x media and 1% agarose. Plates were chilled at room temperature until solid, at which point a 2 ml growth medium with 0.5% agarose layer was poured, consisting of cells suspended (LNCaP-C4-2 cells: 5000 cells per well, LNCaP cells: $1X10^4$ cells per well). Plates were again chilled at room temperature until the growth layer congealed. A further 1 ml of 1x culture media without agarose was added on top of the growth layer. The growth medium was changed every week for 3-4 weeks, after which colonies were fixed with 3.7% PFA and stained with 0.005% crystal violet for 1 minute followed by PBS wash for 3 times of 5 minutes each. A picture was taken and total colonies were counted. Data were obtained from three independent experiments.

Cell migration and invasion assays

In vitro analysis of invasion and migration was assessed using the BioCoat invasion system (BD Biosciences) and Transwell system (Corning), respectively, according to the manufacturer's instructions. The cells were trypsinized and resuspended in the medium without serum and/or growth factor at the indicated concentration (RWPE-1: $1.0X10^5$/well, LNCaP $5.0X10^4$/well, C4-2: $5.0X10^4$/well for migration assay; RWPE-1: $5.0X10^4$/well, LNCaP $5.0X10^4$/well, C4-2: $5.0X10^4$/well for invasion assay). 600 µl of basal medium with 10%FBS was added to the bottom of the migration assay chamber, and 750 µl for BioCoat invasion chamber. The insert was carefully placed into each well to avoid leaving

a bubble between insert and the medium in the bottom chamber. 100 µl or 500 µl of the above mentioned cell suspension was added to the insert for migration and invasion assay, respectively. After the incubation at 37°C for 18 to 24 hours, the plate was removed from the incubator. The cells were fixed with 3.7% PFA and the cells inside the inserts were removed with cotton swabs. Then, the invasive and migratory cells were stained with ProLong® Gold Antifade Reagent with DAPI. The relative invading and migrating rate were calculated by the number of cells invading and migrating through the membrane, divided by the number of cells that invaded and migrated in the control group.

Immunohistochemistry (IHC) staining

Tissue microarray slides (TMA) were obtained from the Prostate Cancer Biorepository Network (PCBN, New York University site). The TMA consists of 7 naïve (hormone responsive) and 13 castration-resistant prostate cancer tumors collected from 1983 to 2002 at New York University Langone Medical Center. Slide deparaffinization, antigen retrieval, and blocking were performed as we have described (24). The sections were then stained with anti-YAP antibody (Cell Signaling #4912, at 1:100 dilutions) using a Histostain-Plus IHC kit following the manufacturer's instructions (Invitrogen, Grand Island, NY, USA). Cell nuclei were stained with Hematoxylin. Ventana iScan HT (Roche) was used for slide scanning with a 20X lens. The staining results were independently evaluated by three researchers including two pathologists (S.M.L. and K.F.). Both the YAP staining intensity (a scale of 0 to 3 was used: 0-negative, 1-weak, 2-moderate,

and 3-strong) and nuclear localization (the percentage of tumor cell nuclei stained, 0-no staining, 1-≤10%, 2-10-50%, and 3->50%) were scored (56).

Mouse xenograft Studies

For *in vivo* xenograft studies, LNCaP cells expressing vector or YAP in 50% Cultrex (Trevigen, Gaithersburg, MD, USA) ($2.0x10^6$ each line/0.1 ml) were subcutaneously injected into the left flank of 3-month-old castrated male SCID mice (Charles River, Wilmington, MA, USA). Six or nine animals were used for control (vector) and experimental (YAP) groups, respectively. Mice were euthanized at 8 weeks post-injection and the tumors were excised and fixed for subsequent histopathological examination and IHC analysis. The animals were housed in pathogen-free facilities. All animal experiments were approved by the University of Nebraska Medical Center Institutional Animal Care and Use Committee.

Generation of prostate-specific Tet-on inducible YAPS127A transgenic mice

The Tet-on inducible system was used to generate prostate-specific inducible YAP-S127A mice. We crossed the PB-rtTA mice to Tet-on YAP-S127A mice to generate pups with both PB-rtTA and Tet-YAPS127A alleles. Since rtTA (reverse tetracycline transactivator) is located downstream of the PB promoter, it is specifically expressed in prostate tissue. As a result, in the presence of doxycycline (fed with drinking water), rtTA binds to the tetracycline response element and produces high level of YAP-S127A. Prostate of different ages of

these male mice were dissected and histological analysis were performed to check the formation of prostatic intraepithelial neoplasia (PIN) and adenocarcinoma.

Generation of prostate-specific MST1/2 knockout mice

The Cre-LoxP system was used to generate mice with prostate-specific deletion of Mst1/2. The Mst1 $^{flox/flox}$; Mst2 $^{flox/flox}$ mice were mated with male PB-Cre mice. PCR genotyping was used to determine the genotype of the offspring. Then the male Mst1 $^{flox/+}$; Mst2$^{flox/+}$;Cre^{+} mice were mated with Mst1 $^{flox/flox}$; Mst2 $^{flox/flox}$ mice to generate the homozygous mice with prostate-specific deletion of Mst1/Mst2. Prostate at different age of these male mice were dissected and histological analysis were performed to check the formation of PIN and adenocarcinoma.

Mouse genomic DNA purification

3-week-old mice were weaned and 1/3-1/2 cm mice tails were cut for genomic DNA purification. To each tail, 500ml of tail digestion buffer was added (which has been supplemented with proteinase K at a final concentration of 0.5 mg/ml) and placed at 55℃ for 16-24 hours. After vigorously shaking tubes for about 15 seconds, tubes were centrifuged at top speed for 15 minutes. Then the supernatant was transferred to new micro-tubes containing 500ul isopropanol. After 5 minutes incubation at room temperature, tubes were centrifuged at top speed for 4 minutes. The DNA pallets were washed twice by adding 100ul 70%

ethanol. Then add 200ul ddH_2O and incubate for 1 hour at 55℃ to dissolve the DNA. Then DNA was ready to use for PCR genotyping.

Genotyping

The PCR genotyping was performed using Promega GoTaq Flexi DNA polymerase kit. All PCR reactions were set in the following 20ul system: DNA 2ul, 5 X Promega buffer 4ul, 25mM Mg^{2+} 1.6ul, 2.5mM dNTP 2ul, 10uM mixed primer 4ul, Promega enzyme 0.2ul, ddH_2O 6.2ul.

Tissue processing

Mouse tissue was fixed in 3.7% PFA for 16h and then transferred to 70% ethanol. Tissue embedding and slides preparation were performed by Tissue Science Facility in UNMC.

Statistical analysis

Data were analyzed using a two-tailed, unpaired Student's *t*-test. The Wilcoxon rank sum test was used to compare the IHC staining data between groups. A *P* value of <0.05 was considered as indicating statistical significance.

2.3 Results

The Hippo Pathway Effector, YAP, Regulates Motility, Invasion and Castration-Resistant Growth of Prostate Cancer Cells.

2.3.1 Upregulation and activation of YAP in prostate castration-resistant tumors

To explore the functional significance of hippo pathway in prostate cancer, we collected both clinical prostate normal and cancer tissues, and our data showed that YAP was highly expressed in nearly all of the tumor samples examined whereas relatively lower level in normal tissues (Fig. 2.1A). Interestingly, the upstream tumor suppressor Mst1 expression was detected in only one of nine tumor samples but three of the four normal samples (Fig. 2.1A). This suggests that hippo pathway is dysregulated in human prostate cancer. We further mined YAP expression data from large scale studies of prostate cancer. These data confirmed that YAP mRNA was significantly high in CRPC or metastatic prostate tumors compared to primary tumors (Fig. 2.1B,C).

YAP is overexpressed and/or hyperactivated (as shown by nuclear localization) in prostate primary tumor samples (24, 32). However, it is not known to what extent YAP activity/expression correlates with prostate castration resistance. To determine the functional relevance of YAP in CRPC in the clinical setting, we obtained tissue microarrays containing naïve (hormonal responsive) and castration-resistant prostate tumors and performed immunohistochemical (IHC) staining. Immunostaining demonstrated that overall YAP expression was

relatively weak in naïve prostate tumors (Fig. 2.2A-A'', n=7) and no single case was scored moderate or strong for YAP staining (see 'Materials and Methods'). Importantly, we observed dramatic upregulation of YAP in most hormonal therapy resistant tumor samples (Fig. 2.2B-E, n=13). Nine of the resistant tumors showed moderate-strong staining and 4 of them had weak staining (compared with all of the naive tumors showing weak to no staining) (p=0.003, resistant versus naive). Furthermore, strong nucleus-localized (hyperactive) YAP staining was detected in 5 of the resistant tumors (Fig. 2.2B-B'', D-D'' and F) (p=0.001, resistant versus naive). These data indicates that YAP may function as a critical regulator in the castration-resistant growth of prostate cancer.

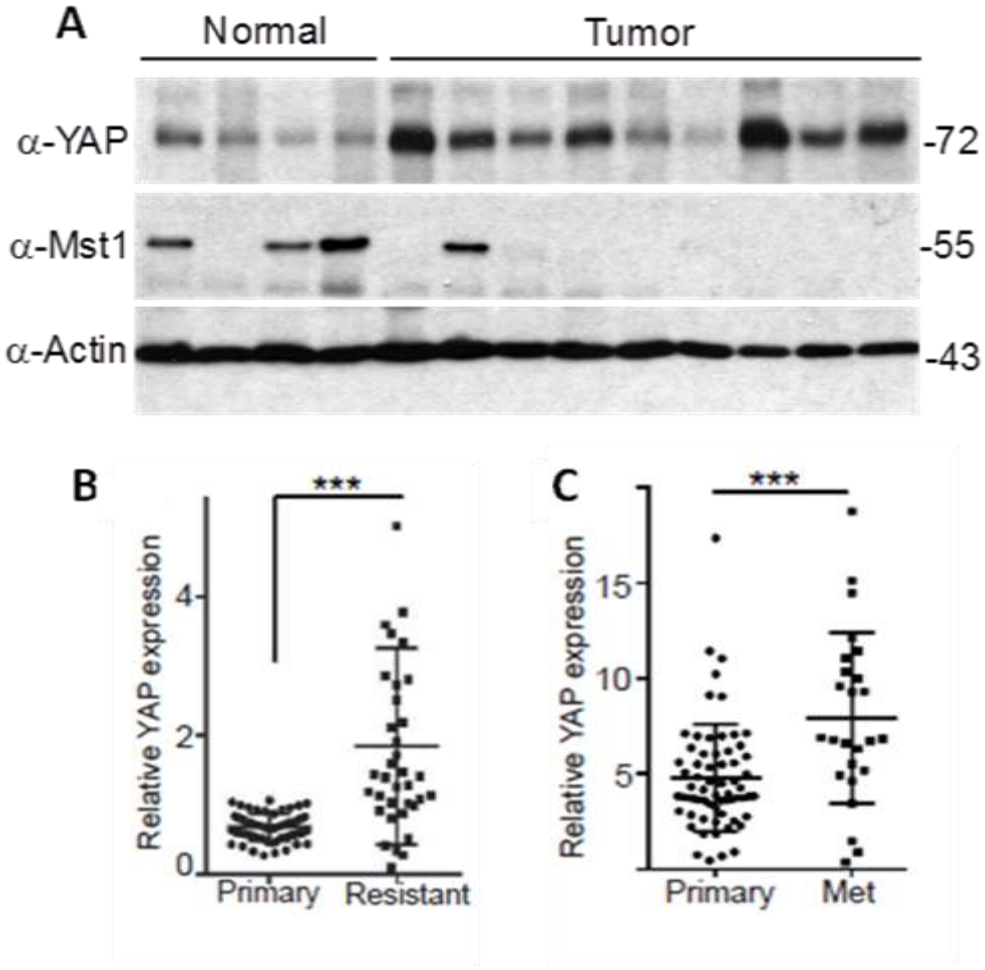

Figure 2.1 Upregulation of YAP in prostate tumors.

A. YAP and Mst1 protein levels in prostate normal and tumor samples.

B, Relative YAP mRNA levels in localized (primary) tumors and CRPC (resistant). Data were mined from Grasso et al., 2012. N=60 (primary) and 36 (resistant). ***: $p<0.001$ (t-test).

C, Relative YAP mRNA levels in primary and metastatic (Met) tumors (most metastases are castration resistant). Data were retrieved from Gene Expression Ominibus/GDS2545. N=65 (primary) and 25 (Met). ***: $p<0.001$ (t-test).

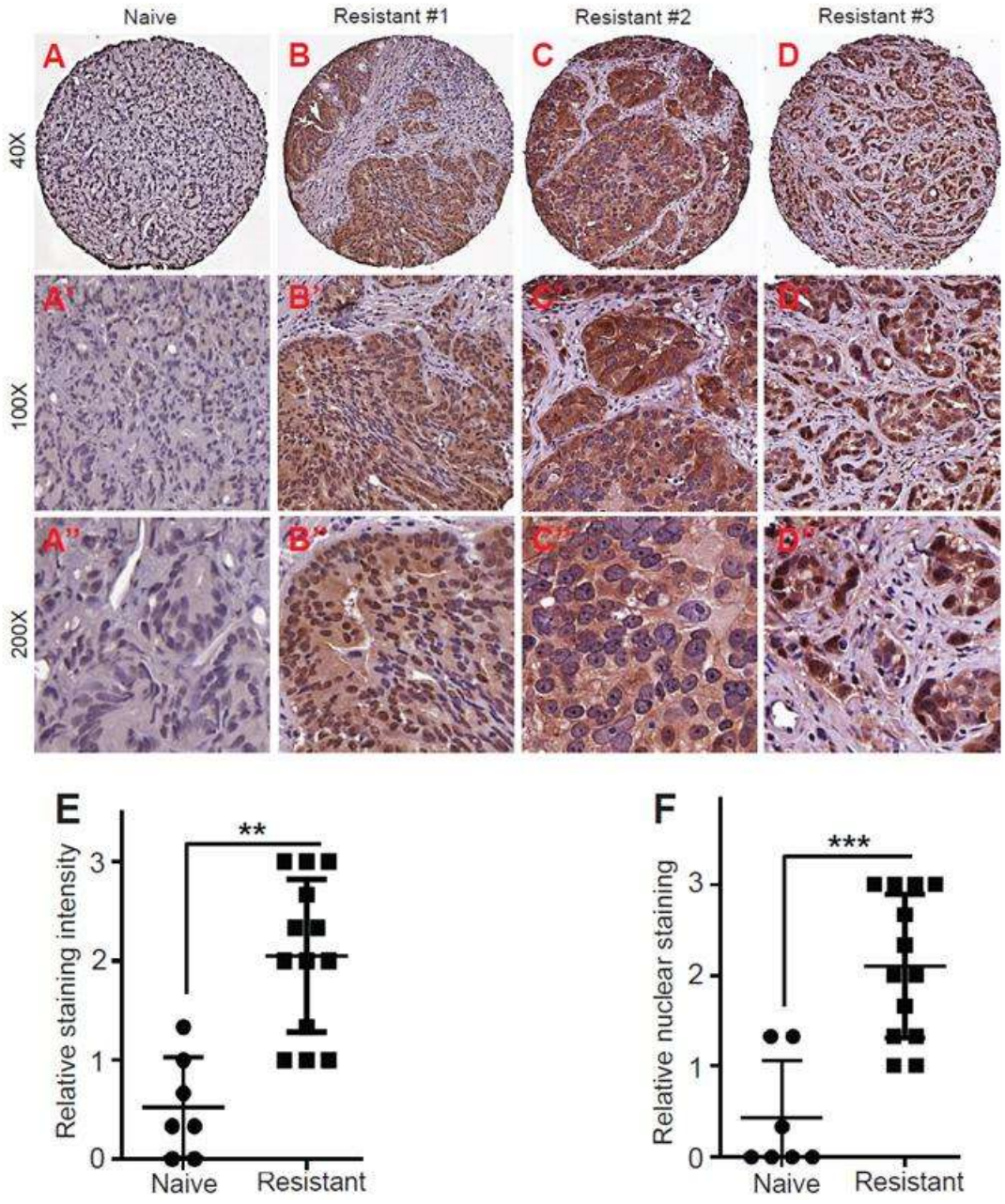

Figure 2.2 Upregulation and activation of YAP in castration-resistant prostate tumors.

A-A'', Representative photos of immunostaining for YAP in naïve (hormonal responsive) prostate tumors.

B-B'', C-C'', and D-D'' Representative photos of YAP IHC staining in hormonal therapy-resistant prostate tumors.

E, Quantification of YAP IHC staining intensity in naive and castration-resistant prostate tumors. Four resistant cases (3254108156, 8322079241, 8842201759, 6756440716) were scored low, five resistant cases (4024863604, 5962887148, 3698735602, 9182583214, 2667199309) were scored moderate and four resistant cases (8063595154, 4976472144, 4729101711, 7346843168) were scored high for YAP staining. All naïve tumors samples have no to low YAP staining (4481786650, 2667199309, 8743000808, 4599423355, 8365207463, 8315345132, 2667199309).

F, Quantification of YAP nuclear localization based on IHC staining in naive and castration-resistant prostate tumors. Four resistant cases (3254108156, 8322079241, 7346843168, 6756440716) were scored low, four resistant cases (8842201759, 4024863604, 4729101711, 2667199309) were scored moderate and five resistant cases (5962887148, 3698735602, 8063595154, 9182583214, 4976472144) were scored high for YAP nuclear staining. All naïve tumors samples have no to low nuclear YAP staining. ***: $p<0.001$; **: $p<0.01$.

2.3.2 YAP transforms prostate epithelial cells and promotes cell motility and invasiveness

Previous studies showed that YAP overexpression induced transformation of immortalized pancreatic and mammary epithelial cells (24, 26, 32). To investigate the biological significance of YAP overexpession/hyperactivation in prostate cancer, we first tested the role of YAP in RWPE-1 cells (immortalized prostate epithelial cells). As shown in Figure 3, ectopic expression of YAP stimulated cell proliferation and induced cellular transformation in RWPE-1 cells (Fig. 2.3A-D). As expected, the expression of the constitutively active YAP-S127A (S127 is the main Hippo-mediated phosphorylation site of YAP) mutant enhanced RWPE-1 cell proliferation and transformation to a greater extent than wild type YAP (Fig. 2.3B-D). YAP expression causes epithelial-mesenchymal transition (EMT) in mammary epithelial cells (MCF10A) (26, 32). Surprisingly, YAP transformed prostate cells without inducing an EMT as the levels of E-cadherin (epithelial marker) and vimentin (mesenchymal marker) remained unchanged in the presence of YAP activation (Fig. 2.4D). Consistent with this observation, YAP was not sufficient to induce a full EMT in a non-transformed mammary epithelial cell line (NMuMG) (35).

Over 90% of cancer deaths are due to metastasis rather than to primary tumors (57, 58). Migration and invasion are essential steps for primary tumor cells to metastasize and grow (58-60). We therefore examined the role of YAP in prostate cell motility. Interestingly, overexpression of YAP or YAP-S127A also

significantly promoted cell migration (Fig. 2.4A) and invasion (Fig. 2.4B, C) in immortalized prostate epithelial cells. Next, we further explored whether enhanced expression of YAP stimulates migration and invasion in prostate cancer (LNCaP) cells. Similarly, YAP or YAP-S127A overexpression resulted in a significant increase in number of LNCaP cells that invaded through Matrigel and migrated through filters compared to vector control cells, respectively (Fig. 2.5A-D). These data indicate that YAP activation is a positive regulator for prostate cell oncogenic activity.

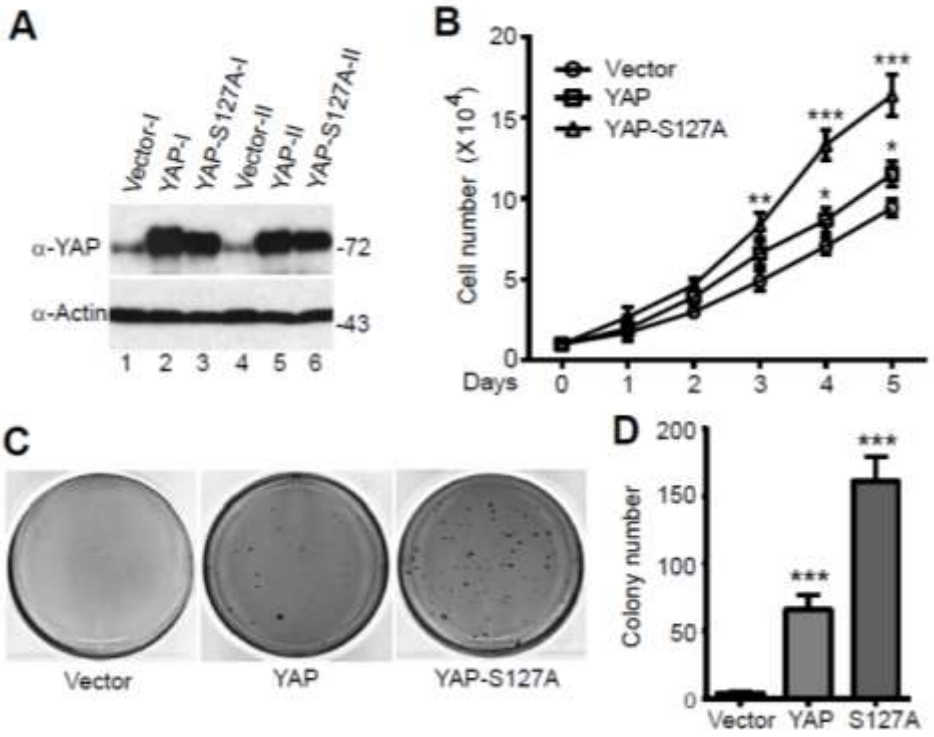

Figure 2.3 YAP promotes cell proliferation and cellular transformation of RWPE-1 cells.

A, Establishment of RWPE-1 cell lines stably expressing YAP.

B, Expression of YAP/YAP-S127A stimulates proliferation in RWPE-1 cells.

C, D, Anchorage-independent growth (colony formation assay) in soft agar.

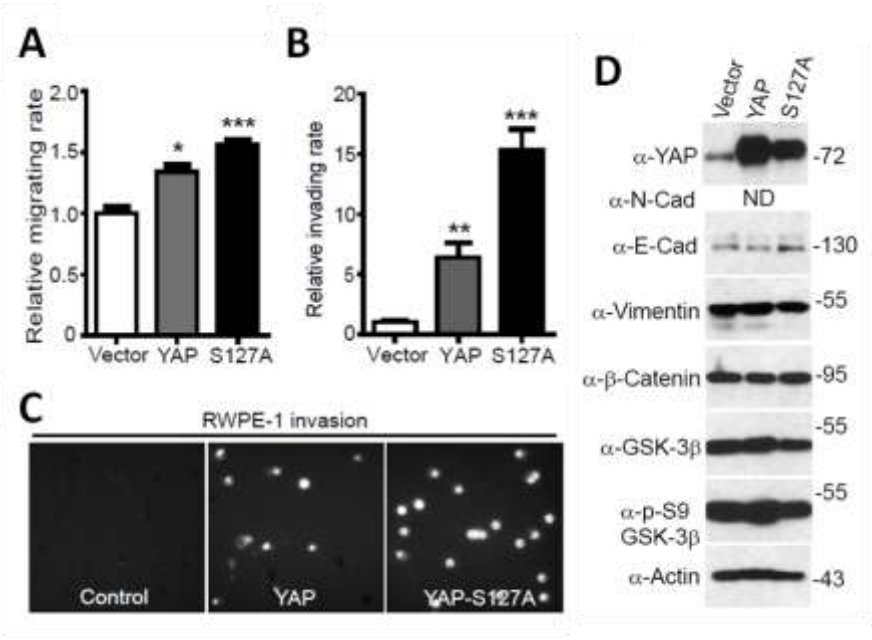

Figure 2.4 YAP promotes migration and invasion in RWPE-1 cells.

A-C, Cell migration (A) and invasion (B) assays with RWPE-1 cells expressing vector, YAP or YAP-S127A constructs. Migrating and invading cells were stained with DAPI and representative fields are shown (C). Quantitative data are expressed as the mean ± s.e.m of three independent experiments. ***: $p<0.001$, **: $p<0.01$, *: $p<0.05$ (t-test).

D, Westen blotting analysis with the indicated antibodies in YAP-expressing RWPE-1 cells. ND: not detectable.

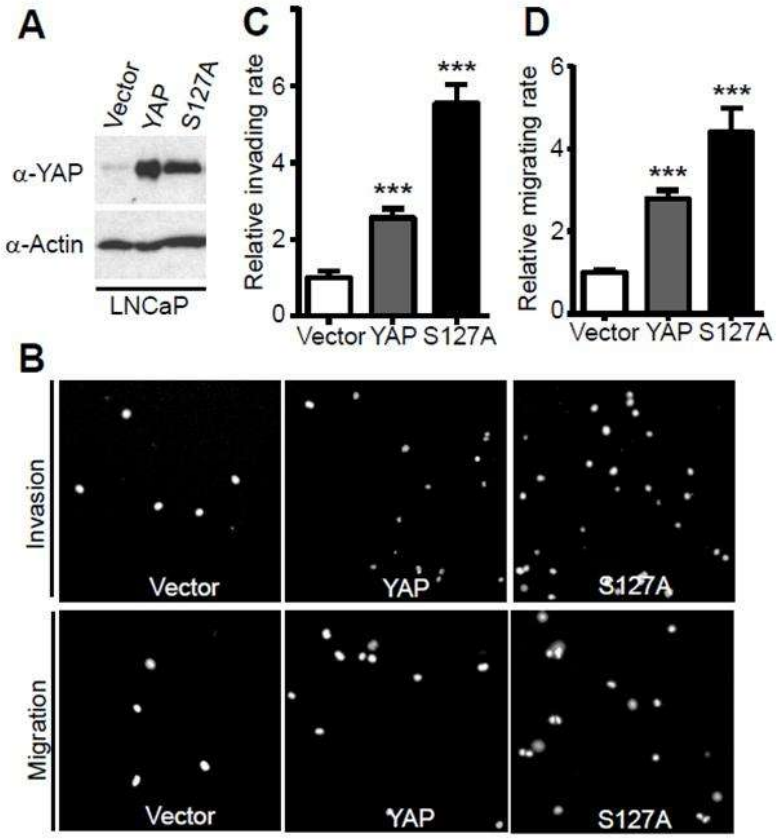

Figure 2.5 YAP promotes migration and invasion in LNCaP cells.

A, Establishment of LNCaP cells expressing vector, YAP or YAP-S127A.

B-D, Cell invasion (B,C) and migration (B,D) assays with LNCaP cell lines established in (A).

2.3.3 YAP promotes castration-resistant growth of LNCaP cells

Most prostate cancer patients with metastatic disease progress to CRPC. We next assessed whether YAP expression is sufficient to induce castration-resistant growth in LNCaP cells, which grow completely in an androgen-sensitive/-dependent manner. YAP overexpression stimulated proliferation of LNCaP cells (Fig. 2.6A, B). Interestingly, the most significant change in these cells upon YAP expression was the ability to proliferate normally under androgen-deprivation conditions (using charcoal-stripped serum [CSS] to deplete the media of androgens), in contrast, the control parental cells stopped dividing without androgen (Fig. 2.6A, B). These data indicate that enhanced expression of YAP was sufficient to convert LNCaP cells from androgen-sensitive to castration-resistant.

YAP was able to induce Akt and ERK activation in a cellular context-dependent manner (49, 50). Interestingly, we also detected moderate but reproducible increased phosphorylation of Akt on T308 (but not S473) upon YAP expression (Fig. 2.6C). Both Akt and ERK were strongly activated upon androgen depletion (Fig. 2.6C), suggesting that multiple cellular pathways are involved in prostate cancer cell survival upon androgen deprivation.

TEAD1-4 (TEA domain containing protein) are the major transcriptional factors of the Hippo pathway. Most of the known YAP/TEADs targets including ANKRD1 (ankyrin repeat domain 1), SOX4 (SRY(sex determining region Y)-box 4), CTGF

(connective tissue growth factor) and Cyr61 (cysteine-rich angiogenic inducer 61) were induced by YAP expression in LNCaP cells (Fig. 2.7A), indicating that YAP signaling is on in LNCaP-YAP cells. Survivin and ITGB2 (integrin beta 2) were not induced by YAP-overexpressing LNCaP cells (data not shown).

We further explored whether YAP could regulate androgen signaling activity. Indeed, the AR (androgen receptor) targets PSA (prostate specific antigen), NKX3.1 (NK3 homeobox 1), PGC-1(Peroxisome proliferator-activated receptor gamma coactivator 1-alpha) and KLK2 (Kallikrein-2) were all greatly induced by YAP overexpression (Fig. 2.7B), suggesting that YAP promotes AR activation.

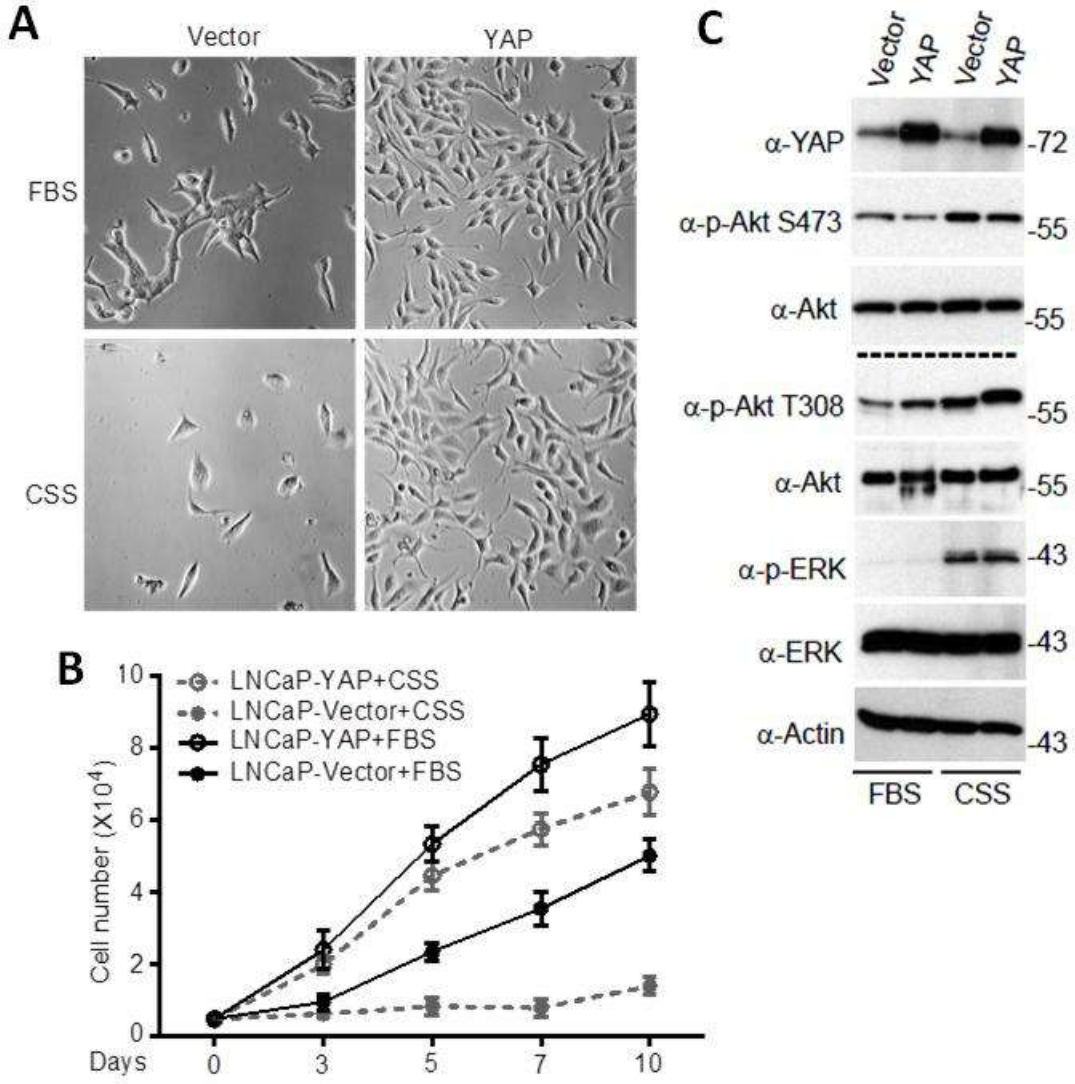

Figure 2.6 YAP promotes androgen-insensitive growth and Akt activation in LNCaP cells.

A, Representative photos of LNCaP cells expressing vector or YAP that have been cultured under normal (FBS) or androgen deprivation (CSS) media for 3 (FBS) or 5 (CSS) days. FBS: fetal bovine serum; CSS: charcoal-stripped serum.

B, Cell proliferation curve for various LNCaP cells.

C, LNCaP cells expressing vector or YAP were cultured under normal (FBS) or androgen deprivation (CSS) media for 3 days. The total lysates were probed with the indicated antibodies.

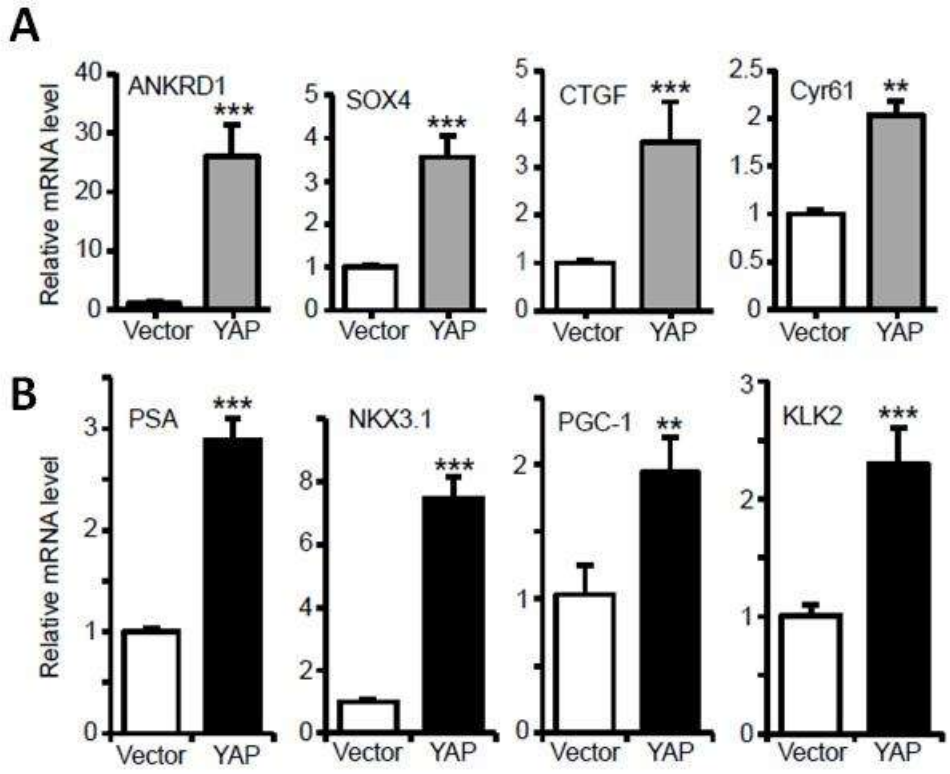

Figure 2.7 YAP induces its targets and AR activation in LNCaP cells.

A, Relative mRNA levels of known targets of YAP (by quantitative RT-PCR) in LNCaP cells expressing vector or YAP.

B, Relative mRNA levels of known targets of androgen receptor (by quantitative RT-PCR) in LNCaP cells expressing vector or YAP. Quantitative data are expressed as the mean ± s.e.m of three independent experiments. ***: $p<0.001$, **: $p<0.01$ (t-test).

2.3.4 Upregulation of YAP in castration-resistant prostate cancer cells

We further assessed the extent to which YAP expression/activity is altered during androgen-sensitive to castration-resistant progression. For this purpose, we took advantage of a well-established prostate cancer cell model system. LNCaP cells grow slowly and completely rely on androgen, whereas LNCaP-C81 and LNCaP-C4-2 sub-lines (both of which are castration-resistant) grow aggressively even under androgen-deprivation conditions. These cancer cell models closely represent the transition of the initial androgen-sensitive disease to castration-resistant state (61, 62). Interestingly, we found that, compared to LNCaP cells, YAP expression levels were dramatically upregulated in both LNCaP-C4-2 and LNCaP-C81 castration-resistant cells (Fig. 2.8A). Phosphorylation of YAP on S127 (the major phosphorylation site for the Hippo pathway) was proportionally increased. Cell fractionation assays confirmed that the cytoplasmic-nuclear localization of YAP was not significantly altered (Fig. 2.8B). In line with this observation, no change was detected in the expression and activity of upstream Hippo core components (Fig. 2.8A and data not shown). Consistent with previous studies (63), AR levels were increased in LNCaP-C4-2 and LNCaP-C81 cells compared to parental LNCaP cells (Fig. 2.8A). Finally, qRT-PCR showed that YAP but not its paralog TAZ mRNA levels were significantly elevated in LNCaP-C4-2 and LNCaP-C81 cells, indicating that transcriptional regulation was involved in YAP upregulation (Fig. 2.8C and data not shown). Consistently, YAP targets were induced in LNCaP-C4-2 cells (Fig. 2.8D). TEAD4 but not TEAD1-3 mRNA was upregulated in LNCaP-C4-2 cells (Fig. 2.8E). YAP protein stability was

similar in both LNCaP and LNCaP-C4-2 cells (data not shown). Together, these results suggest that YAP was transcriptionally upregulated during the transition of LNCaP cells to castration-resistant growth.

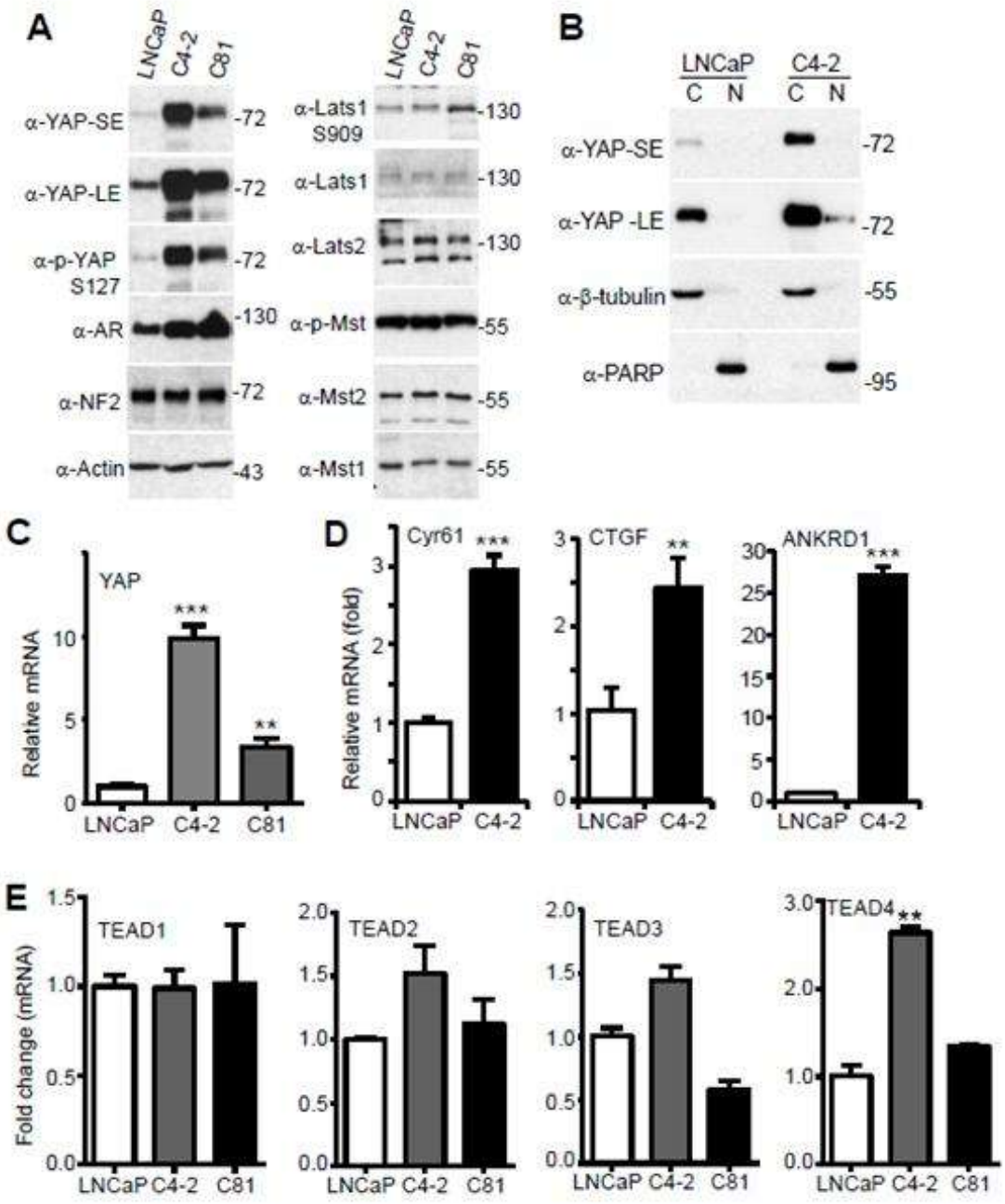

Figure 2.8 YAP is upregulated in castration-resistant prostate cancer cells.

A, LNCaP (androgen-sensitive) and LNCaP-C81/LNCaP-C4-2 (castration-resistant) cell lysates were probed with the indicated antibodies. SE: short exposure; LE: long exposure (A,B).

B, Cell fractionation assay in LNCaP and C4-2 cells. The cells were harvested at 70-80 percent confluence. β-tubulin and PARP serve as cytoplasmic and nuclear markers, respectively. C: cytoplasmic; N: nuclear.

C,D, Quantitative RT-PCR of YAP and its known targets in LNCaP and castration-resistant sublines.

E, Quantitative RT-PCR of TEAD1-4 in LNCaP and castration-resistant sublines.

2.3.5 YAP promotes castration-resistant growth *in vivo*

We next evaluated the influence of YAP on castration resistance in animals. LNCaP-vector control and –YAP-expressing cells were subcutaneously inoculated into castrated male mice (SCID). As expected, most of the mice (except one) injected with LNCaP-vector cells did not form palpable tumors (n=6). However, about 67% (6/9) mice injected with LNCaP-YAP cells grew large tumors at the end point of the experiment (Fig. 2.9A,B). The tumors on the mice harboring YAP-expressing LNCaP cells were visible at one month post-injection (data not shown). Histopathological examination revealed extensive tumor necrosis and hemorrhage (Fig. 2.9C, H&E staining), which is an indicator of aggressiveness. Most of these tumor cells express AR and YAP (Fig. 2.9C). These data strongly suggest that YAP confers castration-resistant growth of prostate cancer cells *in vitro* and *in vivo*.

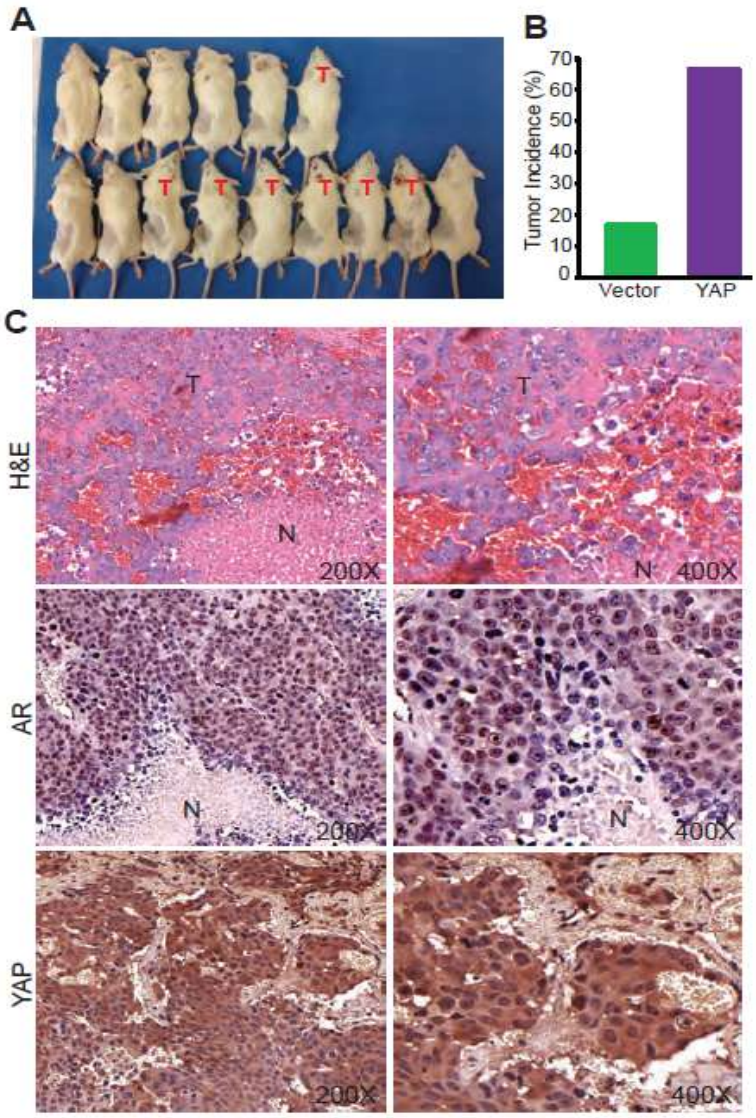

Figure 2.9 YAP confers castration resistance *in vivo.*

A, Castrated male SCID mice were implanted LNCaP-vector (top 6 mice) or LNCaP-YAP-expressing (bottom row) cells and photographed at 8 weeks post injection. T marks the tumor-harboring mice.

B, Tumor incidence of mice in A.

C, Hematoxylin and Eosin (H&E) and IHC staining of androgen receptor (AR) and YAP. T: tumor area; N: necrotic area.

2.3.6 YAP knockdown impairs migration and invasion in castration-resistant prostate cancer cells

To explore the biological significance of YAP upregulation in castration-resistant prostate cancer cells, we reduced YAP expression by shRNA (constitutive) or siRNA (transient) in LNCaP-C4-2 cells (Fig. 2.10A,B). Using Transwell and Matrigel assays, we demonstrated that YAP knockdown greatly impaired migration and invasion in LNCaP-C4-2 prostate cancer cells (Fig. 2.10C-J). These data, together with gain-of-function of YAP (Figs. 2.3-7), suggest that YAP plays an important role in motility and invasion in prostate cancer cells.

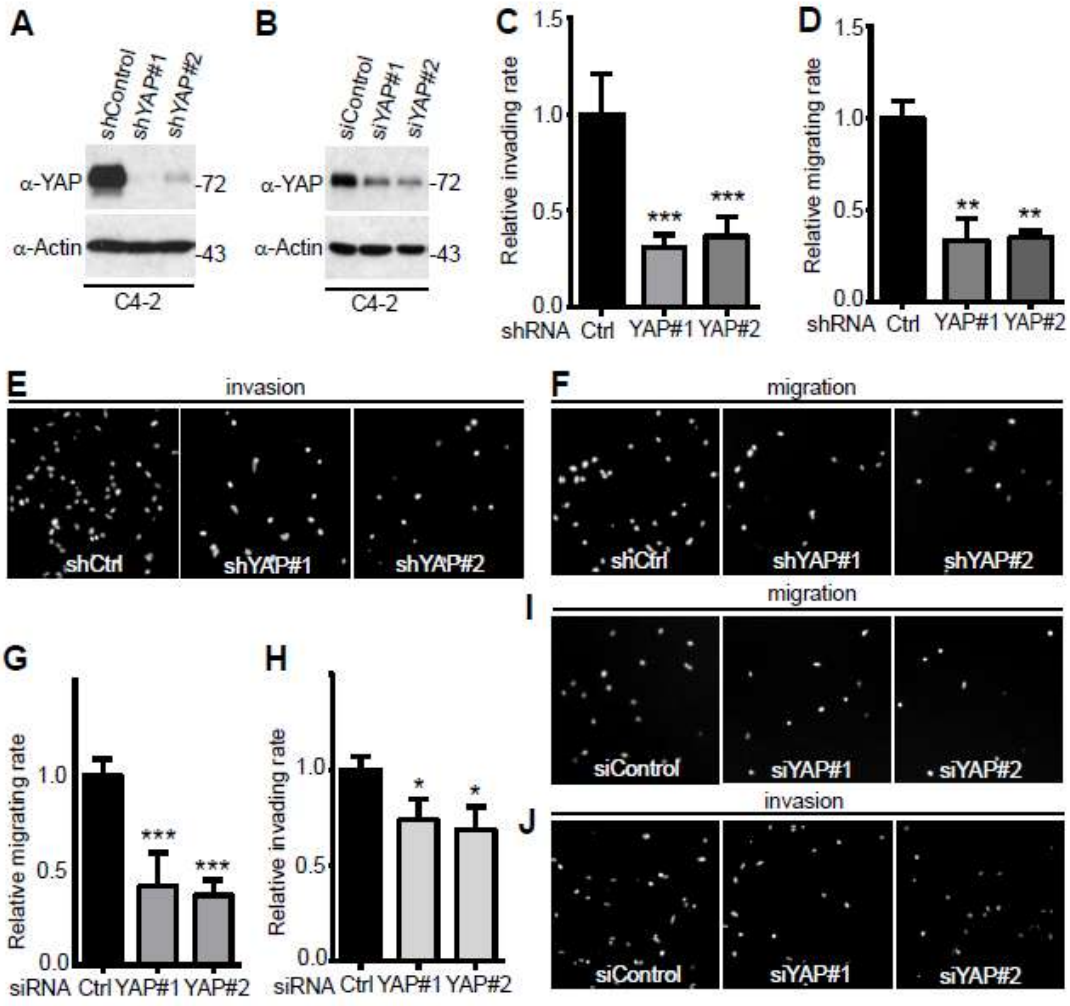

Figure 2.10 YAP knockdown in LNCaP-C4-2 cells impairs cell migration and invasion.

A, Establishment of cells stably expressing shRNA vector, and shRNAs against YAP (shYAP#1 and shYAP#2) in LNCaP-C4-2 cells.

B, LNCaP-C4-2 cells were transiently transfected with control siRNA or siRNA targeting YAP and YAP expression were analyzed by Western blotting.

C-F, Cell migration and invasion assays with LNCaP-C4-2 cells established in A.

G-J, Cell migration and invasion assays with LNCaP-C4-2 cells transfected with siRNA in B. Cell migration assays with Transwell and invasion assays with Matrigel were performed as we previously described(64). Migrating and invading cells were stained with DAPI, and representative fields are shown. Data are expressed as the mean ± s.e.m. of three independent experiments. ***: $p<0.001$, **: $p<0.01$, *: $p<0.05$ (t-test).

2.3.7 YAP is essential for castration-resistant growth of prostate cancer cells

The upregulation of YAP in castration-resistant cell lines led us to further determine whether YAP is required for growth without androgens in these cells. Under normal growth conditions, LNCaP-C4-2 cells with YAP knockdown showed only moderately slower proliferation than control LNCaP-C4-2 cells with YAP expression (Fig. 2.11A, top panels, B). However, while LNCaP-C4-2 cells were still able to proliferate (albeit at a slow rate) in the absence of androgens (CSS media), YAP knockdown cells failed to divide under androgen deprivation conditions (Fig. 2.11A,B). Consistent with this observation, LNCaP-C4-2 cells with reduced YAP form colonies well in soft agar with complete serum (Fig. 2.11C,D); however, these cells failed to grow under CSS conditions (Fig. 2.11E,F). Again, LNCaP-C4-2 control cells, but not LNCaP-C-2 cells lacking YAP, formed colonies even when androgens were removed (Fig. 2.11E,F). In total, these studies implicate that YAP is essential for castration-resistant growth of prostate cancer cells.

Consistent with our observations that YAP activated AR targets (Fig. 2.7B), YAP knockdown reduced basal levels of PSA and NKX3.1 mRNA and partially blocked the AR targets induced by R1881 (Fig. 2.12), further suggesting that YAP regulates AR signaling activity.

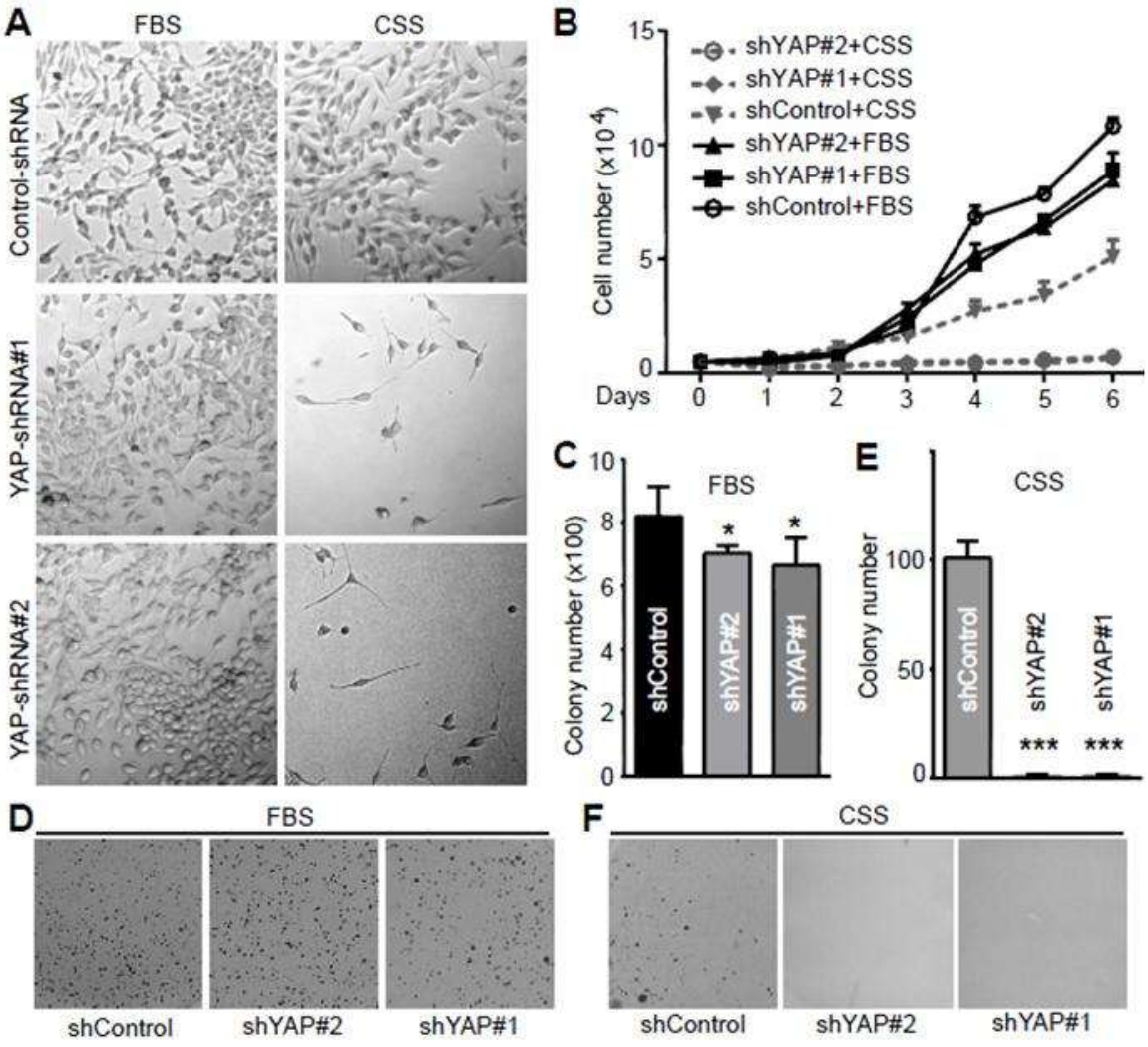

Figure 2.11 YAP is required for castration-resistant growth of LNCaP-C4-2 cells.

A, Representative photos of LNCaP-C4-2 cells expressing control shRNA or YAP shRNA that have been cultured under normal (FBS) or androgen deprivation (CSS) medium for 5 days. FBS: fetal bovine serum; CSS: charcoal stripped serum.

B, Cell proliferation curve of various LNCaP-C4-2 cells.

C-F, Anchorage-independent growth assay of LNCaP-C4-2 cells in soft agar under normal (FBS) or androgen deprivation (CSS) conditions.

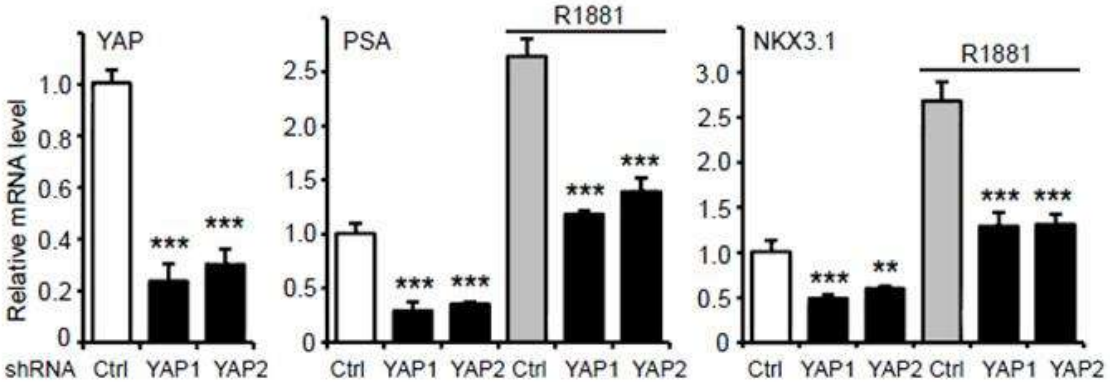

Figure 2.12 YAP partially blocks the AR targets induced by androgen analog.

Quantitative RT-PCR of YAP, PSA and NKx3.1 in LNCaP-C4-2 cells. Control and YAP knockdown cells lines were cultured in serum-free medium for 24 h and treated with or without R1881 (1 nM) for an additional 24 h. Data were derived from three independent experiments and expressed as mean ± s.e.m. *: $p<0.05$; **: $p<0.01$; ***: $p<0.001$ (t-test) when compared to control.

2.3.8 YAP is required for ERK-RSK signaling activation upon androgen depletion in LNCaP-C4-2 cells

We next explored the downstream signaling of YAP in castration-resistant growth of prostate cancer cells. The PTEN/Akt axis and MEK-ERK signaling are critical regulators in prostate tumor survival and progression (13, 65). Both Akt and MEK-ERK pathways have been recently linked with YAP activity (34, 49, 50, 66). Interestingly, we found that both Akt and ERK-RSK signaling pathways were strongly activated upon androgen depletion (Fig. 2.13A,B), suggesting that LNCaP-C4-2 cells proliferated without androgen, at least in part, by activating these survival pathways. Importantly, ERK1/2 and downstream RSK1/2 activation (revealed by phosphorylation) was largely blocked in YAP knockdown cells when androgens were removed (Fig. 2.13B). However, Akt activity was only moderately reduced when YAP was knocked down (Fig. 2.13A). Together, these data suggest that YAP is required for ERK-RSK activation in LNCaP-C4-2 cells under androgen depletion conditions.

To determine the functional role of ERK activation upon androgen depletion, we inhibited MEK-ERK signaling with the inhibitor U0126 and analyzed migratory and invasive activity in LNCaP-C4-2 cells. ERK inhibition partially suppressed migration under normal conditions and to a greater extent in media without androgens (Fig. 2.14A,B). Interestingly, treatment with U0126 had no effect on invasion under complete media, however, U0126 greatly impaired the invasive ability of LNCaP-C4-2 cells under androgen-deprivation conditions (Fig. 2.14C,D).

As expected, knockdown of YAP significantly reduced migration and invasion in LNCaP-C4-2 cells (Fig. 2.14A-D). Taken together, our data indicate that ERK activation (probably downstream YAP) is essential for LNCaP-C4-2 cells to promote survival and migration/invasion under androgen depletion conditions.

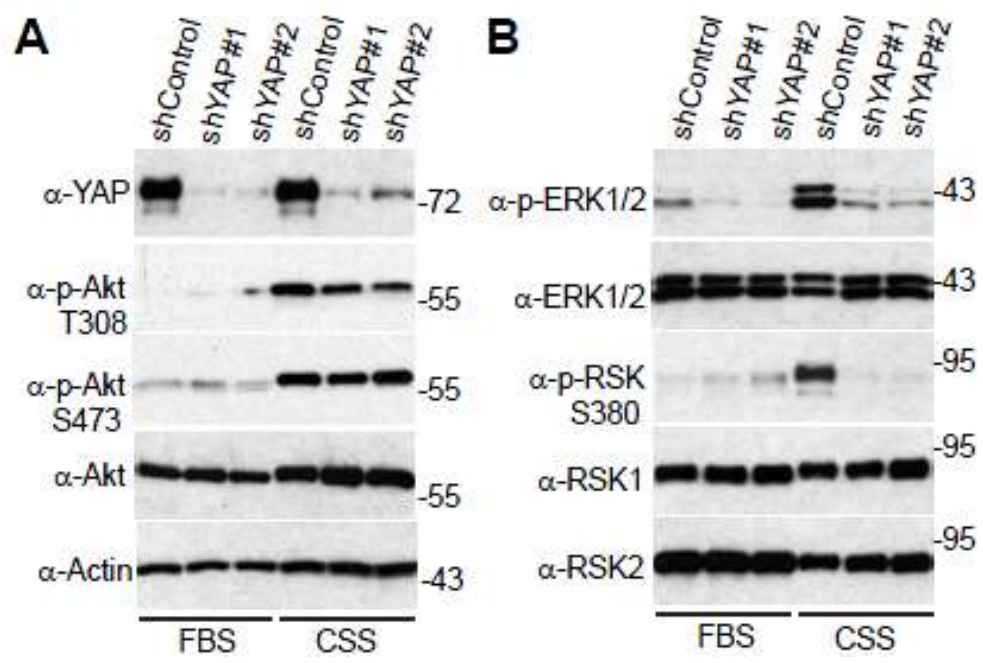

Figure 2.13 YAP is required for ERK-RSK activation upon androgen depletion in LNCaP-C4-2 cells.

A,B, Cells were harvested at day 3 under normal (FBS) or androgen-depleted (CSS) conditions and the total lysates were probed with the indicated antibodies.

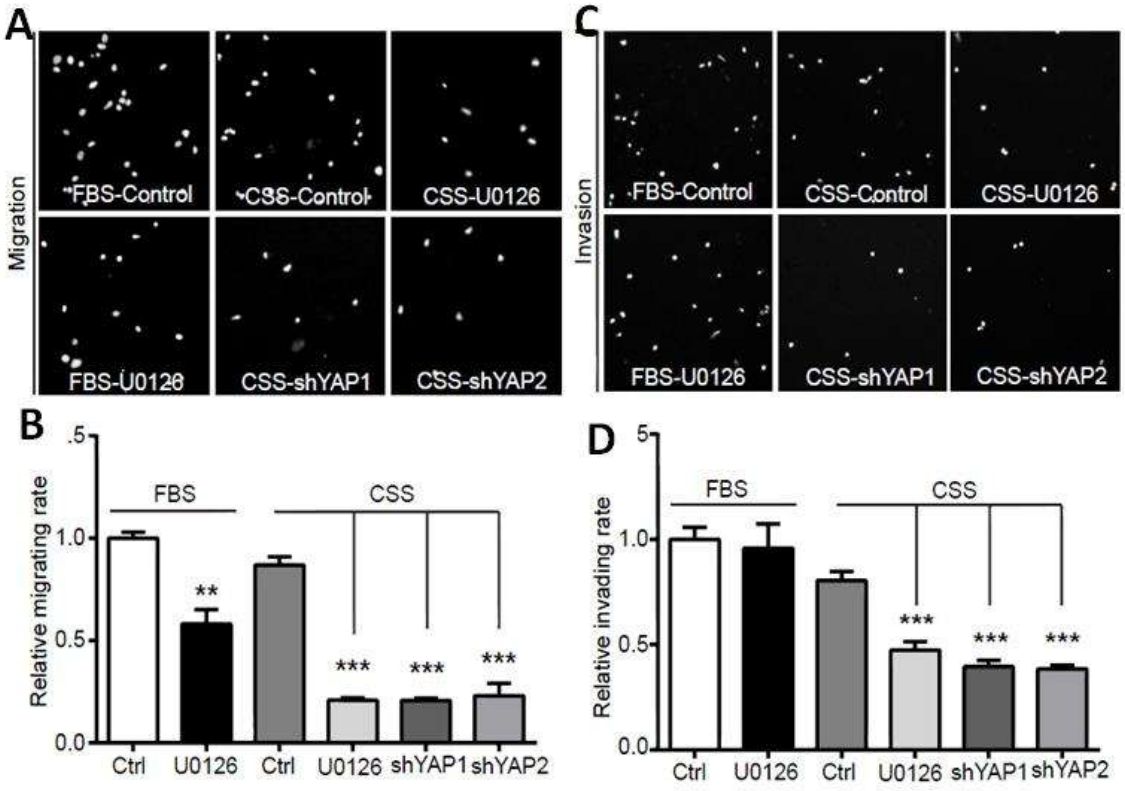

Figure 2.14 MEK-ERK inhibitor largely reduces migration and invasion ability of LNCaP-C4-2 cells under androgen-deprivation condition.

A-D, Cell migration (A,B) and invasion (C,D) assays under normal (FBS) and androgen-deprivation (CSS) conditions with or without MEK-ERK inhibitor U0126. FBS: fetal bovine serum; CSS: charcoal stripped serum. ***: $p<0.001$(t-test); **: $p<0.01$(t-test) when compared to control.

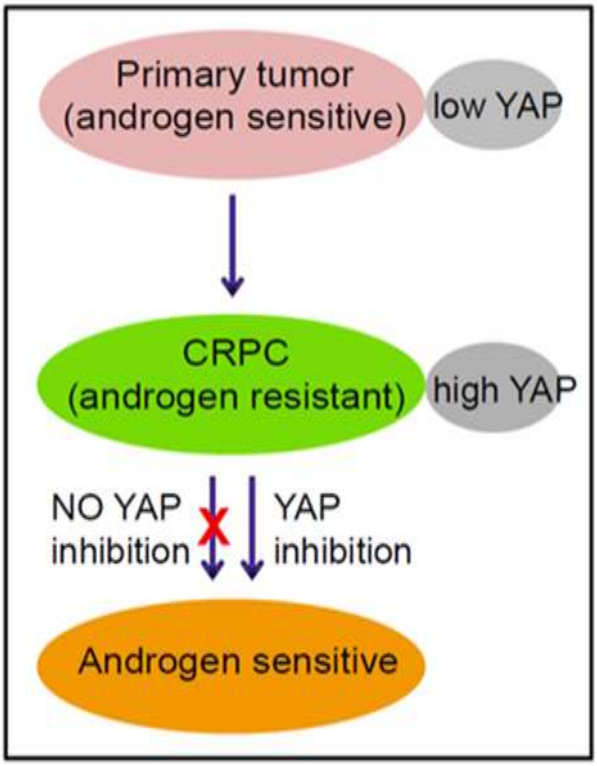

Figure 2.15 A model for YAP signaling in castration-resistant prostate cancer.

2.3.9 Activated YAP promotes mouse prostate cell proliferation at early age but is not sufficient to promote tumorigenesis in the mouse prostate

Having established the biological function of YAP in prostate tumorigenesis and CRPC in cell culture and immunodeficient mouse, we further explored role of Hippo-YAP signaling in prostate tumorigenesis by genetic transgenic mouse models. First, we want to examine whether activated YAP is sufficient to induce mouse prostate tumorigenesis or PIN. We crossed the PB-rtTA male mice to Tet-on YAP-S127A female mice to generate prostate-specific bi-transgenic mice (Fig. 2.16). Since rtTA is located downstream of the PB promoter, it is specifically expressed in prostate tissue. As a result, in the presence of doxycycline (administered through drinking water), rtTA binds to the tetracycline response element and produces high levels of hyper-active YAP-S127A (Fig. 2.16).

After 10 days induction of doxycycline, activated YAP is more obviously detected in the epithelial cells of mice prostate compared to the control mice, and ki67 staining showed increased proliferating cells (Fig. 2.17A). At 1 month, YAP is more dramatically expressed in the transgenic mice prostate compared to the control mice, and also more proliferating cells were detected (Fig. 2.17B), indicating YAP stimulates prostate epithelial cell proliferation at the early state of prostate development. However, after 14 months induction, we did not observe any PIN lesion or adenocarcinoma formation in the mouse prostate although YAP is still highly expressed (Fig. 2.18), suggesting that YAP is not sufficient to promote prostate tumorigenesis in our transgenic mouse model.

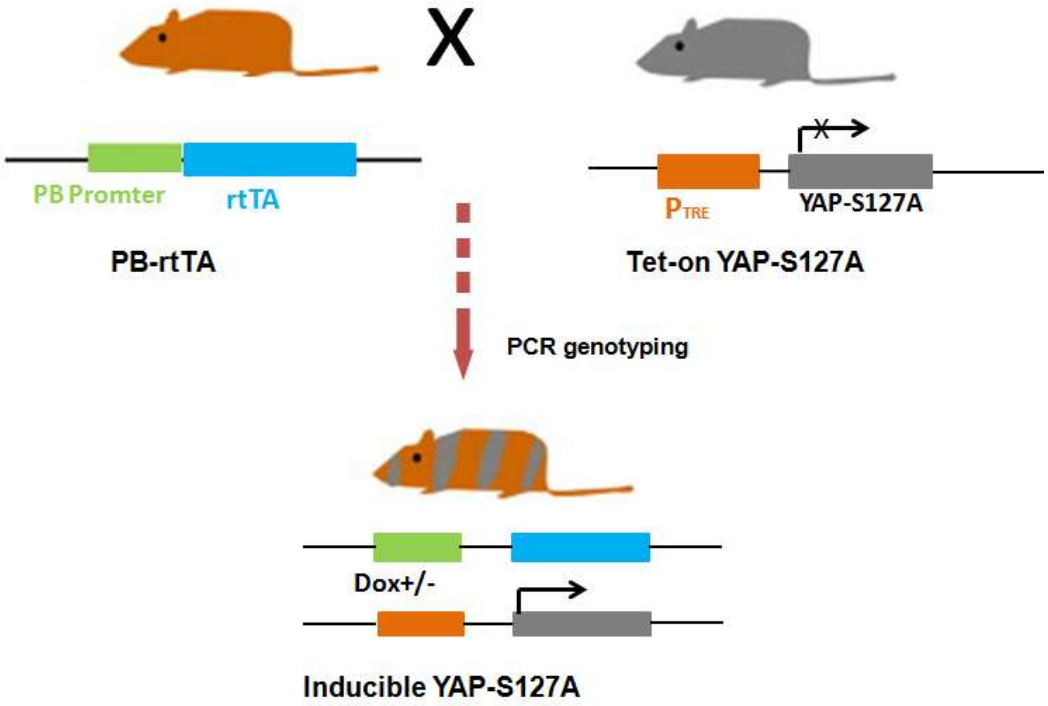

Figure 2.16 Generation of prostate-specific Tet-on inducible YAP-S127A mice.

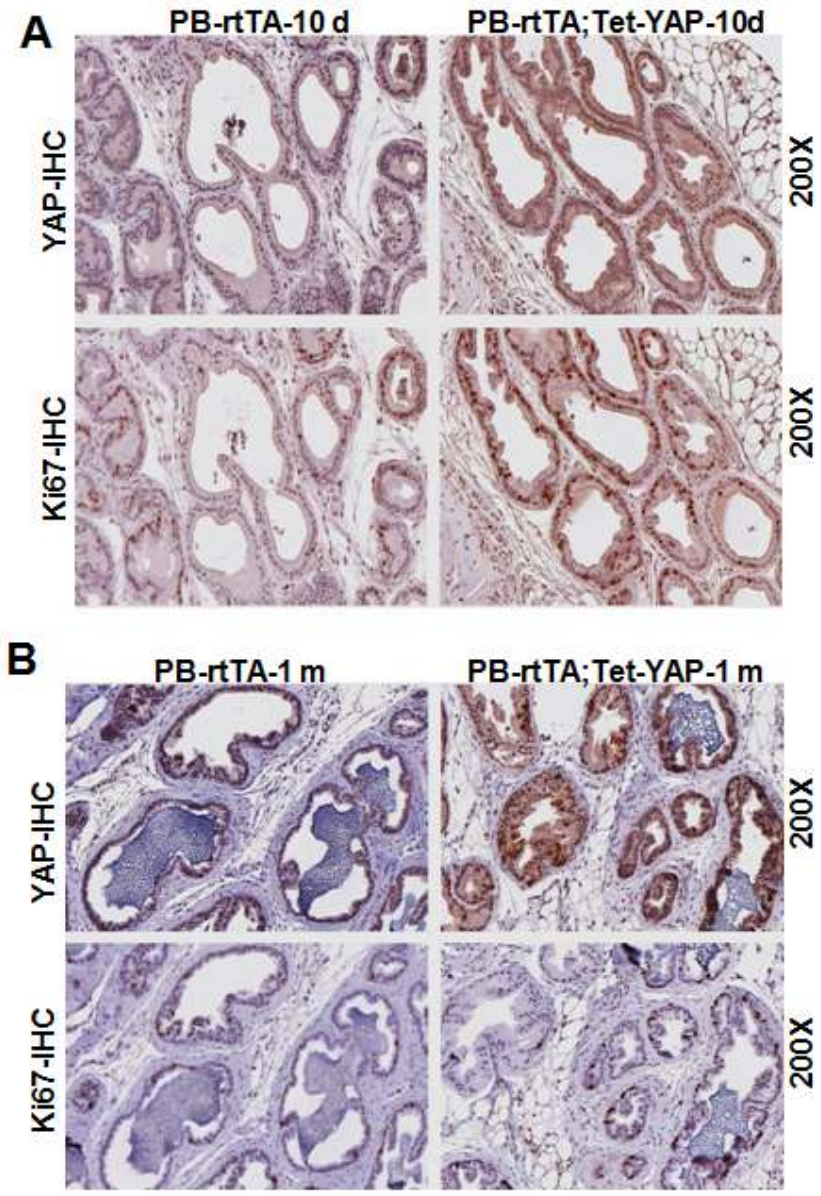

Figure 2.17 Doxycycline induces YAP expression and epithelial cell proliferation at early stage.

A, Adult single (left) or double (right) transgenic mice were fed with Doxycycline water for 10 days, and prostate tissue were analyzed for histology. YAP or ki67 IHC staining were performed.

B, Adult single (left) or double (right) transgenic mice were fed with Doxycycline water for 1 month, and prostate tissue were analyzed for histology. YAP or ki67 IHC staining were performed.

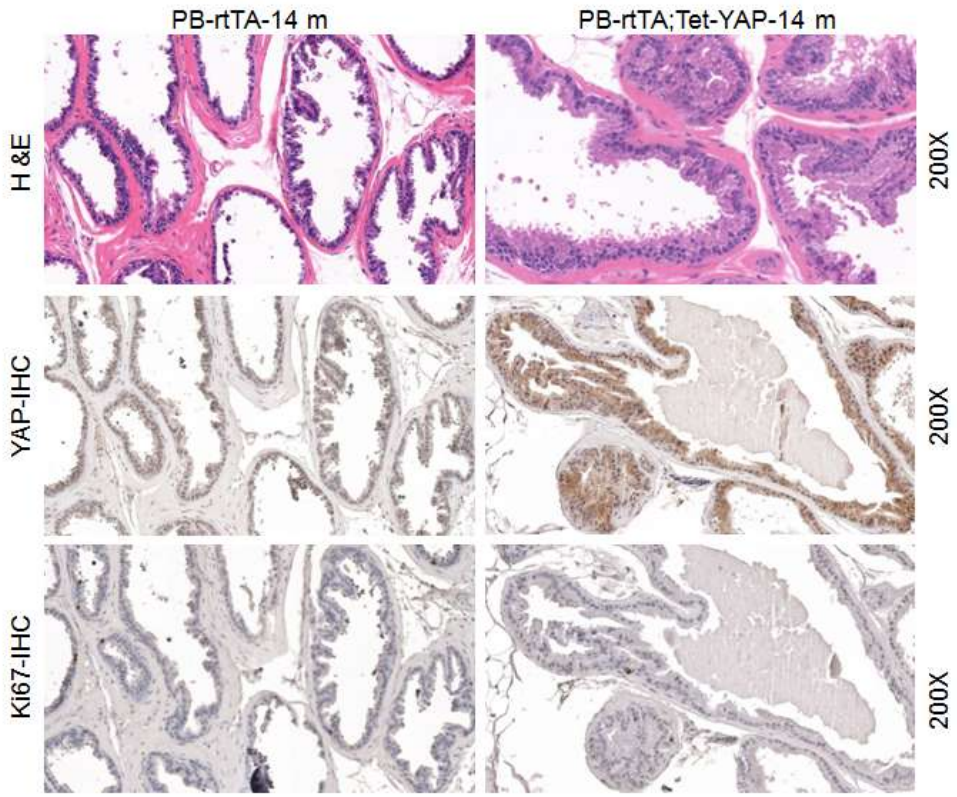

Figure 2.18 Activated YAP is not sufficient to promote tumorigenesis in the mouse prostate.

Adult single (left) or double (right) transgenic mice were fed with Doxycycline water for 14 months, and prostate tissue were analyzed for histology. Hematoxylin & Eosin staining and YAP or ki67 IHC staining were performed.

2.3.10 MST1/2 deletion is not sufficient to promote tumorigenesis in the mouse prostate

We further explored whether deletion of tumor suppressor genes MST1/2 is able to promote tumorigenesis in the mouse prostate. The $Mst1^{flox/flox}$; $Mst2^{flox/flox}$ mice were mated with male PB-Cre mice (Fig. 2.19). PCR-based genotyping was used to determine the genotype of the offspring. Homozygous prostate-specific deletion of Mst1/Mst2 were generated by breeding male PB-Cre+; $Mst1^{flox/flox}$; $Mst2^{flox/flox}$ to $Mst1^{flox/flox}$; $Mst2^{flox/flox}$ mice. Littermates without PB-Cre were used as controls.

As shown in (Fig. 2.20A), 45 days deletion of MST1/2 in prostate increased cell proliferation indicated by ki67 staining. After 1 year deletion of MST1/2, still no PIN or adenocarcinoma observed in the mouse prostate (Fig. 2.20B). Our results suggest that specific deletion of MST1/2 in the prostate promotes cell proliferation at early age but is not sufficient to induce prostate tumorigenesis.

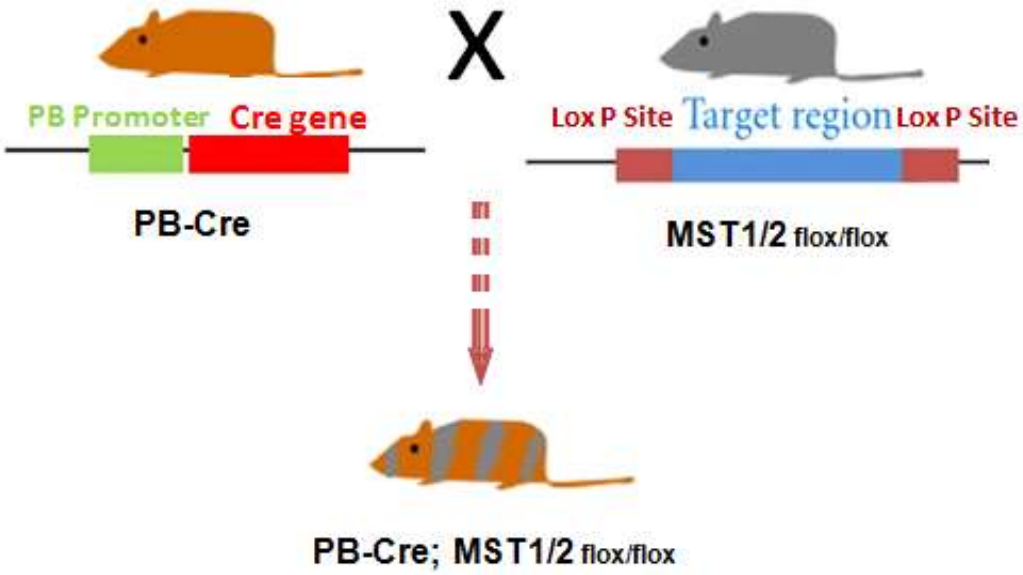

Figure 2.19 Generation of prostate-specific MST1/2 deletion.

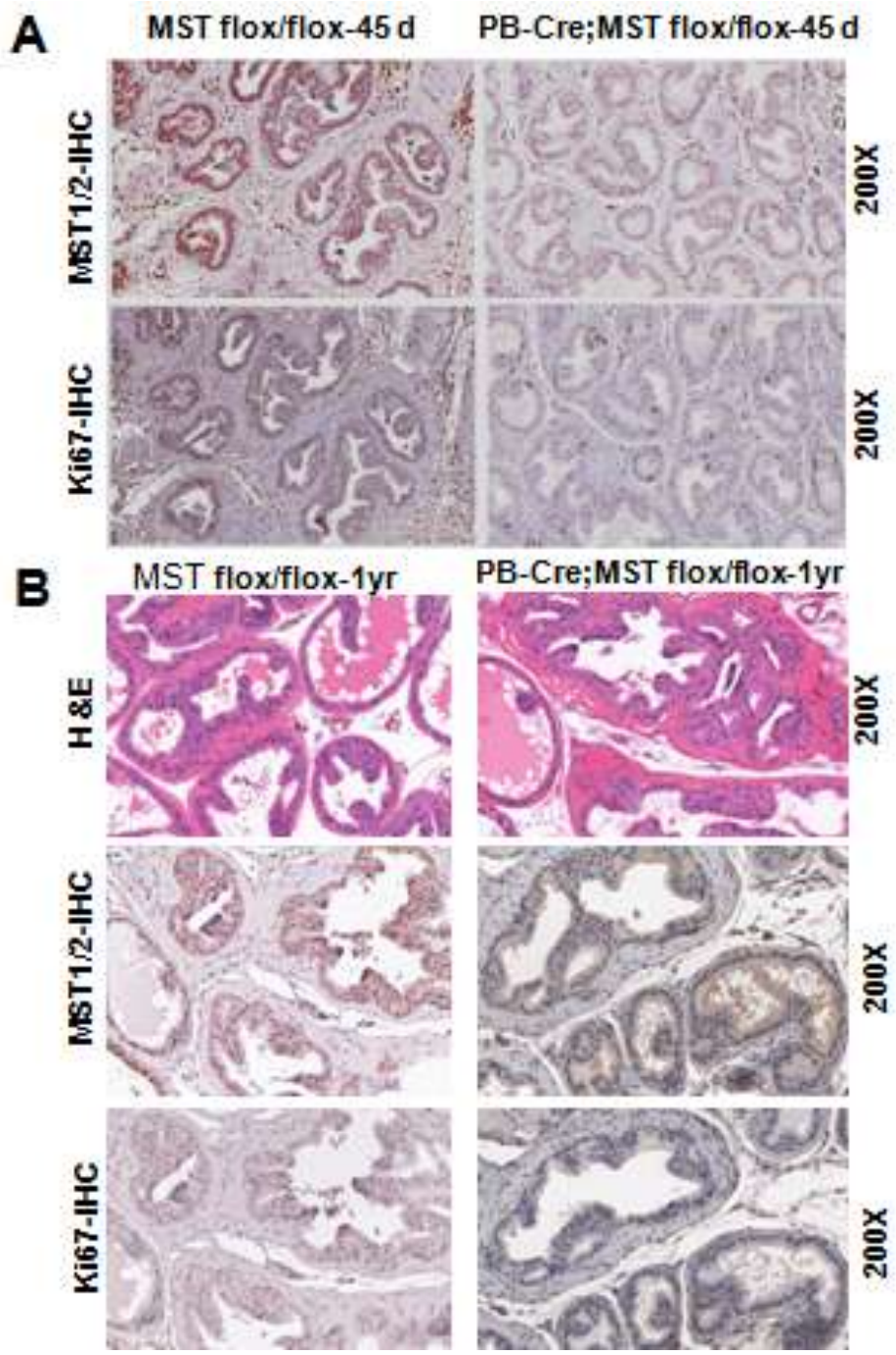

Figure 2.20 MST1/2 specific deletion is not sufficient to promote tumorigenesis in the mouse prostate.

A, Adult control (left) or prostate specific MST1/2 deletion (right) mice with conditional MST1/2 knockout for 45 days, and prostate tissue were analyzed for histology. MST1/2 or ki67 IHC staining were performed.

B, Adult controls (left) or prostate specific MST1/2 deletion (right) mice with conditional MST1/2 knockout for 1 year, and prostate tissue were analyzed for histology. Hematoxylin & Eosin staining and MST1/2 or ki67 IHC staining were performed.

DISCUSSION

Androgen deprivation therapy initially decreases the volume of both primary and metastatic lesions, however most men experience eventual relapse. Recurring prostate cancer is typically ‘castration-resistant’ since removal of testicular androgen by chemical or surgical castration does not affect tumor growth or metastasis. Ultimately, the vast majority of CRPC is lethal. Thus, there is an urgent need to identify drug targets, and develop new therapeutic strategies to treat CRPC. Although the underlying mechanisms of castration resistance are not fully understood, both androgen receptor-dependent and –independent signaling pathways are known to be involved (67). Androgen receptor overexpression, activation and androgen secretion are the major contributors to androgen receptor-dependent CRPC (67-69). For example, androgen receptor selectively upregulates M-phase cell-cycle genes to promote CRPC (70). Interestingly, a recent study found that a gain-of-function mutation in dihydrotestosterone (the most potent androgen) synthesis partially accounts for castration resistance (71). However, some other studies have challenged the androgen receptor-dependent mechanism, as castration induces many kinases activation (72) and increases the expression of anti-apoptotic genes independent of the androgen receptor (73). Furthermore, prostate cancer stem cells have been proposed to be the origin of prostate cancer progression and they may not express androgen receptor (74). Our current study implicates YAP as a potent regulator for CRPC *in vitro* and *in vivo* (Figs. 2.3-9) and in clinical samples (Figs.

2.1,2), thus identifying YAP as a potential alternative regulator/pathway for the acquisition of castration resistance of prostate tumor cells.

Hippo-YAP signaling is often deregulated in cancer and is a potential target for cancer therapy (37, 75, 76). Among the components, the YAP/TEAD complex represents the most attractive target for several reasons. First, TEAD transcription factors are required for YAP's oncogenic activity both in cell culture and *in vivo* (77, 78). Second, TEAD is largely dispensable during normal tissue growth in the mouse liver (78) and in *Drosophila* (64) (i.e., TEAD becomes critical only when YAP is hyperactivated/overexpressed). Thus, there is a strong rationale for developing YAP-TEAD complex-disrupting agents as anti-cancer therapeutics against YAP-driven oncogenesis. Indeed, Liu-Chittenden *et al*. screened a small molecule library (consisting of 3,300 FDA-approved drugs) for agents that inhibit YAP/TEAD activity in a cell-based assay (78). Verteporfin was identified as an compound effective at preventing hepatic tumorigenesis driven by YAP overexpression (78) and the growth of xenograft tumors in immunodeficient mice (56, 57). Thus, verteporfin is an effective pharmacologic approach to inhibit YAP signaling, and these studies strongly support the feasibility of targeting YAP in human cancer in which Hippo-YAP is deregulated. Importantly, the current study showed that depletion of YAP could cause castration-resistant prostate cancer cells to stop growing and become androgen-sensitive (Figs. 2.6,10,11,13). Therefore, inhibiting YAP (e.g. by verteporfin)

combined with hormonal therapy is a potential novel therapeutic strategy for prostate cancer patients with CRPC (Fig. 2.15).

Previous studies, including ours, demonstrated that YAP is overexpressed or hyperactivated in prostate tumor samples (24, 32). Furthermore, Lats2 expression is significantly lower in metastatic prostate tissues when compared to normal prostate samples (79). Interestingly, Lats2 and Mst1 have been shown to be associated with androgen receptor and regulate its activity (80, 81). These reports suggest that the Hippo-YAP pathway plays a role in the pathogenesis of prostate cancer. This study adds further evidence showing that the Hippo effector YAP regulates cell motility, invasion and castration-resistant growth of prostate cancer cells. Together, these studies demonstrated the biological significance of the Hippo-YAP signaling in prostate cancer. There are several questions that need to be addressed. How is YAP upregulated in castration-resistant prostate cancer cells? Our observations suggest that the upregulation of YAP is androgen receptor-independent and methylation is dispensable for YAP transcription in LNCaP and C4-2 cells (L.Z. and J.D., unpublished observations). Large scale studies failed to identify YAP amplification and mutation in CRPC. Therefore, future studies are needed to address the underlying mechanisms of YAP upregulation in CRPC. Furthermore, how is Hippo-YAP deregulated and what are the clinical outcomes? Answers and understanding from these questions may provide additional insights into the pathogenesis of prostate cancer.

Genetically engineered mouse alleles of the most Hippo components are available and these animal models provided compelling evidence showing the importance of Hippo-YAP signaling in human malignancies (18-20, 23-27, 82, 83). However, no single such model has been developed in the prostate. Our transgenic mouse studies showed that activated YAP or specific deletion of MST1/2 promotes mouse prostate cell proliferation at early age but is not sufficient to promote tumorigenesis in the mouse prostate. It is possible that only YAP activation or loss of MST1/2 is not sufficient to induce prostate tumorigenesis, and combination of additional alleles is necessary to induce prostate cancer. Since PTEN is an important tumor suppressor in prostate cancer, and specific deletion of PTEN in prostate leads to metastatic prostate cancer and castration resistance (84, 85), we are currently trying to combine the PTEN alleles with the Hippo (loss-of-function)-YAP (gain-of-function) signaling. A recent report showed that Mst1/2 deletion or YAP activation could downregulate PTEN, suggesting a potential link between Hippo-YAP pathway and PTEN signaling (66).

References

1. Kyprianou N, English HF, and Isaacs JT. Programmed cell death during regression of PC-82 human prostate cancer following androgen ablation. *Cancer research.* 1990;50(12):3748-53.
2. Isaacs JT. The biology of hormone refractory prostate cancer. Why does it develop? *The Urologic clinics of North America.* 1999;26(2):263-73.
3. Oh WK, and Kantoff PW. Management of hormone refractory prostate cancer: current standards and future prospects. *The Journal of urology.* 1998;160(4):1220-9.
4. Vogiatzi P, Cassone M, Claudio L, and Claudio PP. Targeted therapy for advanced prostate cancer: Looking through new lenses. *Drug news & perspectives.* 2009;22(10):593-601.
5. Petrylak DP. New paradigms for advanced prostate cancer. *Reviews in urology.* 2007;9 Suppl 2(S3-S12.
6. Linja MJ, Savinainen KJ, Saramaki OR, Tammela TL, Vessella RL, and Visakorpi T. Amplification and overexpression of androgen receptor gene in hormone-refractory prostate cancer. *Cancer research.* 2001;61(9):3550-5.
7. Visakorpi T, Hyytinen E, Koivisto P, Tanner M, Keinanen R, Palmberg C, Palotie A, Tammela T, Isola J, and Kallioniemi OP. *In vivo* amplification of the androgen receptor gene and progression of human prostate cancer. *Nature genetics.* 1995;9(4):401-6.

8. Koivisto P, Kononen J, Palmberg C, Tammela T, Hyytinen E, Isola J, Trapman J, Cleutjens K, Noordzij A, Visakorpi T, et al. Androgen receptor gene amplification: a possible molecular mechanism for androgen deprivation therapy failure in prostate cancer. *Cancer research.* 1997;57(2):314-9.

9. Zhao XY, Malloy PJ, Krishnan AV, Swami S, Navone NM, Peehl DM, and Feldman D. Glucocorticoids can promote androgen-independent growth of prostate cancer cells through a mutated androgen receptor. *Nature medicine.* 2000;6(6):703-6.

10. Robzyk K, Oen H, Buchanan G, Butler LM, Tilley WD, Mandal AK, Rosen N, and Caplan AJ. Uncoupling of hormone-dependence from chaperone-dependence in the L701H mutation of the androgen receptor. *Molecular and cellular endocrinology.* 2007;268(1-2):67-74.

11. Steinkamp MP, O'Mahony OA, Brogley M, Rehman H, Lapensee EW, Dhanasekaran S, Hofer MD, Kuefer R, Chinnaiyan A, Rubin MA, et al. Treatment-dependent androgen receptor mutations in prostate cancer exploit multiple mechanisms to evade therapy. *Cancer research.* 2009;69(10):4434-42.

12. Thomas GV, Horvath S, Smith BL, Crosby K, Lebel LA, Schrage M, Said J, De Kernion J, Reiter RE, and Sawyers CL. Antibody-based profiling of the phosphoinositide 3-kinase pathway in clinical prostate cancer. *Clinical cancer research : an official journal of the American Association for Cancer Research.* 2004;10(24):8351-6.

13. Mulholland DJ, Dedhar S, Wu H, and Nelson CC. PTEN and GSK3beta: key regulators of progression to androgen-independent prostate cancer. *Oncogene.* 2006;25(3):329-37.

14. Paweletz CP, Charboneau L, Bichsel VE, Simone NL, Chen T, Gillespie JW, Emmert-Buck MR, Roth MJ, Petricoin IE, and Liotta LA. Reverse phase protein microarrays which capture disease progression show activation of pro-survival pathways at the cancer invasion front. *Oncogene.* 2001;20(16):1981-9.

15. Kinkade CW, Castillo-Martin M, Puzio-Kuter A, Yan J, Foster TH, Gao H, Sun Y, Ouyang X, Gerald WL, Cordon-Cardo C, et al. Targeting AKT/mTOR and ERK MAPK signaling inhibits hormone-refractory prostate cancer in a preclinical mouse model. *The Journal of clinical investigation.* 2008;118(9):3051-64.

16. Greenberg NM, DeMayo F, Finegold MJ, Medina D, Tilley WD, Aspinall JO, Cunha GR, Donjacour AA, Matusik RJ, and Rosen JM. Prostate cancer in a transgenic mouse. *Proceedings of the National Academy of Sciences of the United States of America.* 1995;92(8):3439-43.

17. Kim MJ, Bhatia-Gaur R, Banach-Petrosky WA, Desai N, Wang Y, Hayward SW, Cunha GR, Cardiff RD, Shen MM, and Abate-Shen C. Nkx3.1 mutant mice recapitulate early stages of prostate carcinogenesis. *Cancer research.* 2002;62(11):2999-3004.

18. Zhou D, Conrad C, Xia F, Park JS, Payer B, Yin Y, Lauwers GY, Thasler W, Lee JT, Avruch J, et al. Mst1 and Mst2 maintain hepatocyte

quiescence and suppress hepatocellular carcinoma development through inactivation of the Yap1 oncogene. *Cancer cell.* 2009;16(5):425-38.

19. Song H, Mak KK, Topol L, Yun K, Hu J, Garrett L, Chen Y, Park O, Chang J, Simpson RM, et al. Mammalian Mst1 and Mst2 kinases play essential roles in organ size control and tumor suppression. *Proceedings of the National Academy of Sciences of the United States of America.* 2010;107(4):1431-6.

20. Lu L, Li Y, Kim SM, Bossuyt W, Liu P, Qiu Q, Wang Y, Halder G, Finegold MJ, Lee JS, et al. Hippo signaling is a potent *in vivo* growth and tumor suppressor pathway in the mammalian liver. *Proceedings of the National Academy of Sciences of the United States of America.* 2010;107(4):1437-42.

21. Song JY, Lee JH, Joe CO, Lim DS, and Chung JH. Retrotransposon-specific DNA hypomethylation and two-step loss-of-imprinting during WW45 haploinsufficiency-induced hepatocarcinogenesis. *Biochemical and biophysical research communications.* 2011;404(2):728-34.

22. Murakami H, Mizuno T, Taniguchi T, Fujii M, Ishiguro F, Fukui T, Akatsuka S, Horio Y, Hida T, Kondo Y, et al. LATS2 is a tumor suppressor gene of malignant mesothelioma. *Cancer research.* 2011;71(3):873-83.

23. Schlegelmilch K, Mohseni M, Kirak O, Pruszak J, Rodriguez JR, Zhou D, Kreger BT, Vasioukhin V, Avruch J, Brummelkamp TR, et al. Yap1 acts downstream of alpha-catenin to control epidermal proliferation. *Cell.* 2011;144(5):782-95.

24. Dong J, Feldmann G, Huang J, Wu S, Zhang N, Comerford SA, Gayyed MF, Anders RA, Maitra A, and Pan D. Elucidation of a universal size-control mechanism in Drosophila and mammals. *Cell.* 2007;130(6):1120-33.

25. Camargo FD, Gokhale S, Johnnidis JB, Fu D, Bell GW, Jaenisch R, and Brummelkamp TR. YAP1 increases organ size and expands undifferentiated progenitor cells. *Current biology : CB.* 2007;17(23):2054-60.

26. Overholtzer M, Zhang J, Smolen GA, Muir B, Li W, Sgroi DC, Deng CX, Brugge JS, and Haber DA. Transforming properties of YAP, a candidate oncogene on the chromosome 11q22 amplicon. *Proceedings of the National Academy of Sciences of the United States of America.* 2006;103(33):12405-10.

27. Tremblay AM, Missiaglia E, Galli GG, Hettmer S, Urcia R, Carrara M, Judson RN, Thway K, Nadal G, Selfe JL, et al. The Hippo transducer YAP1 transforms activated satellite cells and is a potent effector of embryonal rhabdomyosarcoma formation. *Cancer cell.* 2014;26(2):273-87.

28. Zender L, Spector MS, Xue W, Flemming P, Cordon-Cardo C, Silke J, Fan ST, Luk JM, Wigler M, Hannon GJ, et al. Identification and validation of oncogenes in liver cancer using an integrative oncogenomic approach. *Cell.* 2006;125(7):1253-67.

29. Steinhardt AA, Gayyed MF, Klein AP, Dong J, Maitra A, Pan D, Montgomery EA, and Anders RA. Expression of Yes-associated protein in common solid tumors. *Human pathology.* 2008;39(11):1582-9.

30. Fernandez LA, Northcott PA, Dalton J, Fraga C, Ellison D, Angers S, Taylor MD, and Kenney AM. YAP1 is amplified and up-regulated in hedgehog-associated medulloblastomas and mediates Sonic hedgehog-driven neural precursor proliferation. *Genes & development.* 2009;23(23):2729-41.

31. Xu MZ, Yao TJ, Lee NP, Ng IO, Chan YT, Zender L, Lowe SW, Poon RT, and Luk JM. Yes-associated protein is an independent prognostic marker in hepatocellular carcinoma. *Cancer.* 2009;115(19):4576-85.

32. Zhao B, Wei X, Li W, Udan RS, Yang Q, Kim J, Xie J, Ikenoue T, Yu J, Li L, et al. Inactivation of YAP oncoprotein by the Hippo pathway is involved in cell contact inhibition and tissue growth control. *Genes & development.* 2007;21(21):2747-61.

33. Zhang X, George J, Deb S, Degoutin JL, Takano EA, Fox SB, group AS, Bowtell DD, and Harvey KF. The Hippo pathway transcriptional co-activator, YAP, is an ovarian cancer oncogene. *Oncogene.* 2011;30(25):2810-22.

34. Zhang W, Nandakumar N, Shi Y, Manzano M, Smith A, Graham G, Gupta S, Vietsch EE, Laughlin SZ, Wadhwa M, et al. Downstream of mutant KRAS, the transcription regulator YAP is essential for neoplastic

progression to pancreatic ductal adenocarcinoma. *Science signaling.* 2014;7(324):ra42.

35. Lamar JM, Stern P, Liu H, Schindler JW, Jiang ZG, and Hynes RO. The Hippo pathway target, YAP, promotes metastasis through its TEAD-interaction domain. *Proceedings of the National Academy of Sciences of the United States of America.* 2012;109(37):E2441-50.

36. Chan SW, Lim CJ, Guo K, Ng CP, Lee I, Hunziker W, Zeng Q, and Hong W. A role for TAZ in migration, invasion, and tumorigenesis of breast cancer cells. *Cancer research.* 2008;68(8):2592-8.

37. Park HW, and Guan KL. Regulation of the Hippo pathway and implications for anticancer drug development. *Trends in pharmacological sciences.* 2013;34(10):581-9.

38. Yu FX, and Guan KL. The Hippo pathway: regulators and regulations. *Genes & development.* 2013;27(4):355-71.

39. Rosenbluh J, Nijhawan D, Cox AG, Li X, Neal JT, Schafer EJ, Zack TI, Wang X, Tsherniak A, Schinzel AC, et al. beta-Catenin-driven cancers require a YAP1 transcriptional complex for survival and tumorigenesis. *Cell.* 2012;151(7):1457-73.

40. Varelas X, Miller BW, Sopko R, Song S, Gregorieff A, Fellouse FA, Sakuma R, Pawson T, Hunziker W, McNeill H, et al. The Hippo pathway regulates Wnt/beta-catenin signaling. *Developmental cell.* 2010;18(4):579-91.

41. Imajo M, Miyatake K, Iimura A, Miyamoto A, and Nishida E. A molecular mechanism that links Hippo signalling to the inhibition of Wnt/beta-catenin signalling. *The EMBO journal.* 2012;31(5):1109-22.

42. Heallen T, Zhang M, Wang J, Bonilla-Claudio M, Klysik E, Johnson RL, and Martin JF. Hippo pathway inhibits Wnt signaling to restrain cardiomyocyte proliferation and heart size. *Science.* 2011;332(6028):458-61.

43. Konsavage WM, Jr., Kyler SL, Rennoll SA, Jin G, and Yochum GS. Wnt/beta-catenin signaling regulates Yes-associated protein (YAP) gene expression in colorectal carcinoma cells. *The Journal of biological chemistry.* 2012;287(15):11730-9.

44. Azzolin L, Zanconato F, Bresolin S, Forcato M, Basso G, Bicciato S, Cordenonsi M, and Piccolo S. Role of TAZ as mediator of Wnt signaling. *Cell.* 2012;151(7):1443-56.

45. Azzolin L, Panciera T, Soligo S, Enzo E, Bicciato S, Dupont S, Bresolin S, Frasson C, Basso G, Guzzardo V, et al. YAP/TAZ incorporation in the beta-catenin destruction complex orchestrates the Wnt response. *Cell.* 2014;158(1):157-70.

46. Alarcon C, Zaromytidou AI, Xi Q, Gao S, Yu J, Fujisawa S, Barlas A, Miller AN, Manova-Todorova K, Macias MJ, et al. Nuclear CDKs drive Smad transcriptional activation and turnover in BMP and TGF-beta pathways. *Cell.* 2009;139(4):757-69.

47. Ferrigno O, Lallemand F, Verrecchia F, L'Hoste S, Camonis J, Atfi A, and Mauviel A. Yes-associated protein (YAP65) interacts with Smad7 and potentiates its inhibitory activity against TGF-beta/Smad signaling. *Oncogene.* 2002;21(32):4879-84.

48. Varelas X, Sakuma R, Samavarchi-Tehrani P, Peerani R, Rao BM, Dembowy J, Yaffe MB, Zandstra PW, and Wrana JL. TAZ controls Smad nucleocytoplasmic shuttling and regulates human embryonic stem-cell self-renewal. *Nature cell biology.* 2008;10(7):837-48.

49. Xin M, Kim Y, Sutherland LB, Qi X, McAnally J, Schwartz RJ, Richardson JA, Bassel-Duby R, and Olson EN. Regulation of insulin-like growth factor signaling by Yap governs cardiomyocyte proliferation and embryonic heart size. *Science signaling.* 2011;4(196):ra70.

50. Xu MZ, Chan SW, Liu AM, Wong KF, Fan ST, Chen J, Poon RT, Zender L, Lowe SW, Hong W, et al. AXL receptor kinase is a mediator of YAP-dependent oncogenic functions in hepatocellular carcinoma. *Oncogene.* 2011;30(10):1229-40.

51. Thalmann GN, Anezinis PE, Chang SM, Zhau HE, Kim EE, Hopwood VL, Pathak S, von Eschenbach AC, and Chung LW. Androgen-independent cancer progression and bone metastasis in the LNCaP model of human prostate cancer. *Cancer research.* 1994;54(10):2577-81.

52. Lin MF, Meng TC, Rao PS, Chang C, Schonthal AH, and Lin FF. Expression of human prostatic acid phosphatase correlates with

androgen-stimulated cell proliferation in prostate cancer cell lines. *The Journal of biological chemistry.* 1998;273(10):5939-47.

53. Igawa T, Lin FF, Lee MS, Karan D, Batra SK, and Lin MF. Establishment and characterization of androgen-independent human prostate cancer LNCaP cell model. *The Prostate.* 2002;50(4):222-35.

54. Xiao L, Chen Y, Ji M, and Dong J. KIBRA regulates Hippo signaling activity via interactions with large tumor suppressor kinases. *The Journal of biological chemistry.* 2011;286(10):7788-96.

55. Johnson KR, Lewis JE, Li D, Wahl J, Soler AP, Knudsen KA, and Wheelock MJ. P- and E-cadherin are in separate complexes in cells expressing both cadherins. *Experimental cell research.* 1993;207(2):252-60.

56. Song S, Ajani JA, Honjo S, Maru DM, Chen Q, Scott AW, Heallen TR, Xiao L, Hofstetter WL, Weston B, et al. Hippo coactivator YAP1 upregulates SOX9 and endows esophageal cancer cells with stem-like properties. *Cancer research.* 2014;74(15):4170-82.

57. Hanahan D, and Weinberg RA. Hallmarks of cancer: the next generation. *Cell.* 2011;144(5):646-74.

58. Chambers AF, Groom AC, and MacDonald IC. Dissemination and growth of cancer cells in metastatic sites. *Nature reviews Cancer.* 2002;2(8):563-72.

59. Chaffer CL, and Weinberg RA. A perspective on cancer cell metastasis. *Science.* 2011;331(6024):1559-64.

60. Nguyen DX, Bos PD, and Massague J. Metastasis: from dissemination to organ-specific colonization. *Nature reviews Cancer.* 2009;9(4):274-84.

61. Karan D, Schmied BM, Dave BJ, Wittel UA, Lin MF, and Batra SK. Decreased androgen-responsive growth of human prostate cancer is associated with increased genetic alterations. *Clinical cancer research : an official journal of the American Association for Cancer Research.* 2001;7(11):3472-80.

62. Karan D, Kelly DL, Rizzino A, Lin MF, and Batra SK. Expression profile of differentially-regulated genes during progression of androgen-independent growth in human prostate cancer cells. *Carcinogenesis.* 2002;23(6):967-75.

63. Qin J, Xie Y, Wang B, Hoshino M, Wolff DW, Zhao J, Scofield MA, Dowd FJ, Lin MF, and Tu Y. Upregulation of PIP3-dependent Rac exchanger 1 (P-Rex1) promotes prostate cancer metastasis. *Oncogene.* 2009;28(16):1853-63.

64. Wu S, Liu Y, Zheng Y, Dong J, and Pan D. The TEAD/TEF family protein Scalloped mediates transcriptional output of the Hippo growth-regulatory pathway. *Developmental cell.* 2008;14(3):388-98.

65. Rodriguez-Berriguete G, Fraile B, Martinez-Onsurbe P, Olmedilla G, Paniagua R, and Royuela M. MAP Kinases and Prostate Cancer. *Journal of signal transduction.* 2012;2012(169170.

66. Tumaneng K, Schlegelmilch K, Russell RC, Yimlamai D, Basnet H, Mahadevan N, Fitamant J, Bardeesy N, Camargo FD, and Guan KL. YAP

mediates crosstalk between the Hippo and PI(3)K-TOR pathways by suppressing PTEN via miR-29. *Nature cell biology.* 2012;14(12):1322-9.

67. Tanaka H, Kono E, Tran CP, Miyazaki H, Yamashiro J, Shimomura T, Fazli L, Wada R, Huang J, Vessella RL, et al. Monoclonal antibody targeting of N-cadherin inhibits prostate cancer growth, metastasis and castration resistance. *Nature medicine.* 2010;16(12):1414-20.
68. Chen CD, Welsbie DS, Tran C, Baek SH, Chen R, Vessella R, Rosenfeld MG, and Sawyers CL. Molecular determinants of resistance to antiandrogen therapy. *Nature medicine.* 2004;10(1):33-9.
69. Harris WP, Mostaghel EA, Nelson PS, and Montgomery B. Androgen deprivation therapy: progress in understanding mechanisms of resistance and optimizing androgen depletion. *Nature clinical practice Urology.* 2009;6(2):76-85.
70. Wang Q, Li W, Zhang Y, Yuan X, Xu K, Yu J, Chen Z, Beroukhim R, Wang H, Lupien M, et al. Androgen receptor regulates a distinct transcription program in androgen-independent prostate cancer. *Cell.* 2009;138(2):245-56.
71. Chang KH, Li R, Kuri B, Lotan Y, Roehrborn CG, Liu J, Vessella R, Nelson PS, Kapur P, Guo X, et al. A gain-of-function mutation in DHT synthesis in castration-resistant prostate cancer. *Cell.* 2013;154(5):1074-84.
72. Drake JM, Graham NA, Lee JK, Stoyanova T, Faltermeier CM, Sud S, Titz B, Huang J, Pienta KJ, Graeber TG, et al. Metastatic castration-resistant prostate cancer reveals intrapatient similarity and interpatient

heterogeneity of therapeutic kinase targets. *Proceedings of the National Academy of Sciences of the United States of America.* 2013;110(49):E4762-9.

73. Gleave M, Miyake H, and Chi K. Beyond simple castration: targeting the molecular basis of treatment resistance in advanced prostate cancer. *Cancer chemotherapy and pharmacology.* 2005;56 Suppl 1(47-57.

74. Sharifi N, Kawasaki BT, Hurt EM, and Farrar WL. Stem cells in prostate cancer: resolving the castrate-resistant conundrum and implications for hormonal therapy. *Cancer biology & therapy.* 2006;5(8):901-6.

75. Harvey KF, Zhang X, and Thomas DM. The Hippo pathway and human cancer. *Nature reviews Cancer.* 2013;13(4):246-57.

76. Johnson R, and Halder G. The two faces of Hippo: targeting the Hippo pathway for regenerative medicine and cancer treatment. *Nature reviews Drug discovery.* 2014;13(1):63-79.

77. Zhao B, Ye X, Yu J, Li L, Li W, Li S, Yu J, Lin JD, Wang CY, Chinnaiyan AM, et al. TEAD mediates YAP-dependent gene induction and growth control. *Genes & development.* 2008;22(14):1962-71.

78. Liu-Chittenden Y, Huang B, Shim JS, Chen Q, Lee SJ, Anders RA, Liu JO, and Pan D. Genetic and pharmacological disruption of the TEAD-YAP complex suppresses the oncogenic activity of YAP. *Genes & development.* 2012;26(12):1300-5.

79. Zhao B, Li L, Wang L, Wang CY, Yu J, and Guan KL. Cell detachment activates the Hippo pathway via cytoskeleton reorganization to induce anoikis. *Genes & development.* 2012;26(1):54-68.

80. Cinar B, Collak FK, Lopez D, Akgul S, Mukhopadhyay NK, Kilicarslan M, Gioeli DG, and Freeman MR. MST1 is a multifunctional caspase-independent inhibitor of androgenic signaling. *Cancer research.* 2011;71(12):4303-13.

81. Powzaniuk M, McElwee-Witmer S, Vogel RL, Hayami T, Rutledge SJ, Chen F, Harada S, Schmidt A, Rodan GA, Freedman LP, et al. The LATS2/KPM tumor suppressor is a negative regulator of the androgen receptor. *Molecular endocrinology.* 2004;18(8):2011-23.

82. Lee KP, Lee JH, Kim TS, Kim TH, Park HD, Byun JS, Kim MC, Jeong WI, Calvisi DF, Kim JM, et al. The Hippo-Salvador pathway restrains hepatic oval cell proliferation, liver size, and liver tumorigenesis. *Proceedings of the National Academy of Sciences of the United States of America.* 2010;107(18):8248-53.

83. Cai J, Zhang N, Zheng Y, de Wilde RF, Maitra A, and Pan D. The Hippo signaling pathway restricts the oncogenic potential of an intestinal regeneration program. *Genes & development.* 2010;24(21):2383-8.

84. Mulholland DJ, Tran LM, Li Y, Cai H, Morim A, Wang S, Plaisier S, Garraway IP, Huang J, Graeber TG, et al. Cell autonomous role of PTEN in regulating castration-resistant prostate cancer growth. *Cancer cell.* 2011;19(6):792-804.

85. Wang S, Gao J, Lei Q, Rozengurt N, Pritchard C, Jiao J, Thomas GV, Li G, Roy-Burman P, Nelson PS, et al. Prostate-specific deletion of the murine Pten tumor suppressor gene leads to metastatic prostate cancer. *Cancer cell.* 2003;4(3):209-21.